DESIGN AND FUNCTION OF TRILOBITE EXOSKELETONS

by

NADINE VIVIENNE WILMOT

Doctor of Philosophy

THE UNIVERSITY OF ASTON IN BIRMINGHAM

October 1988

The University of Aston in Birmingham

DESIGN AND FUNCTION OF TRILOBITE EXOSKELETONS

NADINE VIVIENNE WILMOT

Thesis submitted for the degree of Doctor of Philosophy

1988

SUMMARY

The fossil arthropod Class Trilobita is characterised by the possession of a highly mineralised dorsal exoskeleton with an incurved marginal flange (doublure). This cuticle is usually the only part of the organism to be preserved. Despite the common occurrence of trilobites in Palaeozoic sediments, the original exoskeletal mineralogy has not been determined previously. Petrographic data involving over seventy trilobite species, ranging in age from Cambrian to Carboniferous, together with atomic absorption and stable isotope analyses, indicate a primary low-magnesian calcite composition.

Trilobite cuticles exhibit a variety of preservational textures which are related to the different diagenetic realms through which they have passed. A greater knowledge of post-depositional processes and the specific features they produce, has enabled post-mortem artefacts to be distinguished from primary cuticular microstructures. Alterations of the cuticle can either enhance or destroy primary features, and their effects are best observed in thin-sections, both under transmitted light and cathodoluminescence.

Well preserved trilobites often retain primary microstructures such as laminations, canals, and pustules. These have been examined in stained thin-sections and by scanning electron microscopy, from as wide a range of trilobites as possible. Construction of sensory field maps has shown that although the basic organisation of the exoskeleton is the same in all trilobites, the types of microstructures found, and their distribution is species-specific.

The composition, microstructure, and architecture of the trilobite exoskeleton have also been studied from a biomechanical viewpoint. Total cuticle thickness, and the relative proportions of the different layers, together with the overall architecture all affected the mechanical properties of the exoskeleton.

KEY WORDS: trilobite cuticle biomineralisation microstructure biomechanics

ACKNOWLEDGEMENTS

I thank Dr A. T. Thomas for his encouragement and supervision throughout the project, and for assistance during fieldwork. Funding was provided by an Aston University Research Studentship Award. I also thank Dr R. J. Aldridge (University of Nottingham) for providing scanning electron microscope facilities, and Mr A. Swift for technical assistance.

Dr A. E. Fallick (S.U.R.R.C., Glasgow) obtained the stable isotope analyses, and Dr K. T. Ratcliffe (Kingston Polytechnic) discussed aspects of carbonate diagenesis as well as providing fieldwork assistance. My biomechanical studies have benefitted from valuable discussions on structural mechanics and architectural design with my father.

The project would not have been possible without generous donations of specimens from Dr B. D. E. Chatterton, Dr E. N. K. Clarkson, Dr N. Eldredge, Dr R. A. Fortey, Dr G. Helbert, Dr P. D. Lane, Dr A. W. Owen, Dr L. Ramsköld, Mr S. J. Tull and Prof H. B. Whittington. I also thank Dr J. E. Dalingwater for the loan of his thesis material, and the curators of the following institutions for loaning additional specimens: British Geological Survey, Keyworth; British Museum (Natural History), London; Geology Museum Louisiana State University, Baton Rouge; National Museum of Wales, Cardiff; Naturhistoriska Riksmuseet, Stockholm; Paleontologisk Museum, Oslo; and the Sedgwick Museum, Cambridge.

I also give special thanks to my fiancé Simon Tull for always being there when I needed him.

CONTENTS

LIST OF FIGURES

LIST OF PLATES

LIST OF APPENDICES

CHAPTER 1

INTRODUCTION AND METHODS

1.1. Introduction

THE Phylum Arthropoda is characterised by the possession of a rigid but jointed, chitinous exoskeleton which is used for both protection and muscle attachment. Periodic moulting (ecdysis) is necessary to allow growth. Cuticle is material secreted onto the outer surfaces of epidermal cells which solidifies to form the exoskeleton (Richards 1951).

The basic structure of arthropod cuticle is the same throughout the phylum, and consists of several layers which are distinguishable on structural and histochemical grounds (Figure 1.1). The main divisions are a thin outer epicuticle, and an underlying procuticle which forms the bulk of the exoskeleton. The procuticle is divisible into the exocuticle and an inner endocuticle. Although all arthropod cuticles are composed at least in part of a chitin-protein complex (for chemistry see Richards 1951), the various arthropodan groups are characterised by variations in the overall composition and proportions of the different layers (see review by Dalingwater 1981). Trilobite exoskeletons are characteristically highly calcified. Laminae and canals in the procuticle are almost universal in the Arthropoda.

Laminations within the procuticle can be seen in thin-sections of specimens viewed in transmitted light, as a series of light and dark bands parallel to the cuticle surface (Plate 4.1a). There has been some dispute as to whether these laminations are discrete entities (Dennell

Figure 1.1. Subdivisions of arthropod cuticle.

Based on Richards (1951, p. 147).

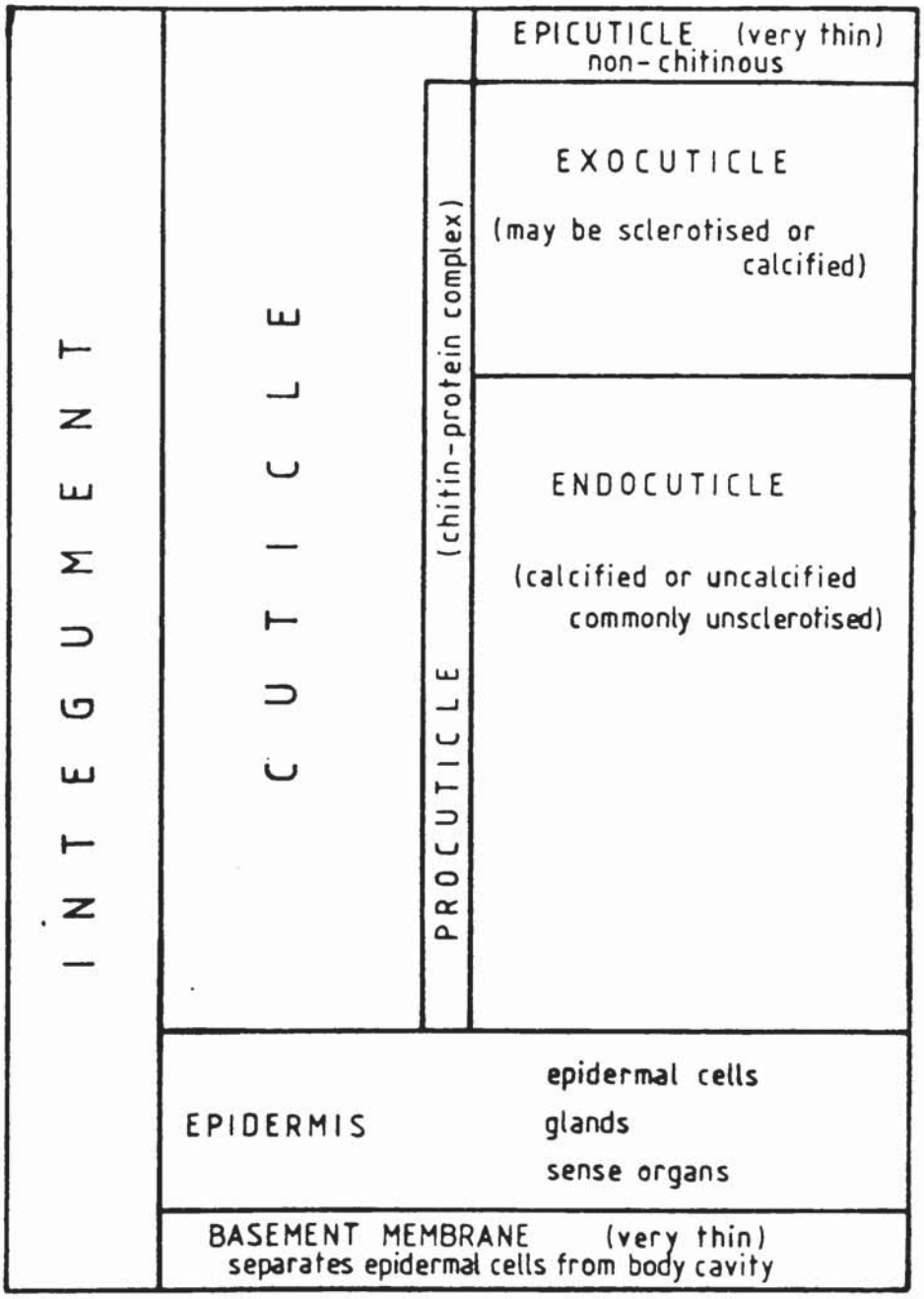

1960, 1973, 1974, 1976, 1978; Mutvei 1974, 1977, 1981; Dalingwater 1975a, 1975b; Dalingwater and Miller 1977) composed of horizontal layers interconnected by 'parabolic arcs' (Mutvei 1977); or artefacts resulting from cutting through helically arranged flat sheets of fibres (Bouligand 1965, 1972; Livolant et al. 1978). Today the Bouligand model (1965) is widely accepted. This theory suggests that chitin fibrils within the cuticle are arranged in a series of horizontal layers. Fibre orientation within each sheet is unidirectional, but each layer is slightly offset by a few degrees rotation, creating a helicoidal arrangement within the cuticle. A lamina is produced with every 180° rotation. Helically arranged layers within some insect cuticles are produced on a daily circadian rhythm (Neville 1963, 1967b) which is related to the presence of light (Neville 1967a, 1967b).

Helicoidal structure does not occur in all arthropod cuticles. Sometimes the cuticle may be composed of layers all having the same fibre direction, or a mixture of both unidirectional and successively rotating sheets. Spider cuticle (Barth 1973), and that of chelicerates (Dalingwater 1980) show all these fibre arrangements depending on which part is examined. Most exocuticles contain helicoidal structures whereas endocuticles may be mixtures of helicoidal and unidirectional structural arrangements (Neville 1975). In locusts, unidirectional layers are produced during the day, and helicoidal sheets at night (Neville and Luke 1969). Unidirectional fibre orientation is thought to be more advanced than helicoidal structure and is an adaptation for greater strength against particlar forces acting in specific directions (Neville 1975).

Sometimes a reticulate pattern of cell polygons may be observed on the external surface of cuticles, formed by a series of raised ridges. The vertical ridges (interprismatic septa) surrounding each polygon outline the boundaries of the underlying epidermal cells which generated the cuticle (Dennell 1960; Travis 1963; Okada 1981, 1982).

The most numerous canals in arthropod cuticle are pore canals (typically only 1μm diameter) which travel vertically through the cuticle and lie within the cell polygons (Dennell 1960). They are involved in cuticle secretion. In most arthropods, pore canals are shaped like twisted ribbons (see reviews by Neville 1970, 1975), the degree of rotation being directly related to fibre architecture (Rolfe 1962; Neville et al. 1969). Non-twisted pore canals have been reported in some crustaceans (Mutvei 1974). Other larger canals are either gland ducts or parts of sensory receptors.

Most published studies of arthropod cuticle have been carried out on Recent insects as they are by far the most numerous arthropods today, and have the most influence on Man in terms of crop destruction and disease. Knowledge of cuticle construction has been vital in the development of pesticides. For reviews of insect ultrastructure see Neville (1970, 1984).

Insect cuticle is usually hardened by sclerotisation; the incorporation of phenols which become tightly bound within the cuticle, coupled with some loss of water (Vincent and Hillerton 1979). Many marine arthropods however have thicker calcified exoskeletons. This is probably due to the availability of calcium ions in the marine environment which, in those conditions, makes calcified cuticle more economical to construct (Wainwright et al. 1976). Examples of such

calcified groups are cirripedes, some decapod crustaceans and ostracodes, and trilobites. In crustaceans, calcium ions are transported through the cuticle via the pore canals (Yano 1975) but initial precipitation is along the interprismatic septa (Giraud-Guille 1984).

In the following chapters, the composition, microstructural organisation and mechanical properties of exoskeletons from the fossil arthropod Class Trilobita are described. This group has been the subject of few cuticular microstructural studies as their exoskeletons are generally less well preserved than those of eurypterids (Dalingwater 1973b, 1975c, 1980; Mutvei 1977; Selden 1981; Dalingwater and Waterston 1983) and crustaceans (Rolfe 1962; Neville and Berg 1971; Taylor 1973; Dalingwater 1977). This preservational variability is related to the different cuticle compositions of these groups.

Until the 1970's, descriptions of trilobite cuticle were mainly limited to brief comments included in taxonomic works (see review by Dalingwater 1973a). Since then, trilobite cuticular microstructure has been studied in its own right, with the recognition of two main layers in the exoskeleton (Dalingwater 1973a; Osmólska 1975; Teigler and Towe 1975; Dalingwater and Miller 1977; Mutvei 1981) and the identification of various microstructures, some of which may have contained sensory receptors, for example those described by Miller (1975, 1976) and Størmer (1980).

Each chapter in this thesis has been written as a discrete unit in publication style, in accordance with the recommendation of C.H.U.G.D. Chapter 2 is already in press with Palaeontology, and that journal's format is used throughout. Trilobites were marine arthropods that were

distinctive in the high degree of mineralisation of their exoskeletons, and in Chapter 2 their original mineralogy is identified as low-magnesian calcite. The various preservational states that trilobite exoskeletons may exhibit are then documented and related to the different diagenetic regimes through which the fossils have passed (Chapter 3).

New, more extensive data on trilobite cuticular microstructures are discussed in Chapter 4, and detailed accounts of the cuticular features of specimens from the trilobite orders Proetida and Agnostida are given in Chapters 5 and 6. It is shown that although some structures are common to all trilobites (such as laminations and canals), others are restricted to particular groups. The distribution and types of cuticular microstructures in trilobites are species-specific, and may be used as an aid in taxonomy.

The final chapter discusses the composition, microstructural organisation and architecture of trilobite exoskeletons from a biomechanical viewpoint. The relative proportion of exocuticle to endocuticle, as well as overall cuticle thickness and architecture, strongly affect the mechanical properties of trilobite exoskeletons.

1.2. MATERIAL AND METHODS

Specimens belonging to over seventy species of trilobite, ranging in age from Cambrian to Carboniferous (see Appendix 6) were embedded in Araldite (epoxy resin) and made into uncovered thin-sections. They were then examined by cathodoluminescence, using a Technosyn cold cathode luminoscope, model 8200 Mk11 at a gun current of 15-18kV and 400-600mA.

The thin-sections were later stained (Dickson 1966) and protected by coverslips before examination in transmitted light.

Other specimens were trimmed to a diameter of no more than 12.5mm and a height of 5mm, for mounting on ½ inch aluminium pin stubs (Agar Aids, Stansted, Essex. CM24 8DA) with carbon glue (Polaron Equipment Ltd., Watford, Herts). Occasionally specimens were first etched for 10 seconds in concentrated HCl diluted to 10% by volume, to enhance relief. After being allowed to dry for 24 hours, the stubs were gold-coated using a Polaron E5000C (PS3) sputter coater timed at 70 seconds. The material was then examined with an International Scientific Instruments scanning electron microscope, model ISI-SX-30 which had been adapted to hold stubs of the above dimensions. Additional chemical and isotopic analyses have also been carried out, detailed descriptions of which are given in Section 2.2.

As the material studied had to be as well preserved as possible, most of the specimens have been loaned by museums. However, additional collecting was carried out in the West Midlands, Shropshire, and Malvern Hills, England, from the Much Wenlock Limestone and Woolhope Limestone formations (Wenlock).

Unless otherwise stated, all material is housed at the National Museum of Wales, Cardiff; accession number NMW 88.22G. Specimens figured in the thesis loaned by other institutions or individuals are indicated by initials (designated below) at the start of the specimen number: Dr J. E. Dalingwater (University of Manchester) (JED); British Geological Survey, Keyworth (BGS); British Museum (Natural History), London (BM); Geology Museum, Louisiana State University, Baton Rouge (LSU); National Museum of Wales, Cardiff (NMW); Naturhistoriska

Riksmuseet, Stockholm (NRS); Paleontologisk Museum, Oslo (PMO), Sedgwick Museum, Cambridge (SM).

1.3. REFERENCES

BARTH, F. G. 1973. Microfibre reinforcement of an arthropod cuticle. Z. Zellforsch. mikrosk. Anat. 144, 409-433.

BOULIGAND, Y. 1965. Sur une architecture torsadée répandue dans de nombreuses cuticules d'arthropodes. C. r. hebd. Séanc. Acad. Sci. Paris, 261, 3665-3668.

BOULIGAND, Y. 1972. Twisted fibrous arrangements in biological materials and cholesteric mesophases. Tissue and Cell, 4, 189-217.

DALINGWATER, J. E. 1973a. Trilobite cuticle microstructure and composition. Palaeontology, 16, 827-839, pls. 107-109.

DALINGWATER, J. E. 1973b. The cuticle of a eurypterid. Lethaia, 6, 179-186.

DALINGWATER, J. E. 1975a. S.E.M. observations on the cuticles of some decapod crustaceans. Zool. J. Linn. Soc., 56, 327-330.

DALINGWATER, J. E. 1975b. Further observations of eurypterid cuticles. Fossils Strata, 4, 271-280.

DALINGWATER, J. E. 1975c. The reality of arthropod cuticular laminae. Cell Tissue Res., 163, 411-413.

DALINGWATER, J. E. 1977. Cuticular ultrastructure of a Cretaceous decapod crustacean. Geol. J. 12, 25-32.

DALINGWATER, J. E. 1980. S.E.M. observations on the cuticles of some chelicerates. Proc. 8th Int. Cong. Arach. Vienna., 285-289.

DALINGWATER, J. E. 1981. Studying fossil arthropod cuticles with the S.E.M. Int. Symp. Concept. Meth. Paleo. Barcelona., 319-324.

DALINGWATER, J. E. and MILLER, J. 1977. The laminae and cuticular organisation of the trilobite Asaphus raniceps. Palaeontology, 20, 21-32, pls. 9-10.

DALINGWATER, J. E. and WATERSTON, C. D. 1983. An arthropod fragment from the Scottish Namurian and its remarkably preserved cuticular ultrastructure. In BRIGGS, D. E. G. and LANE, P. D. (eds.). Trilobites and other early arthropods. Spec. Pap. Palaeont., 30, 221-228, pls. 29-30.

DENNELL, R. 1960. Integument and exoskeleton. In WATERMAN, T. H. (ed.). The physiology of Crustacea. 1. 449-472. Academic Press, New York.

DENNELL, R. 1973. The structure of the shore crab Carcinus maenas (L.). Zool. J. Linn. Soc., 56, 327-330.

DENNELL, R. 1974. The cuticle of the crabs Cancer pagurus (L.) and Carcinus maenas (L.). Zool. J. Linn. Soc., 54, 241-245.

DENNELL, R. 1976. The structure and lamination of some arthropod cuticles. Zool. J. Linn. Soc., 58, 159-164.

DENNELL, R. 1978. The cuticle of the hoplocarid crustacean Squilla desmaresti Risso. Zool. J. Linn. Soc., 62, 309-316, 3 pls.

DICKSON, J. A. D. 1966. Carbonate identification and genesis as revealed by staining. J. sedim. Petrol., 12, 133-149.

GIRAUD-GUILLE, M. M. 1984. Calcification initiation sites in the crab cuticle: the interprismatic septa. Cell Tissue Res., 236, 413-420.

LIVOLANT, F., GIRAUD, M. M. and BOULIGAND, Y. 1978. A goniometric effect observed in sections of twisted fibrous materials. Biol. Cellulaire, 31, 159-168.

MILLER, J. 1975. Structure and function of trilobite terrace lines. Fossils Strata, 4, 155-178.

MILLER, J. 1976. The sensory fields and life mode of Phacops rana (Green, 1832) (Trilobita). Trans. R. Soc. Edinb., 69, 337-367, pls. 1-4.

MUTVEI, H. 1974. S.E.M. studies on arthropod exoskeletons, Part 1: Decapod crustaceans Homarus gammarus L. and Carcinus maenas (L.). Bull. geol. Instn Univ. Upsala, N. S., 4, 73-80.

MUTVEI, H. 1977. S.E.M. studies on arthropod exoskeletons. Part 2: Horseshoe crab Limulus polyphemus (L.) in comparison with extinct eurypterids and Recent scorpions. Zool. Scr., 6, 203-213.

MUTVEI, H. 1981. Exoskeletal structure in the Ordovician trilobite Flexicalymene. Lethaia, 14, 225-234.

NEVILLE, A. C. 1963. Daily growth layers for determining the age of grasshopper populations. Oikos, 14, 1-8, figs. 1-16.

NEVILLE, A. C. 1967a. A dermal light sense influencing skeletal structure in locusts. J. Insect. Physiol., 13, 933-939.

NEVILLE, A. C. 1967b. Daily growth layers in animals and plants. Biol. Rev., 42, 421-441.

NEVILLE, A. C. 1970. Cuticle ultrastructure in relation to the whole insect. Symp. R. entomol. Soc. Lond., 5, 17-39.

NEVILLE, A. C. 1975. Biology of arthropod cuticle. Springer, Berlin.

NEVILLE, A. C. 1984. Cuticle: organisation. In BEREITER-HAHN, J., MATOLTSY, A. G. and SYLVIA RICHARDS, K. (eds.). Biology of the integument, Volume 1. 611-625. Springer-Verlag, Berlin.

NEVILLE, A. C. and BERG, C. W. 1971. Cuticle ultrastructure of a Jurassic crustacean (Eryma stricklandi). Palaeontology, 14, 201-205.

NEVILLE, A. C. and LUKE, B. M. 1969. Molecular architecture of adult locust cuticle at the electron-microscope level. Tissue and Cell, 1, 355-366.

NEVILLE, A. C., THOMAS, M. G. and ZELAZNY, B. 1969. Pore canal shape related to molecular architecture of arthropod cuticle. Tissue and Cell, 1, 183-200.

OKADA, Y. 1981. Development of cell arrangement in ostracod carapaces. Paleobiology, 7, 276-280.

OKADA, Y. 1982. Structure and cuticle formation of the reticulated carapace of the ostracode Bicornucythere bisanensis. Lethaia, 15, 85-101.

OSMÓLSKA, H. 1975. Fine morphological characters of some Upper Palaeozoic trilobites. Fossils Strata, 4, 201-207.

RICHARDS, A. G. 1951. The integument of arthropods. xvi + 411pp. University of Minnesota Press, Minneapolis.

ROLFE, W. D. I. 1962. The cuticle of some middle Silurian ceratiocaridid Crustacea from Scotland. Palaeontology, 5, 30-51.

SELDEN, P. A. 1981. Functional morphology of the prosoma of Baltoeurypterus tetragonophthalmus (Fischer) (Chelicerata; Eurypterida). Trans. R. Soc. Edinb., 72, 9-48.

STØRMER, L. 1980. Sculpture and microstructure of the exoskeleton in chasmopinid and phacopid trilobites. Palaeontology, 23, 237-271, pls. 25-34.

TAYLOR, B. J. 1973. The cuticle of Cretaceous macrurous Decapoda from Alexander and James Ross Islands. Br. Antarct. Surv. Bull., 35, 91-100.

TEIGLER, D. J. and TOWE, K. M. 1975. Microstructure and composition of the trilobite exoskeleton. Fossils Strata, 4, 137-149, pls. 1-9.

TRAVIS, D. F. 1963. Structural features of mineralisation from tissue to macromolecular levels of organisation in the decapod Crustacea. Ann. N. Y. Acad. Sci. Ser. 5, 109, 177-245.

VINCENT, J. F. V. and HILLERTON, J. E. 1979. The tanning of insect cuticle - a critical review and a revised mechanism. J. Insect Physiol., 25, 653-658.

WAINWRIGHT, S. A., BIGGS, W. D., CURREY, J. D. and GOSLINE, J. M. 1976. Mechanical design in organisms 423pp. Edward Arnold, London.

YANO, I. 1975. An electron microscope study on the calcification of the exoskeleton in a shore crab. Bull. Jap. Soc. scient. Fish., 41, 1079-1082.

CHAPTER 2

ORIGINAL MINERALOGY OF TRILOBITE EXOSKELETONS

ABSTRACT. The mineralised exoskeletons of well-preserved trilobites are now composed of low-magnesian calcite. However, as this is the only form of calcium carbonate to survive in Lower Palaeozoic rocks, such a mineralogy may be a function of diagenetic processes rather than reflecting primary cuticle composition. Ferroan calcite replacement has previously been used to infer an original high-magnesian calcite mineralogy for trilobite exoskeletons. By contrast, petrographic data involving over seventy trilobite species, ranging in age from Cambrian to Devonian, together with carbon and oxygen stable isotope analyses of specimens from the Much Wenlock Limestone Formation, England (Wenlock), are here used to infer that trilobites constructed low-magnesian calcite exoskeletons. Petrographically, the trilobite cuticles share the same preservational characteristics as low-magnesian calcite organisms such as articulate brachiopods. They also have very similar isotopic signatures to those of brachiopods, yet differ from crinoids which secreted high-magnesian calcite ossicles and now commonly contain microdolomite inclusions and secondary voids. Together, these separate lines of evidence strongly suggest that trilobite exoskeletons originally had a low-magnesian calcite mineralogy.

2.1. Introduction

MOST trilobites had heavily-mineralised exoskeletons, a characteristic shared by some other marine arthropods such as decapod crustaceans,

cirripedes, and ostracodes. Three trilobite species with entirely organic cuticles have been described (Whittington 1977, 1985; Dzik and Lendzion 1988), but this chapter is concerned only with those trilobites that had mineralised exoskeletons. In such trilobites the dorsal exoskeleton and hypostome were predominantly composed of calcium carbonate with a small proportion of organic matter. If the exoskeleton is decalcified in E.D.T.A. the remains of the organic framework become apparent as a delicate brown residue of unknown composition, still retaining the general structure of the cuticle (Dalingwater 1973; Teigler and Towe 1975; Miller 1976; Dalingwater and Miller 1977). The ultrastructure of the exoskeleton comprises an outer prismatic layer with a much thicker principal layer below (Plate 2.1d). Several types of cuticular microstructure may also occur, including laminations, tubercles and canals (Dalingwater 1973; Miller 1976; Størmer 1980; Mutvei 1981). Despite increasing understanding of the structure of the exoskeleton, its original mineralogy has not previously been determined.

Marine invertebrates construct their skeletons from a variety of forms of calcium carbonate. Scleractinian corals use aragonite (A), echinoderms have high-magnesian calcite (HMC) hard parts (>5% $MgCO_3$), and articulate brachiopods construct low-magnesian calcite (LMC) valves (<5% $MgCO_3$); sometimes combinations of these may be used, as in certain molluscs (Milliman 1974; Wolf et al. 1976; Morrison and Brand 1987). Among modern arthropods, decapod crustaceans utilise HMC and small amounts of calcium phosphate, whereas most ostracodes use LMC, and cirripedes form their lateral plates from LMC with some species having A basal plates (Richards 1951; Milliman 1974; Morrison and Brand 1987).

When trilobite exoskeletons are well preserved and still exhibit primary microstructures, examination of stained thin-sections and X-ray diffraction show they are composed of calcite (Dalingwater 1973; Teigler

and Towe 1975). Analyses by microprobe (Teigler and Towe 1975; Miller and Clarkson 1980) and atomic absorption indicate a LMC mineralogy; shown in the data below of the average composition of ten trilobite specimens from the Much Wenlock Limestone Formation, England (Wenlock).

$\%Ca^{2+}$	$\%CaCO_3$	$\%Mg^{2+}$	$\%MgCO_3$	Total $CaMgCO_3$	$\%Fe^{2+}$
35.18	87.94	0.81	2.82	89.89	0.50
$\pm$ 2.73	$\pm$6.81	$\pm$0.57	$\pm$1.98	$\pm$6.83	$\pm$0.19

Specimens were obtained from localities 43 and 64 of Thomas (1978). Impurities such as organic matrix, ferroan calcite, pyrite, and water account for incomplete percentage totals. Isolated reports of phosphate within trilobite cuticle (Dalingwater 1973, p. 829; Teigler and Towe 1975) probably represent secondary deposits. A LMC mineralogy is to be expected for Palaeozoic fossils, for although the primary composition of extant organisms or well-preserved Tertiary fossils can be determined directly, the older the fossil, the more its composition is likely to have been altered by diagenetic processes. The original composition of Lower Palaeozoic fossils may be inferred by comparisons with living taxa of the same class, from petrographic evidence (Lohmann and Meyers 1977; Richter and Füchtbauer 1978), and from stable isotope data. These principles are used for trilobites which have no close modern relatives, and in the following sections, data are presented which indicate an original LMC mineralogy.

2.2. MATERIAL AND METHODS

Ten samples of five trilobite species from the Much Wenlock Limestone Formation, England (Wenlock) were prepared for atomic absorption

analyses. Unweathered specimens were scraped with a scalpel to obtain approximately 50mg of exoskeleton in powder form. Each sample was then dissolved in 10ml of concentrated HCl diluted 50%, and boiled on a hot plate for 2 minutes until the solution became clear, adding more distilled water as necessary. The solutions were allowed to cool and made up to 100ml volume with distilled water, before running on a Perkin-Elmer atomic absorption spectrophotometer, model 460.

Pieces of trilobite cuticle, brachiopod valves, and individual crinoid ossicles from the Much Wenlock Limestone Formation were prepared for carbon and oxygen stable isotope analyses. Unweathered specimens were scraped with a scalpel to obtain 5mg of powder, great care being taken to avoid contamination from the surrounding matrix. Isotopic ratios were then obtained by Dr A. E. Fallick at S.U.R.R.C. Glasgow, following established methods (McCrea 1950). All isotopic values are in per mil with respect to PDB. Precision is around 0.1% (1σ) or better for both $\delta^{13}C$ and $\delta^{18}O$. See Appendices 1 and 2 for tabulation of all data.

2.3. PETROGRAPHY

Trilobite exoskeletons are best preserved in dark, fine-grained limestones and calcareous mudstones. Fine primary microstructures such as canals and laminations are often retained in such cases, and eye lenses may remain capable of focussing sharp images (Towe 1973). Loss of most primary structure is inevitable during the inversion of aragonite to calcite. Occasionally, traces of organic inclusions outline former structures and produce pseudopleochroic calcite in neomorphically altered aragonite (Hudson 1962). As the preservation of trilobite exoskeletons is generally much better than this, a primary A mineralogy can be discounted.

Richter and Füchtbauer (1978) suggested that replacement by ferroan calcite is indicative of a former HMC composition, as LMC is more stable

and therefore not replaced. Trilobite cuticles are, very occasionally, preserved in this way. The former existence of HMC can also be indicated by the presence of microdolomites that formed in a closed system during the conversion to LMC (Lohmann and Meyers 1977). During this process, the excess magnesium ions which are not incorporated into the LMC lattice form microdolomite inclusions 1-10μm diameter, which are readily identified with cathodoluminescence (CL). Microdolomites have never been found within trilobite exoskeletons, despite them often occurring in close association with inclusion-rich components, suggesting that they may have had an original LMC mineralogy. These differences are well illustrated by petrological examination of fossils from the Much Wenlock Limestone Formation, which show clear preservational variations between taxa (Plate 2.1). Gastropods which had an original A exoskeleton have been replaced by a void-filling cement (Bathurst 1975) with total loss of primary microstructure. Crinoid ossicles, originally HMC, have abundant microdolomite inclusions and often contain secondary voids. Both brachiopods (primary LMC) and trilobites show good preservation, with laminae and canals still visible. Neither taxon ever has any microdolomite inclusions, nor shows evidence of secondary dissolution in this formation, suggesting that they were both composed of LMC.

2.4. CARBON AND OXYGEN STABLE ISOTOPE ANALYSES

The principles involved in carbon and oxygen isotope analyses are outlined below; for a more detailed introduction to stable isotopes and their geological uses, see Hoefs (1980) and Arthur *et al.* (1983). The isotopic fractionation of oxygen between calcium carbonate and water is temperature dependent (McCrea 1950). Although the isotopic composition of meteoric waters (as measured from atmospheric precipitation) varies considerably with temperature, altitude and latitude, the isotopic

composition of seawater remains relatively constant at a given temperature because of its much larger mass. It would be expected that marine invertebrates secreting a calcium carbonate exoskeleton would do so in isotopic equilibrium with the surrounding seawater. This is the case in certain organisms, such as articulate brachiopods and Recent cirripedes, though other groups such as echinoderms exhibit a 'vital effect' and secrete exoskeletons that are not in isotopic equilibrium. This non-equilibrium is thought to result from variations in their physiological processes, such as use of metabolic carbon dioxide (Milliman 1974; Morrison and Brand 1987). Hence different marine invertebrate groups possess distinctive 'isotopic signatures', related both to the temperature of the seawater they inhabit and their physiology. In general, forms with LMC exoskeletons tend to be in isotopic equilibrium whereas those secreting A or HMC hard parts show a vital effect.

Isotopic signatures can be determined for fossils and coexisting inorganically-precipitated carbonate, including cements. For any locality, the relative differences in carbon and oxygen isotopic values between organisms and the seawater at the time of their formation should still be apparent, even with diagenetic effects superimposed, provided the components did not reach isotopic equilibrium with pore fluids.

On this basis, the composition of trilobite exoskeletons was determined using specimens from the Much Wenlock Limestone Formation, which contains some of the best preserved trilobites in Britain. Conodont elements from this formation have suffered very minor thermal maturation, 50-90°C (Aldridge 1986) suggesting burial to only 1-1.5km. Previous carbon and oxygen isotope studies from this formation (Ratcliffe 1987) revealed a clear distinction between the isotopic values of brachiopods and crinoid ossicles. These data from primary and secondary LMC are then

Figure 2.1. Carbon and oxygen stable isotope compositions for allochems and cements from the Much Wenlock Limestone Formation.

Based partly on unpublished data from K. T. Ratcliffe.

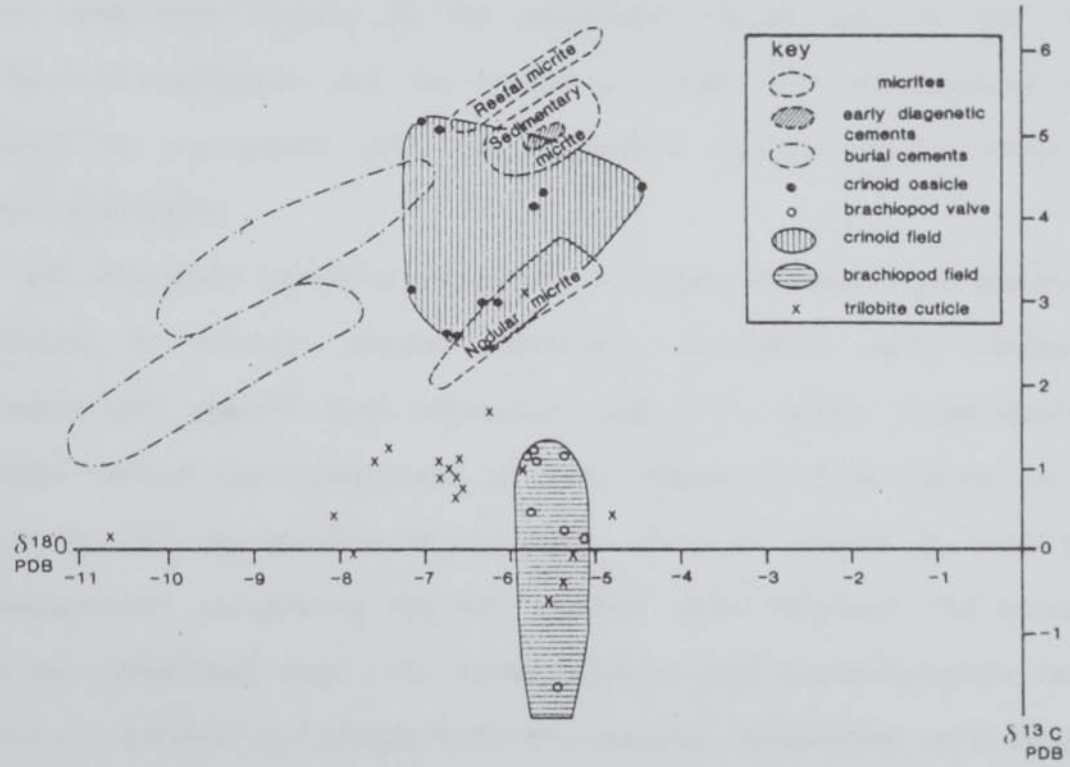

used here for comparison with the isotopic signature obtained from trilobite cuticles.

2.5. Discussion

The isotope data (Figure 2.1) show no relationship between the trilobite species used, or the locality from which they came. The trilobite data plot much more closely to the brachiopod values than to the other limestone components, and the spread of points can be explained when viewed in conjunction with the diagenetic history of the formation (Ratcliffe 1987).

All originally unstable components now have elevated $\delta^{13}C$ signatures relative to Silurian marine carbonates. Similarly, early diagenetic primary LMC cements have relatively high $\delta^{13}C$ values. These elevated values reflect the development of early diagenetic pore fluids, so the more porous the constituent analysed, the more cement it will have incorporated, influencing the net isotopic value obtained. The micrites all have relatively high $\delta^{13}C$ values compared with the brachiopods, which were in isotopic equilibrium with the seawater (Lowenstam 1961; Popp *et al.* 1986). This is probably because they include small amounts of early diagenetic cements with a high $\delta^{13}C$ value. They also show a NE/SW trend similar to that of the burial cements, again indicating incorporation of burial cement in the micrite micro-pores. Crinoid ossicles also have high $\delta^{13}C$ values, but with a relatively wide distribution. The composition of these originally HMC skeletal parts is a reflection of their original isotopic signature, and partial equilibration with the pore fluids that generated the early diagenetic primary LMC cements.

The brachiopods, being primary LMC and hence very stable have low $\delta^{13}C$ values. They also show very little spread in data due to their low porosity. These factors give brachiopods great stability, making them

suitable for palaeotemperature determinations. The trilobite cuticles also have low $\delta^{13}C$ values and are distinct from both the micritic and cement phases, suggesting that they, like the brachiopods, were constructed from LMC. Trilobite exoskeletons contain numerous canals which were liable to have been infilled by either early cements or burial cement; the degree to which this happened being reflected in the variation of their isotopic values. When these effects are taken into account, it can be seen that the isotopic signature of trilobites was originally very similar to that of the brachiopods, close to isotopic equilibrium with seawater.

The degree of porosity within trilobite exoskeletons makes them unsuitable for palaeotemperature determinations despite their primary LMC mineralogy; eye lenses are a possible exception. Similar problems arise in using belemnite rostra for this purpose (Veizer 1974). It is notable that the isotopic composition of Silurian seawater obtained from these data is lower in $\delta^{13}C$ than previously published results from the Silurian of Gotland (Frykman 1986). However, as the $\delta^{18}O$ values are in the same range, implying the same temperatures, this is probably due to differing productivity levels between England and Gotland.

The present study emphasises that fossils should not be studied in isolation, since the isotopic values of the trilobite specimens can only be interpreted when viewed in conjunction with data from other limestone allochems and cements. Only in this way can diagenetic effects be identified and their influences evaluated.

2.6. CONCLUDING REMARKS

Comparison of the petrographic and chemical characteristics of taxa of known mineralogy with those of trilobites occurring in the same samples strongly suggests that mineralised trilobite exoskeletons were constructed from LMC. This contrasts with Richter and Füchtbauer's (1978)

inferred HMC composition based on replacement by ferroan calcite. However, this type of replacement in trilobites is very rare and probably results merely from local diagenetic conditions. Where ferroan calcite trilobites have been found in the Much Wenlock Limestone Formation, they occur in a ferruginous crinoidal grainstone lithofacies which had major diagenetic interaction with nearby iron-rich mudstones (Ratcliffe 1987), so that the vast majority of the other limestone components have been affected. Trilobite cuticles were basically stable, being composed of LMC, but nevertheless subject to alteration by highly reactive pore fluids. Microstructure (Walter 1985) and the amount and composition of the organic matter within the exoskeleton all influence the rate of ionic exchange. Even brachiopods, which are recognised as having had a LMC composition may occasionally be replaced by ferroan calcite (A. M. Searl pers. comm.). The total absence of microdolomites from trilobite cuticles, the absence of secondary voids, and the similarity in type of preservation and isotopic composition between trilobites and brachiopods, indicates that trilobites had a primary LMC mineralogy. Given the early appearance of trilobites in the Phanerozoic record, this is compatible with the general evolutionary trend of biomineralisation. This began with a brief use of calcium phosphate in the Tommotian followed by a change to carbonate; first LMC, then HMC, until today the majority of marine organisms use A (Wilkinson 1979; Lowenstam 1981; Lowenstam and Weiner 1983).

2.7. REFERENCES

ALDRIDGE, R. J. 1986. Conodont palaeobiogeography and thermal maturation in the Caledonides. J. geol. Soc. Lond. 143, 177-184.

ARTHUR, M. A., ANDERSON, T. F., KAPLAN, I. R., VEIZER, J. and LAND, L. S. (eds.). 1983. Stable isotopes in sedimentary geology 435pp. Soc. econ. Paleont. Miner. Short Course 10, Dallas.

BATHURST, R. G. C. 1975. Carbonate sediments and their diagenesis (2nd ed.). xix + 658pp. Elsevier, Amsterdam.

DALINGWATER, J. E. 1973. Trilobite cuticle microstructure and composition. Palaeontology, 16, 827-839, pls. 107-109.

DALINGWATER, J. E. and MILLER, J. 1977. The laminae and cuticular organisation of the trilobite Asaphus raniceps. Palaeontology, 20, 21-32, pls. 9-10.

DICKSON, J. A. D. 1966. Carbonate identification and genesis as revealed by staining. J. sedim. Petrol. 12, 133-149.

DZIK, J. and LENDZION, K. 1988. The oldest arthropods of the East European Platform. Lethaia, 21, 29-38.

FRYKMAN, P. 1986. Diagenesis of Silurian bioherms in the Klinteberg Formation, Gotland, Sweden. In SHROEDER, J. A. and PURSER, B. H. (eds.). Reef diagenesis 399-423pp. Springer-Verlag, Berlin, Heidelberg, New York.

HOEFS, J. 1980. Stable isotope geochemistry (2nd ed.). xii + 208pp. Springer-Verlag, Berlin, Heidelberg, New York.

HUDSON, J. D. 1962. Pseudo-pleochroic calcite in recrystallised shell-limestones. Geol. Mag. 99, 492-500.

LOHMANN, K. C. and MEYERS, W. J. 1977. Microdolomite inclusions in cloudy prismatic calcites: a proposed criterion for former high-magnesian calcites. J. sedim. Petrol. 47, 1078-1088.

LOWENSTAM, H. A. 1961. Mineralogy, $^{18}O/^{16}O$ ratios, and strontium and magnesium contents of Recent and fossil brachiopods and their bearing on the history of the oceans. J. Geol. 69, 241-260.

LOWENSTAM, H. A. 1981. Minerals formed by organisms. Science, N. Y. 211, 1126-1131.

LOWENSTAM, H. A. and WEINER, S. 1983. Mineralization by organisms and the evolution of biomineralization. In WESTBROEK, P. and De JONG, E. W. (eds.). Biomineralization and biological metal accumulation, 191-203. D. Reidel, Dordrecht, Holland.

McCREA, J. M. 1950. On the isotopic chemistry of carbonates and a paleotemperature scale. J. chem. Phys. 18, 849-857.

MILLER, J. 1976. The sensory fields and mode of life of Phacops rana (Green 1832) (Trilobita). Trans. R. Soc. Edinb. 69, 337-367, pls. 1-4.

MILLER, J. and CLARKSON, E. N. K. 1980. The post-ecdysial development of the cuticle and the eye of the Devonian trilobite Phacops rana milleri Stewart, 1927. Phil. Trans. R. Soc. Ser. B, 288, 461-480, pls. 1-7.

MILLIMAN, J. D. 1974. Recent sedimentary carbonates, Part 1: marine carbonates. xv + 375pp. Springer-Verlag, Berlin, Heidelberg, New York.

MORRISON, J. O. and BRAND, U. 1987. Geochemistry of Recent marine invertebrates. Geoscience Canada, 13, 237-254.

MUTVEI, H. 1981. Exoskeletal structure in the Ordovician trilobite Flexicalymene. Lethaia, 14, 225-234.

POPP, B. N., ANDERSON, T. F. and SANDBERG, P. A. 1986. Brachiopods as indicators of original isotopic compositions in some Paleozoic limestones. Bull. geol. Soc. Am. 97, 1262-1269.

RATCLIFFE, K. T. 1987. Sedimentology, palaeontology and diagenesis of the Much Wenlock Limestone Formation. Ph.D. thesis (unpubl.), Aston University.

RICHARDS, A. G. 1951. The integument of arthropods. xvi + 411pp. University of Minnesota Press, Minneapolis.

RICHTER, D. K. and FÜCHTBAUER, H. 1978. Ferroan calcite replacement indicates former high-magnesian calcite skeletons. Sedimentology, 25, 843-860.

STØRMER, L. 1980. Sculpture and microstructure of the exoskeleton in chasmopinid and phacopid trilobites. Palaeontology, 23, 237-271, pls. 25-34.

TEIGLER, D. J. and TOWE, K. M. 1975. Microstructure and composition of the trilobite exoskeleton. Fossils Strata, 4, 137-149, pls. 1-9.

THOMAS, A. T. 1978. British Wenlock trilobites (Part 1). Palaeontogr. Soc. [Monogr.], 1, 1-56, pls. 1-14.

TOWE, K. M. 1973. Trilobite eyes: calcified lenses in vivo. Science, N.Y. 179, 1007-1009.

VEIZER, J. 1974. Chemical diagenesis of belemnite shells and possible consequences for paleotemperature determinations. Neues Jb. Geol. Paläont. Abh. 147, 91-111.

WALTER, L. M. 1985. Relative reactivity of skeletal carbonates during dissolution: implications for diagenesis. In SCHNEIDERMANN, N. and HARRIS, P. M. (eds.). Carbonate cements 3-16. Soc. econ. Paleont. Miner. Sp. Pub. 36, Tulsa, Oklahoma.

WHITTINGTON, H. B. 1977. The Middle Cambrian trilobite Naraoia, Burgess Shale, British Columbia. Phil. Trans. R. Soc. Ser. B, 280, 409-443.

WHITTINGTON H. B. 1985. Tegopelte gigas, a second soft-bodied trilobite from the Burgess Shale, Middle Cambrian, British Columbia. J. Paleont. 59, 1251-1274.

WILKINSON, B. 1979. Biomineralization, paleo-oceanography and the evolution of calcareous marine organisms. Geology, 7, 524-527.

WOLF, K. H., CHILLINGAR, G. V. and BEALES, F. W. 1976. Elemental composition of carbonate skeletons, minerals and sediments. In CHILLINGAR, G. V., BISSELL, H. J. and FAIRBRIDGE, R. W. (eds.). Carbonate rocks: Physical and chemical aspects. 23-149. Elsevier, Amsterdam.

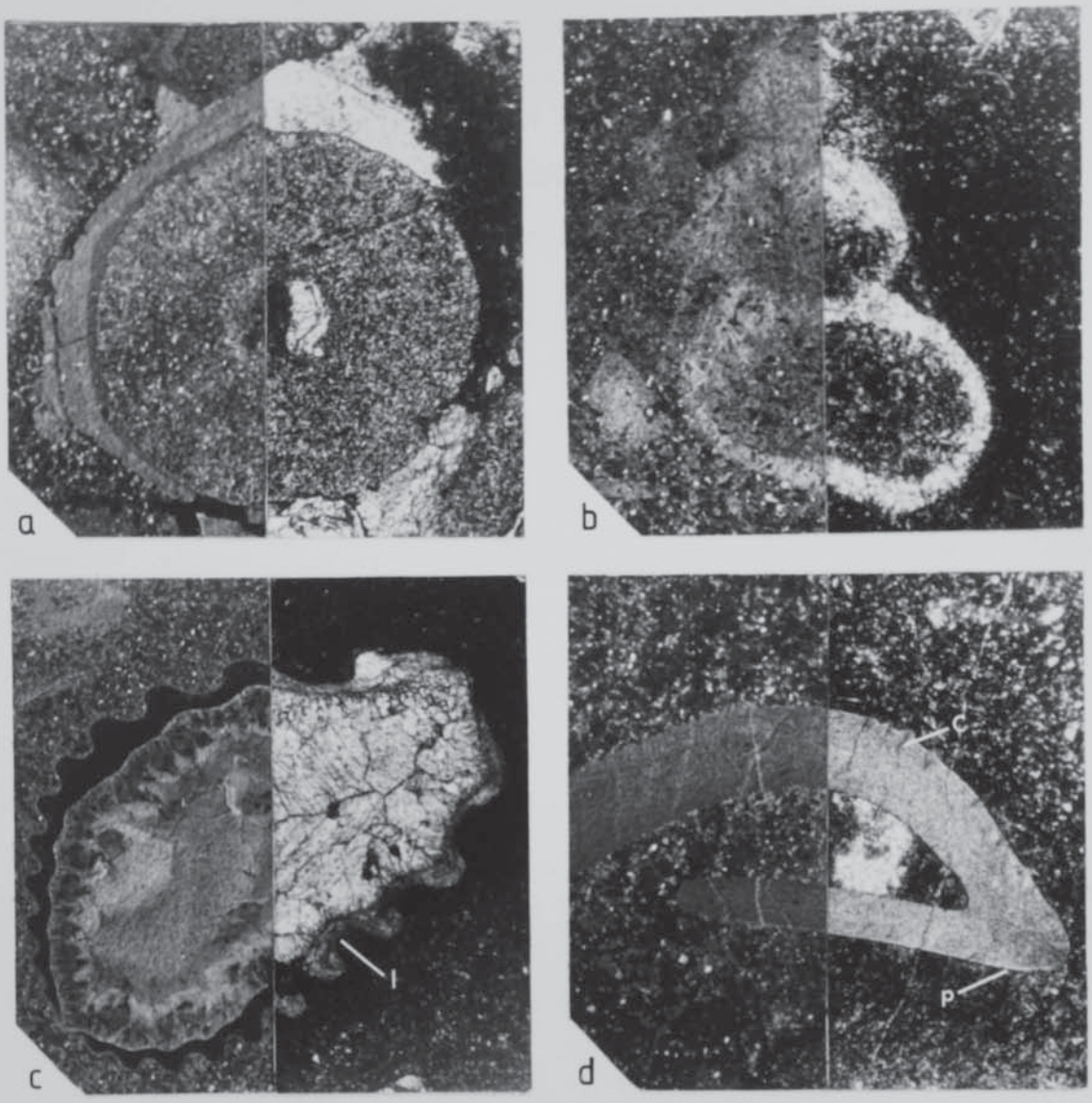

Plate 2.1. Composite photomicrographs of fossils from the Much Wenlock Limestone Formation.

In each case, the left hand side is taken under cathodoluminescence (CL) and the right hand side under plane polarised light (PPL). a, crinoid ossicle, NMW 88.22G.1. originally HMC, now with syntaxial overgrowth. Internally the ossicle has become coarsely crystalline, and under CL, small bright points mark the positions of microdolomites which formed during the conversion to LMC. x 25. b, gastropod, NMW 88.22G.2. originally A which has now been totally replaced by a coarse, clear, void-filling cement. x 30. c, strongly ribbed brachiopod, NMW 88.22G.2. primary LMC retaining its original structure of fine laminations (l). Under CL the brachiopod is non-luminescent and contains no microdolomite inclusions unlike the surrounding matrix. x 30. d, trilobite cuticle, NMW 88.22G.2. with thin, outer prismatic layer (p), and fine canals (c) within small tubercles, still visible under PPL. Under CL the exoskeleton is weakly luminescent, a function of its trace element content, but no microdolomites are present. x 40.

CHAPTER 3

PRESERVATION OF TRILOBITE EXOSKELETONS

ABSTRACT. Trilobite exoskeletons, despite having had a common original mineralogy, exhibit a variety of preservational textures which are related to the different diagenetic realms through which they have passed. These alterations of the cuticle can either destroy or enhance primary microstructures, and their effects are best observed in thin-sections, both under transmitted light and cathodoluminescence. The various features observed, and the processes that generated them, are discussed. Large borings, micritisation, mechanical breakage, and dissolution damage exoskeletons; whereas some types of replacement, such as silicification preserve fine structural details. Pyrite quite commonly infills canals and highlights their positions. Variations in luminescence across trilobite cuticles, such as bright prismatic layers and dark central zones do not reflect primary differences in composition, but are diagenetic effects related to trace element content.

3.1. Introduction

TYPICALLY, well preserved trilobite exoskeleton comprises a thin, outermost prismatic layer, overlying a thicker principal layer. The principal layer may contain laminations parallel to the surface, and the whole cuticle may be pierced by canals of various sizes. Trilobite exoskeletons also have a characteristic sweeping extinction pattern

(Chapter 4) under crossed polars (Dalingwater 1973; Teigler and Towe 1975; Miller 1976).

The ways in which trilobite cuticles are preserved are determined by their original composition and subsequent diagenetic history. Although all heavily mineralised trilobite exoskeletons were constructed from low-magnesian calcite (LMC) (Chapter 2), they still exhibit a variety of preservational textures which may either enhance or destroy original microstructures. The type of feature found reflects the diagenetic environments through which the exoskeleton has passed, and often more than one process can be seen to have operated on the same cuticle.

Recognition of diagenetic effects is vital when interpreting structure: some features can resemble primary microstructures leading to misinterpretation. For example Størmer (1980) mistook a fine overgrowth on one specimen of Phacops granulatus for the prismatic layer, which had considerable implications when interpreting the function of the underlying Osmolska cavities (Chapter 4). Miller (1972, 1976), and Dalingwater (1975) briefly discussed preservational effects on trilobite exoskeletons. In this paper, their observations have been expanded and related to diagenetic processes that are now better understood.

In general, trilobite exoskeletons retain the most primary structure in fine-grained limestones or calcareous mudstones. They have a dark tan to almost black colour in hand specimen, often with a pearly lustre. The colouration is partly due to the remains of the organic matrix which surrounded the constituent calcite crystals. The more oxidised the organic matter, the darker it will be. Colouration is an

indicator of depth of burial for conodont elements (Epstein et al. 1977; Rejebian et al. 1988). However the relationship is more complex in trilobites. Heating trilobite specimens as described for conodont elements (Epstein et al. 1977) produces colour changes, but not similar to any found naturally. The external surface becomes increasingly paler, eventually turning white due to the conversion from calcium carbonate to calcium oxide. However in thin-section the cuticles are seen to become progressively darker brown in colour with increasing temperatures. Pyrite within the cuticle may also darken its appearance, and the presence of this mineral may be difficult to determine except in thin-section. Pyrite darkening is common in trilobites from the Much Wenlock Limestone Formation, Wren's Nest, Dudley (Plate 3.1b).

Although details of internal primary microstructures are generally lost during diagenesis, sometimes the external surfaces of the cuticles may remain well preserved, for example Homagnostus obesus from the Middle Cambrian of Sweden (Chapter 6), which retains primary sculptural features only a few microns in diameter.

The different effects of diagenetic processes operating on trilobite cuticles are most clearly seen when examining thin-sections, both under transmitted light and cathodoluminescence (CL). The range of textures that may be found within exoskeletons, and the diagenetic environments they formed under, are described below.

3.2. Large borings

Attack of the exoskeleton by boring organisms destroys the primary structure of the cuticle. Such bioerosion indicates that the exoskeleton lay on or near the sediment surface for some time before

deeper burial. Although not very common, the borings are recognised by their relatively large size in comparison to primary structures such as canals, and their cross-cutting nature (Plate 3.1a-c). Dalingwater (1975) discussed small borings in trilobite cuticles which fell in two main size groups; 1-4μm and 6-10μm. These are probably caused by the actions of fungi and blue-green algae respsectively (Bathurst 1966). However, other much larger borings may also occur (Plate 3.1c, Plate 3.2d) which may have been produced by molluscs or sponges (Bathurst 1975).

3.3. Micritisation

Micrite envelopes may form around trilobite cuticles and are a more typical type of biological attack. They are produced by the action of boring blue-green algae, fungi, or bacteria (Bathurst 1966) which act in the stagnant marine phreatic realm (Longman 1980) or on the sediment surface (Bathurst 1966, 1975). The fine borings these organisms create are infilled by micrite deposited as a carbonate mud, which forms an irregular external rind to the cuticle (Plate 3.1a). During this process of micritisation, surface structures such as tubercles and small-scale terrace ridges may be obliterated.

Micritisation occurs more commonly along primary canals within the trilobite exoskeleton thus highlighting their positions, especially under plane polarised light (PPL). This is frequently seen in trilobites from the Much Wenlock Limestone Formation of England (Plate 3.1d) . It appears that larger canals were preferentially affected in this way, rather than the more numerous pore canals, presumably because access was easier for the boring organisms. Although the primary canals

now appear two to four times wider than they were originally. their orientation through the exoskeleton is clearly revealed.

3.4. Mechanical damage

This can include injuries sustained while the animal was still alive, such as those resulting from complications during moulting (Šnajdr 1978; Owen 1983), or predatory attack (Alpert and Moore 1975; Ludvigsen 1977; Rudkin 1979; Šnajdr 1981). Most trilobites are not preserved as complete specimens but in fragments. Many are moults rather than dead individuals, but disarticulation in both is usually thought to indicate some degree of transport such as disturbance from currents. However, experiments with tumble barrels have shown that freshly killed arthropods (both soft-bodied and those with mineralised exoskeletons) are quite durable to mechanical damage (Allison 1986), and in fact, abrasion of trilobite cuticles is very rare. Disarticulation is more likely to occur soon after shallow burial, due to the decomposition of the soft parts by bacteria and fungi, enhanced by bioturbation and scavenging (Plotnick 1986). Apart from disarticulation, post-mortem damage is most commonly due to fracturing caused by compaction of the sediment, involving loss of structural detail from the cuticle.

3.5. Dissolution

Trilobite exoskeletons from arenaceous and argillaceous sediments are commonly preserved as moulds, probably because pore fluids generated in these sediments tended to be undersaturated in calcium carbonate and totally dissolved the cuticles. Although moulds of trilobite cuticles in shales tend to be flattened and distorted, counterparts of

exoskeletons from limestones may retain fine details of surface cuticular microstructure that can be examined with a scanning electron microscope (Chapter 6).

Trilobite exoskeletons may be damaged by solution processes (Plate 3.1c) operating in the freshwater vadose and phreatic environments (Longman 1980). As meteoric waters undersaturated in calcium carbonate percolate through the pore spaces, they dissolve the carbonate components of the rock to reach equilibrium. The resulting secondary voids may later be infilled by cements. This is very rare for LMC trilobites compared with other organisms such as gastropods and crinoid ossicles, which were composed respectively of the more unstable A and HMC.

3.6. Replacement

3.6a. Ionic substitution within the crystal lattice. Ions with the same charge and a similar size to the calcium ion may substitute for it within calcium carbonate. The type of ion incorporated also depends on the structure of the crystal lattice. The most common ions to be substituted in calcite are Mg^{2+} and Fe^{2+}, and their presence is readily detected by staining (Chapter 1). Sr^{2+} can be substituted in aragonite in large quantities (Kinsman 1969); up to 10,000 ppm in inorganically precipitated aragonite (Scoffin 1987) and even more in biologically secreted aragonite constructed by organisms exerting a 'vital effect'.

High Sr^{2+} levels, greater than those in inorganically precipitated aragonite have been detected from trilobite cuticles from the Much Wenlock Limestone Formation (Appendix 1). This could be taken to suggest that trilobites secreted aragonitic exoskeletons, and/or had a

strong vital effect (but see Chapter 2). However, similar Sr^{2+} concentrations were also obtained from the surrounding matrix, indicating whole rock equilibration with strontium-rich pore fluids during diagenesis. These are very likely to have originated from nearby mudstones (see Ratcliffe 1987 for a detailed discussion of the diagenesis of the Much Wenlock Limestone Formation).

Trilobite exoskeletons were originally composed of LMC, with less than 5% $MgCO_3$. Dolomitised trilobite cuticles have not been encountered in this study, but replacement by ferroan calcite may sometimes occur; for example, trilobites from the ferruginous crinoidal grainstone lithofacies of the Much Wenlock Limestone Formation (Ratcliffe 1987). In some cases, staining reveals only partial replacement, such as Calymene from the Mulde Beds of Gotland (Wenlock) (Plate 3.2a, b).

McKerrow et al. (1956) analysed the rare earth element content of trilobites from several locations, and found them to be enriched in caesium. There was no consistency in the concentrations found between species or localities. However, no mention was made of the preservational state of the fossils, nor any information about the surrounding matrix, and the enrichment is probably a diagenetic effect. In any event, enrichment in caesium is not unexpected as this is also an ion that can substitute within the calcite lattice.

Trace element content affects the luminescence characteristics of minerals. Cathodoluminescence effects in carbonates (Sippel and Glover 1965) are thought to be controlled primarily by the relative concentrations of Mn^{2+} and Fe^{2+} ions present; Mn^{2+} activating luminescence and Fe^{2+} quenching it (see review by Fairchild 1983). However the processes involved are still only partially understood, as

some carbonates with the same Fe^{2+}/Mn^{2+} chemistry have been found to have different luminescence characteristics (R. Mason pers. comm.). Other factors must also be involved, such as other minor or trace elements, and lattice distortions.

Trilobite cuticles, being composed of LMC, tend to have luminescence colours ranging from pale yellow to orange yellow. Whether or not the cuticle stands out from the surrounding rock depends on any relative difference between their luminescence properties. Sometimes cuticles cannot be distinguished, but usually the general shape is apparent as an area of somewhat brighter luminescence. Cathodoluminescence has been used previously on trilobite exoskeletons to enhance primary structure and indicate the degree of recrystallisation that has occurred (Miller and Clarkson 1980).

Internal structures, such as canals that were visible under plane-polarised light (PPL), tend to disappear under CL, for example in Wenlock trilobites from Britain and Gotland, indicating that the infilling micrite has the same trace element content as the cuticles.

Luminescence variations sometimes occur within a single exoskeleton, such as darker central zones, and brighter prismatic layers. Dark central zones are areas of little or no luminescence that tend to occur in thicker trilobite cuticles, such as the Wenlock trilobites Calymene (Plate 3.1e), Dalmanites, and Encrinurus. Their occurrence is not always uniform along the length of the cuticle. When this is the case, they are most common in the thicker parts, suggesting a diagenetic origin. This is further supported by some partially ferroan exoskeletons from Gotland, where areas of luminescence along canals and outer surfaces correspond to ferroan calcite. Although most

often seen with CL, dark central zones may be also be seen under PPL (Plate 3.2f), and seem to correspond to the "central laminate zone" of Dalingwater and Miller (1977); that is, the diagenetic effect is concentrated in this area.

Occasionally the prismatic layer may have a much brighter luminescence than the rest of the cuticle (Plate 3.1e). However, in some specimens of Phacops rana from the Devonian of New York, both borders of the cuticle were brighter (Plate 3.1f), or the brightly luminescent zone was twice as thick as the actual prismatic layer; all indicating that this is a diagenetic effect rather than reflecting a primary difference in composition between the prismatic and principal layers. The fact that the prismatic layer is most often affected is probably due to its crystal arrangement.

As with other limestones, carbonate cements and neomorphic spars associated with trilobite cuticles may be highlighted by CL (Plate 3.2f). The type of cement associated with the exoskeletons is related to the diagenetic environment in which it formed, rather than being controlled by the structure of the trilobite fragment (Fig. 3.1). For example, bladed cements (Plate 3.2d) form in the phreatic zone.

3.6b. Neomorphism: change in crystal form. Trilobite exoskeletons occurring in limestones are quite commonly recrystallised to neomorphic LMC, with the obliteration of primary microstructures (Plate 3.2c, e, f). See Bathurst (1975) for petrographic criteria that can be used to discriminate between neomorphic spars and cements.

Neomorphism involves ion-exchange across a thin-film migrating solution front. Cuticular calcite is dissolved on one side of the front

FIGURE 3.1. Diagenetic processes affecting trilobite cuticles.

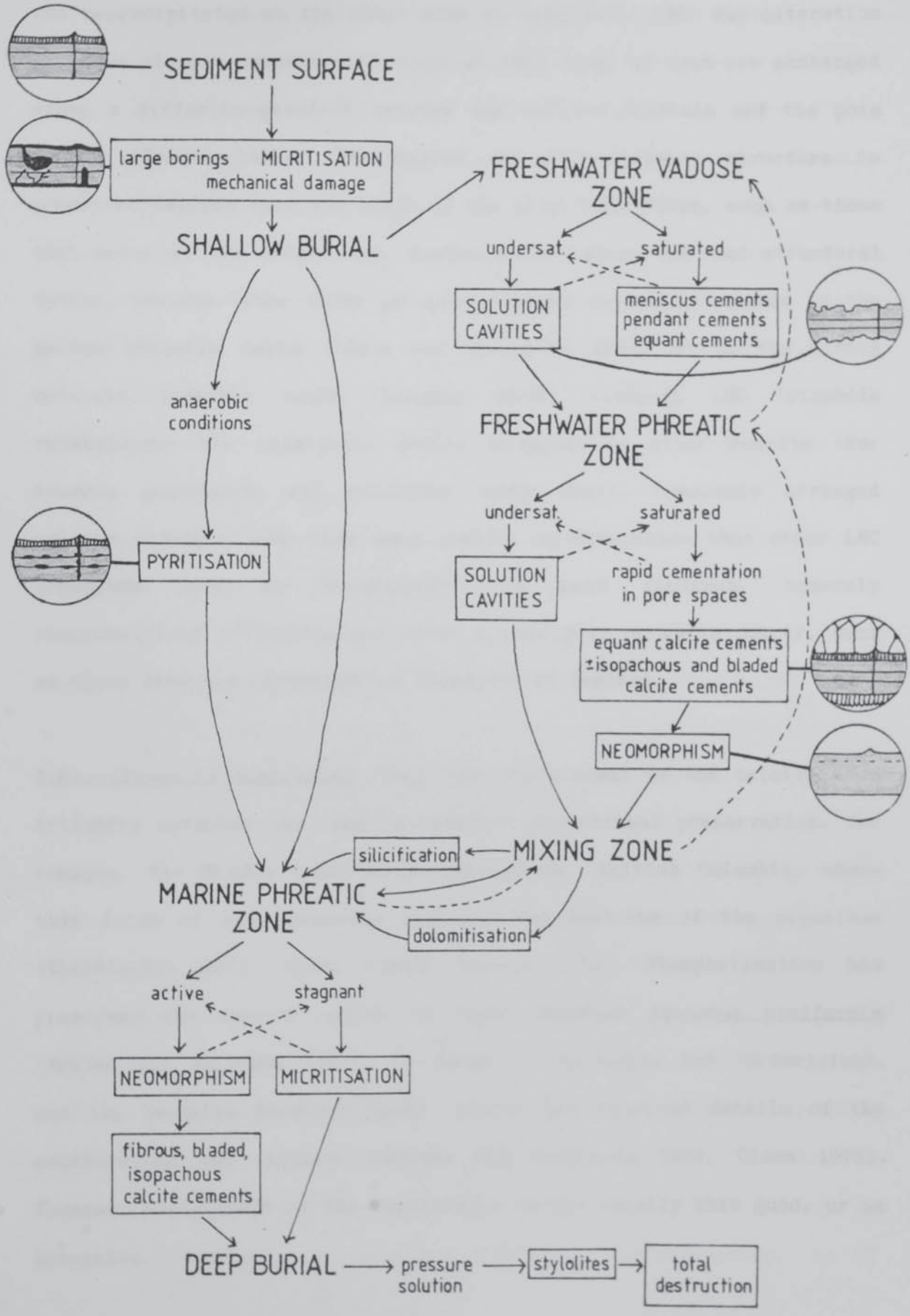

and reprecipitated on the other side as diagenetic LMC. Any alteration in trace element content will occur at this time, as ions are exchanged along a diffusion gradient between the calcite crystals and the pore fluids (Veizer 1983). The degree to which primary structure is preserved depends upon the width of the film. Thin films, such as those that occur in the vadose zone (Leeder 1982) retain the most structural detail, whereas wider films generate coarser crystals, usually in the marine phreatic realm (James and Choquette 1984) or in the active meteoric phreatic realm (Longman 1980). Although LMC trilobite exoskeletons are relatively stable compared to other fossils (for example gastropods and crinoids) their small, complexly arranged calcite crystals make them more subject to alteration than other LMC organisms such as brachiopods. In hand specimen, coarsely recrystallised trilobites are often a pale grey or white colour, such as those from the Carboniferous Limestone of England.

3.6c. Change in mineralogy. Very fine replacement of the calcite from trilobite cuticles can lead to cases of exceptional preservation, for example, the Middle Cambrian Burgess Shale, British Columbia, where thin films of clay minerals preserve the features of the organisms (Whittington 1971, 1975; Conway Morris 1979). Phosphatisation has preserved the ventral organs of Upper Cambrian Agnostus pisiformis (Müller and Walossek 1987). In Beecher's Trilobite Bed (Ordovician), and the Devonian Hunsrück Shale, pyrite has retained details of the exoskeletons and viscera (Stürmer and Bergström 1973; Cisne 1975). However, replacement of the exoskeleton is not usually this good, or as extensive.

Pyrite may commonly occur within trilobite cuticles along laminae or infilling canals, and can be useful in highlighting their positions when seen in thin-section (Plate 3.1b). It tends to form during bacterial decomposition of organic matter under anaerobic conditions (Curtis and Spears 1968; Goldhaber and Kaplan 1974), and therefore implies the former existence of organic membranes and setae. Certain trilobites from the Wenlock of England and Gotland have canals filled with both pyrite and micrite, indicating a variety of microenvironments within the cuticle, some aerobic, others not.

Cuticles may also be silicified, preserving fine surface structural detail, examples of which can be seen from the Middle Ordovician Edinburg Limestone (Whittington and Evitt 1954). Here, small specimens up to 1 or 2cm long are well preserved whereas larger specimens are only partially silicified. In some specimens of Flexicalymene larger canals may be preserved as silicified tubes running between the dorsal and ventral cuticle surfaces (Evitt and Whittington 1953). Silicification occurs when pore fluids are undersaturated in calcium carbonate, but supersaturated with regard to silica. This may be the case at the mixing zone between meteoric phreatic and marine phreatic waters (Knauth 1979). The silicification process does not appear to be related to the original composition of the fossils; trilobites, ostracodes, and bryozoans tend to be replaced, but both brachiopods (constructed from LMC) and echinoids (originally HMC) are only poorly silicified (Whittington and Evitt 1954; Chatterton and Ludvigsen 1976). Silicification may therefore be related to the sizes of the individual components, as in certain examples of phosphatisation (Fortey and Morris 1978; Müller and Valossek 1987), or alternatively, to the

original amount of organic matter present. Decay of the organisms would have released carbon dioxide which locally affected the solubility of calcite and the precipitation of silica (Knauth 1979).

3.7. REFERENCES

ALLISON, P. A. 1986. Soft-bodied animals in the fossil record: the role of decay in fragmentation during transport. Geology, 14, 979-981.

ALPERT, S. P. and MOORE, J. N. 1975. Lower Cambrian trace fossil evidence for predation on trilobites. Lethaia, 8, 222-230.

BATHURST, R. G. C. 1966. Boring algae, micrite envelopes and lithification of molluscan biosparites. Geol. J. 5, 15-32.

BATHURST, R. G. C. 1975. Carbonate sediments and their diagenesis (second edition) xix + 658pp. Elsevier Scientific Publishing Company, Amsterdam.

CHATTERTON, B. D. E. and LUDVIGSEN, R. 1976. Silicified Middle Ordovician trilobites from the South Nahanni River area, District of Mackenzie, Canada. Palaeontographica Abt. A, 154, Lfg.1-3, 1-109, pl.1-22.

CISNE, J. L. 1975. Anatomy of Triarthrus and the relationships of the Trilobita. Fossils Strata 4, 45-63, pls. 1-2.

CONWAY MORRIS, S. 1979. The Burgess Shale (Middle Cambrian) fauna. Ann. Rev. Ecol. Syst. 10, 327-349.

CURTIS, C. D. and SPEARS, D. A. 1968. The formation of sedimentary iron minerals. Econ. Geol. 63, 257-270.

DALINGWATER, J. E. 1973. Trilobite cuticular microstructure and composition. Palaeontology, 16, 827-839, pls.107-109.

DALINGWATER, J. E. 1975. Secondary microstructures in trilobite cuticles. Fossils Strata, 4, 151-154, pl.1.

DALINGWATER, J. E. amd MILLER, J. 1977. The laminae and cuticular organisation of the trilobite Asaphus raniceps. Palaeontology, 20, 21-32, pls.9-10.

EPSTEIN, A. G., EPSTEIN, J. B. and HARRIS, L. D. 1977. Conodont colour alteration - an index to organic metamorphism. Prof. Pap. U.S. geol. Surv., 995, 27pp.

EVITT, W. R. and WHITTINGTON, H. B. 1953. The exoskeleton of Flexicalymene (Trilobita). J. Paleont. 27, 49-55, pls.9-10.

FAIRCHILD, I. J. 1983. Chemical controls of cathodoluminescence of natural dolomites and calcites: new data and review. Sedimentology 30. 579-583.

FORTEY, R. A. and MORRIS, S. F. 1978. Discovery of nauplius-like trilobite larvae. Palaeontology 21, 823-833, pl.94.

GOLDHABER, M. B. and KAPLAN, I. R. 1974. The sulfur cycle. In GOLDBERG, E. D. (ed.). The sea, Volume 5, Marine chemistry. 569-655. Wiley (Interscience), London.

JAMES, N. P. and CHOQUETTE, P. W. 1984. Diagenesis 6: The sea-floor diagenetic environment. Geoscience Canada, 10, 162-179.

KINSMAN, D. J. J. 1969. Interpretation of Sr^{2+} concentrations in carbonate minerals and rocks. J. sedim. Petrol. 39, 486-508.

KNAUTH, L. P. 1979. A model for the origin of chert in limestone. Geology, 7, 247-277.

LEEDER, M. R. 1982. Sedimentology: process and product. xv + 344pp. George Allen and Unwin, London.

LUDVIGSEN, R. 1977. Rapid repair of traumatic injury by an Ordovician trilobite. Lethaia, 10, 205-207.

LONGMAN, M. W. 1980. Carbonate diagenetic textures from nearshore diagenetic environments. Bull. Am. Ass. Petrol. Geol. 64, 461-487.

McKERROW, W. S., TAYLOR, S. R., BLACKBURN, A. L. and AHRENS, L. H. 1956. Rare alkali elements in trilobites. Geol. Mag. 93, 504-516.

MILLER, J. 1972. Aspects of the biology and palaeoecology of trilobites. Ph.D. thesis (unpubl.), University of Manchester.

MILLER, J. 1976. The sensory fields and life mode of Phacops rana (Green, 1832) (Trilobita). Trans. R. Soc. Edinb. 69, 337-367, pls.1-4.

MILLER, J. and CLARKSON, E. N. K. 1980. The post-ecdysial development of the cuticle and the eye of the Devonian trilobite Phacops rana milleri Stewart 1927. Phil. Trans. R. Soc. Ser.B, 288, 461-480, pls. 1-7.

MÜLLER, K. J. and WALOSSEK, D. 1987. Morphology, ontogeny, and life habit of Agnostus pisiformis from the Upper Cambrian of Sweden. Fossils Strata, 19, 1-124, pls. 1-33.

OWEN, A. W. 1983. Abnormal cephalic fringes in the Trinucleidae and Harpetidae (Trilobita). Sp. Pap. Palaeontolgy, 30, 241-247, pl.34.

PLOTNICK, R. E. 1986. Taphonomy of a modern shrimp: implications for the arthropod fossil record. Palaios, 1, 286-293.

RATCLIFFE, K. T. 1987. Sedimentology, palaeontology and diagenesis of the Much Wenlock Limestone Formation. Ph.D. thesis (unpubl.), Aston University.

REJEBIAN, V. A., HARRIS, A. G. and HUEBNER, J. S. 1987. Conodont color and textural alteration: an index to regional metamorphism, contact

metamorphism, and hydrothermal alteration. Bull. geol. Soc. Am., 99, 471-479.

RUDKIN, D. M. 1979. Healed injuries in Ogygopsis klotzi (Trilobita) from the Middle Cambrian of British Colunbia. Life Sci. Occ. Pap. R. Ontario Mus. 32.

SCOFFIN. T. P. 1987. An introduction to carbonate sediments and rocks. ix + 274pp. Blackie, Glasgow and London.

SIPPEL, R. F. and GLOVER, E. D. 1965. Structures made visible by luminescence petrography. Science N. Y. 150, 1283-1287.

ŠNAJDR, M. 1978. Anomalous carapaces of Bohemian paradoxid trilobites. Sb. geol. ved. Paleontologie. 20, 1-31, pls.1-8.

ŠNAJDR, M. 1981. Bohemian Proetidae with malformed exoskeletons. Sb. geol. ved. Paleontologie. 24, 37-61, pls.1-8.

STØRMER, L. 1980. Sculpture and microstructure of the exoskeleton in chasmopinid and phacopid trilobites. Palaeontology, 23, 237-271, pls. 25-34.

STÜRMER, W. and BERGSTRÖM, J. 1973. New discoveries on trilobites by X-rays. Paläont. Z. 47, 1/2, 104-141.

TEIGLER, D. J. and TOWE, K. M. 1975. Microstructure and composition of the trilobite exoskeleton. Fossils Strata, 4, 137-149, pls.1-9.

VEIZER, J. 1983. Chemical diagenesis of carbonates: theory and application of trace element technique. In ARTHUR, M. A., ANDERSON, T. F., KAPLAN, I. R., VEIZER, J. and LAND, L. S. (eds.). Stable isotopes in sedimentary geology 3.1-100. Soc. econ. Paleont. Miner. Short Course 10, Dallas.

WHITTINGTON, H. B. 1971. The Burgess Shale: history of research and preservation of fossils. Proc. N. Am. Paleont. Conv., Chicago 1969. I, 1170-1201.

WHITTINGTON, H. B. 1975. Trilobites with appendages from the Middle Cambrian, Burgess Shale, British Columbia. Fossils Strata, 4, 97-136, pls.1-25.

WHITTINGTON, H. B. and EVITT, W. R. 1954. Silicified Middle Ordovician trilobites. Mem. geol. Soc. Am. 59, 1-135, pls.1-33.

Plate 3.1. Preservational features of trilobite cuticles.

a. Asaphus raniceps Dalman, Lower 'raniceps' Limestone, Öland (Llanvirn). (JED)O1.A.27.1. Borings (2-4μm diam.) through the cuticle, and thick micrite envelope (m). Figured by Dalingwater (1975) Pl. 1, fig. 6. x35.

b. Encrinurus punctatus (Wahlenberg), Much Wenlock Limestone Formation, Wren's Nest, Dudley (Wenlock). (JED)Dy.E.71. Pyrite-infilled borings (b) (1-4μm diam.) and canals (c) within the cuticle. Figured by Dalingwater (1975) Pl. 1, fig. 8. x70.

c. Asaphus sp. Asaphus Limestone, Norway (Ordovician). NV1. Large borings on visceral surface of the exoskeleton 30μm diam. Note also the fine laminations (l) within the principal layer, and the irregular external surfaces due to dissolution of the cuticle. x35.

d. Calymene sp. Much Wenlock Limestone Formation, Wren's Nest, Dudley (Wenlock). D10.1. Longitudinal section through cephalon revealing micrite-infilled canals. x35.

e. Calymene sp. Mulde Beds, Gotland (Wenlock). RCP6.2. Composite photomicrograph of a transverse section through a pygidium. Left hand side in PPL, right hand side under CL. Micrite infilled canals are clearly visible under PPL but fainter with CL. Under CL, a dark central zone is revealed, and a bright prismatic layer. x35.

f. Phacops rana crassituberculata Stumm. Silica Shale, Ohio (Middle Devonian). NE3.2. Longitudinal section through thorax, seen under CL. Note bright 'prismatic layer' on both the external (e) and visceral (v) surfaces of the cuticle. x50.

PLATE 3.1

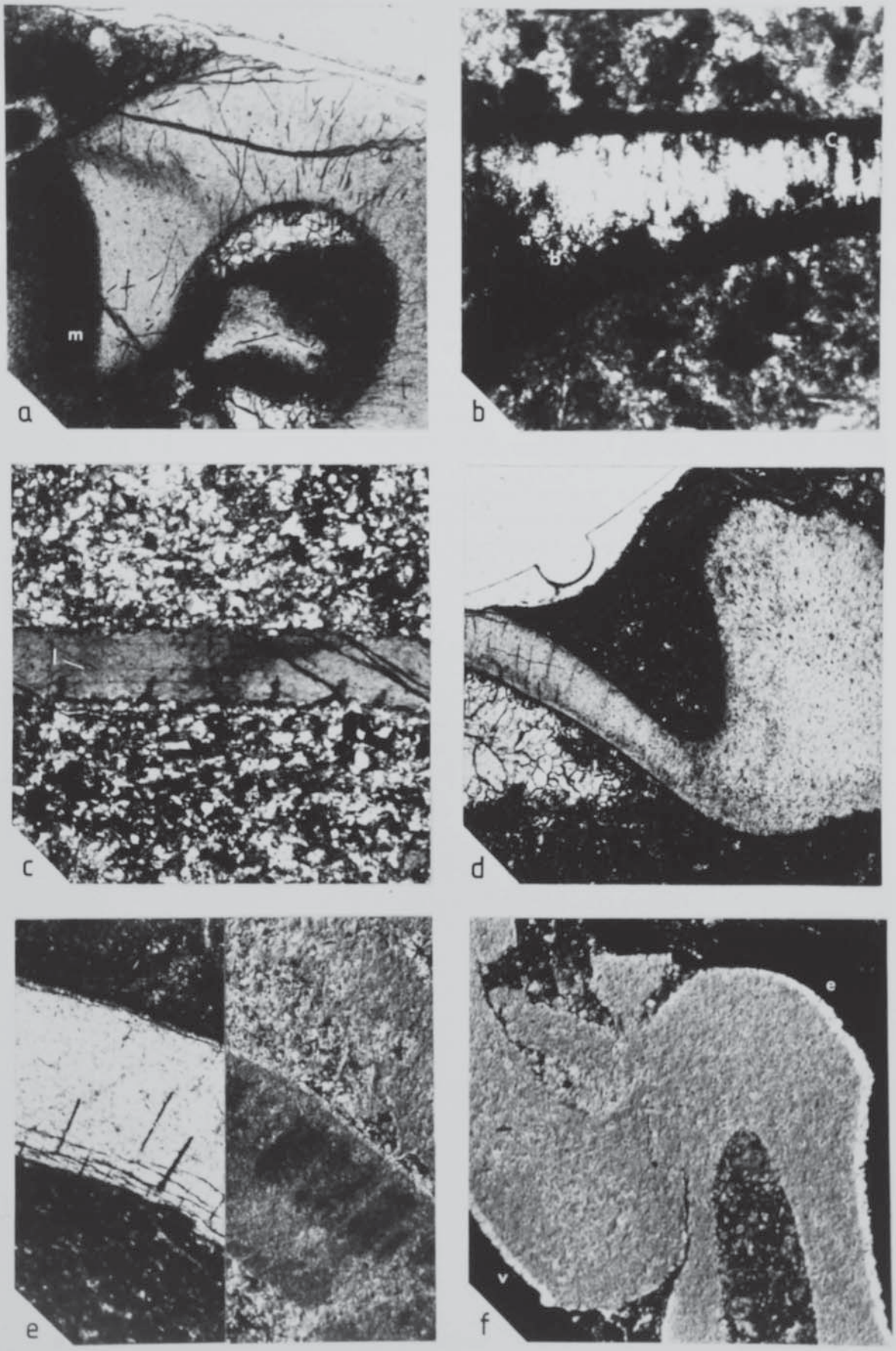

Plate 3.2. Diagenetic features of trilobite cuticles.

a. Calymene sp. Mulde Beds, Gotland (Wenlock). RCC2.1. Stained thin-section through a free cheek. The lighter, central area corresponds to low-magnesian calcite, whereas the darker, outer portions are composed of ferroan calcite. x35.

b. Calymene sp. Mulde Beds, Gotland (Wenlock). RCP6.4. Stained thin-section of a transverse section through a pygidium. Outer sections and remnants of canals are composed of ferroan calcite, whereas the lighter central zone remains calcite. x35.

c. Partially silicified trilobite, Edinburg Limestone, Virginia (Middle Ordovician). From Locality 6 of Whittington and Evitt (1954). NW15. Pale areas correspond to quartz crystals that have grown in from the margins. The remaining cuticle is still composed of calcite, albeit recrystallised. No primary canals are preserved. x70.

d. Section through a trilobite surrounded by a bladed calcite cement. Much Wenlock Limestone Formation, Wren's Nest, Dudley (Wenlock). R2.20.11. Note also the ridges with central canals (c) and a large boring (b). x50.

e. Bumastus? phrix Lane and Thomas. Dolyhir and Nash Scar Limestone Formation, Dolyhir Bridge [SO 2403 5825] (Wenlock). NW10. Thin-section through doublure, with a calcite isopachous rim cement on the prismatic layer. Note small terrace ridge, and finely recrystallised state of the cuticle. Irregular laminations in the exoskeleton are cracks produced when making the thin-section. x70.

f. Bumastus nudus (Angelin). Kullsberg Limestone, Sweden (Ashgill). NW7. Composite photomicrograph of a thin -section through the exoskeleton. Left hand side under PPL, right hand side under CL. The cuticle has a dark central zone both in PPL and CL, and is finely recrystallised. CL highlights the crystal boundaries of the surrounding neomorphic spar. x35.

PLATE 3.2

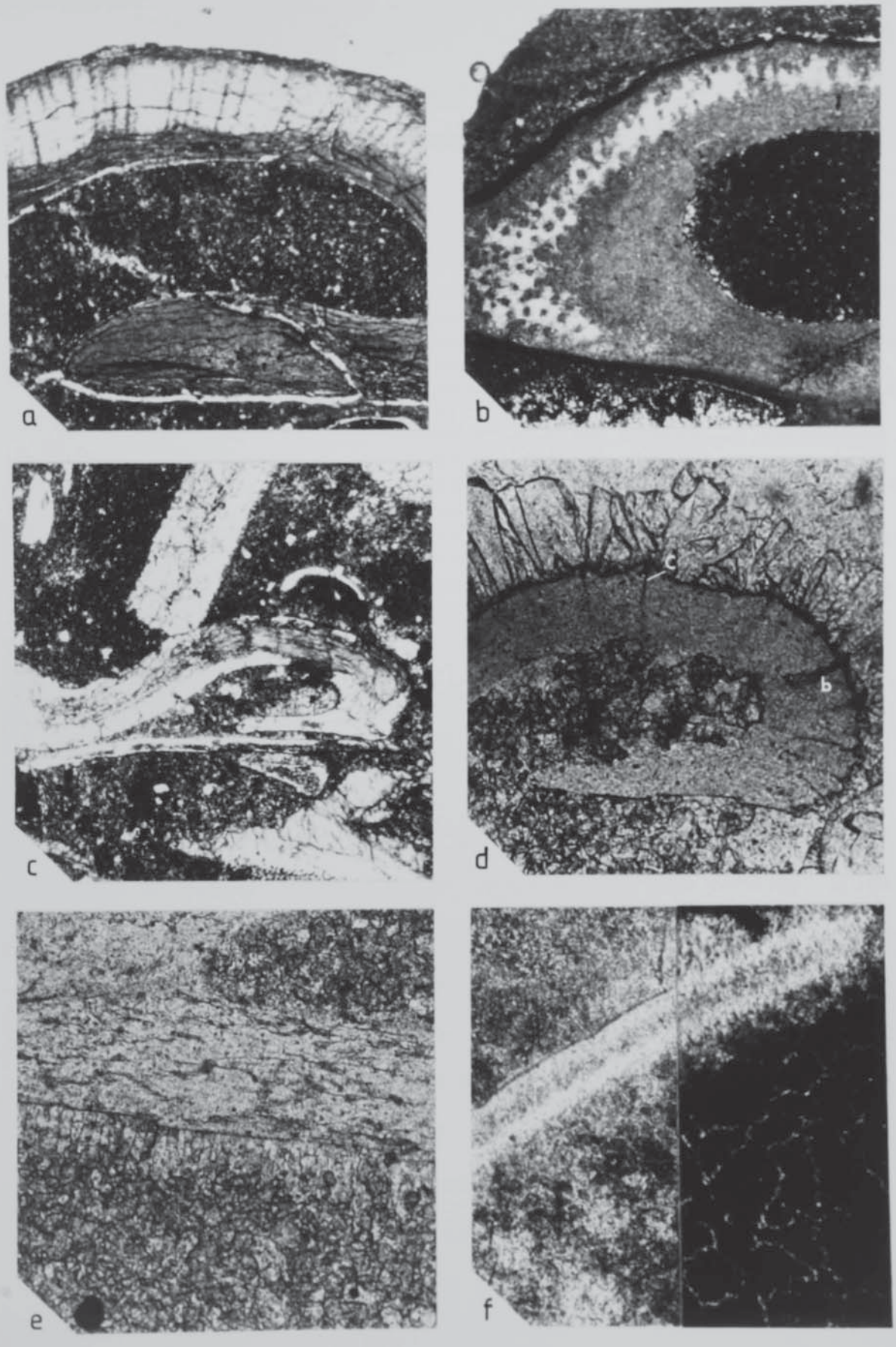

CHAPTER 4

TRILOBITE CUTICULAR MICROSTRUCTURES

ABSTRACT. The ultrastructure of trilobite exoskeletons resembles that of other arthropods in being divisible into three layers; an outer epicuticle (which is rarely preserved), and heavily calcified prismatic and principal layers that together form the procuticle. The procuticle is predominantly composed of calcite crystals orientated with their c-axes perpendicular to the surface, which gives rise to the characteristic sweeping extinction pattern seen under crossed polars. The absolute thickness of the cuticle, and the relative proportion made up of prismatic layer, varies between taxonomic groups.

Laminations and canals may be seen within the trilobite exoskeleton, in addition to surface microstructures such as reticulate patterns, pustules, and terrace ridges. Some of these features are involved in, or produced as a result of, processes of cuticle secretion. Others, especially the larger canals, and pustules, probably represent the sites of former sensory receptors. Knowledge of extant arthropod sense organs is reviewed and discussed in relation to trilobite exoskeletal features. Only a few trilobite cuticular microstructures can be allocated functions with any confidence; such as the Bileus glabellar 'tubercle', and socket pits, as the associated soft-part morphology is generally unknown. A short glossary of microstructural terms is also given.

4.1. TRILOBITE CUTICULAR ULTRASTRUCTURE.

TRILOBITE cuticle, like that of other arthropods, was divided into three units; an unmineralised external epicuticle, a calcified prismatic layer (equivalent to the exocuticle) and an inner calcified principal layer (analogous to the endocuticle) which formed the bulk of the exoskeleton (Mutvei 1981).

Until the late 1960's, trilobite exoskeletal microstructure was usually only briefly commented on within taxonomic descriptions (see review by Dalingwater 1973). Since then, only a few in-depth studies of trilobite cuticle have been published [such as Dalingwater (1973); Osmólska (1975); Teigler and Towe (1975); Miller (1975, 1976); Dalingwater and Miller (1977); Miller and Clarkson (1980); Størmer (1980); and Mutvei (1981)] because preservational effects commonly obscure fine structural details. Usually only the heavily mineralised procuticle which formed the exoskeleton is preserved. In the following sections, the ultrastructure and microstructures of trilobite cuticles are described.

4.1a. Epicuticle

As in other arthropods, the epicuticle was unmineralised and so is rarely preserved in trilobites. It may be represented by a brown residue of unknown composition left after decalcification in E.D.T.A. (Dalingwater 1973; Teigler and Towe 1975; Miller 1976; Dalingwater and Miller 1977). Its presence is also implied by the occurrence of apparently primary colour markings on exoskeletons. These would have been produced either by pigments in the epicuticle or by specialised organs within the procuticle. Colour markings that are distinct from

muscle attachment areas (Section 4.2f) have been described from several trilobites ranging in age from Cambrian to Permian. They are either in the form of dark bands (Raymond 1922; Wells 1942) or spots (Williams 1930; Teichert 1944; Esker 1968).

Esker (1968) suggested that variably-sized spots on Phacops and Greenops specimens were adaptations for camouflage, increasing or decreasing in diameter as necessary. However, re-examination of this material has indicated that at least some of the spots are of secondary origin.

The exoskeleton of Esker's specimen of Greenops boothi is covered by dark spots of variable size (up to 150μm diameter), which are arranged in rows on the thoracic segments (Plate 4.1a). The spots are associated with depressions on the dorsal surface of the cuticle, and on broken edges are seen to continue as vertical pillars through the exoskeleton (Plate 4.1b). Such large-scale penetrating structures are unlikely to have been primary features of the cuticle: no comparable structures have been identified from any other phacopide trilobites in thin-section, despite retention of fine primary canals only 1μm diameter. The large pillars appear to have a ferroan composition and are probably of diagenetic origin, perhaps infilling previously bored canals (see Chapter 3).

Two Phacops rana specimens from the same formation also have dark spots on their external surfaces, but these differ from those on G. boothi. The black spots are of variable size and distribution, but mainly concentrated on the pleurae and eyes (Plate 4.2). Although they appeared to lie only on the external surface, it was not possible to tell whether the spots continued through the cuticle. The spots lack

surface relief and occur in similar positions on both specimens. These facts suggest that the spots of Phacops rana may be primary structures. However if so, and if they do represent photosensitive pigments, it is unclear why they should also occur on the eye lenses: which would appear to interfere with their efficiency.

4.1b. Procuticle

This was predominantly composed of low-magnesian calcite crystals (Chapter 2) arranged with their c-axes perpendicular to the external surface (Teigler and Towe 1975). This is most noticeable in the prismatic layer as these crystals are the largest (average 1x10μm) (Plate 4.3b). The smaller crystals of the principal layer (average 0.5x1.5μm) show a parallel/subparallel alignment with the cuticle surface (Plate 4.3f) yet are still orientated with their c-axes at right-angles to the surface. It is this uniform crystallographic orientation which gives rise to the characteristic sweeping extinction pattern seen in well-preserved trilobite cuticles, observed on rotation of a light-microscope stage under crossed polars (Plate 4.3d). As the cuticle surface is curved, successive zones of crystals are in exinction at different times. The creation of a cuticle composed of calcite crystals in the same orientation is likely to be energetically more economical than constructing an exoskeleton with its component mineral crystallographic axes in a variety of directions. Organic matix surrounded each crystal and controlled growth (Krampitz et al. 1983), so generating elongations in the a-b plane whilst retaining a c-axis orientation perpendicular to the surface.

The absolute thickness of trilobite cuticle varies greatly through the class, from just 5-15μm in the agnostines to over 1mm in some phacopides (Appendix 3). Although fairly uniform for a particular specimen, cuticle thickness increases on various parts of the exoskeleton, for example across apodemes and the doublure, so for comparative purposes it is best to measure thickness from a constant position such as the glabella. In general, larger trilobites have thicker cuticles, and this is certainly true through ontogeny; smaller instars having thinner exoskeletons (Chapter 5). However some groups have characteristically thin exoskeletons for their overall size. The Olenidae have cuticle thicknesses of only 5-50μm, making them the trilobites with the relatively thinnest cuticles. Newly secreted cuticle is very thin, consisting mainly of prismatic layer with only a thin principal layer. However full thickness is quickly restored by growth of the principal layer (Miller and Clarkson 1980). Trilobites did not resorb any of their cuticle before moulting (Miller and Clarkson 1980; Mutvei 1981), resembling most calcified ostracodes in this respect (Rosenfeld 1979, 1982).

The relative proportion of prismatic layer in the cuticle also varies between groups, but usually falls between 5-20% of total procuticle thickness. The proportion of prismatic layer can be characteristic of a whole order, for example it forms 10% of cuticle thickness in the Proetida (Chapter 5). The thickness of prismatic layer and overall exoskeletal thickness will influence the mechanical properties of the cuticle (Chapter 7), and a certain combination may be an adaption to a particular mode of life. For example the very thin cuticles of olenids may reflect the reduced oxygen conditions and low

predation in the 'Olenid Sea' (Fortey 1985); whereas trilobites having relatively thick, tuberculate exoskeletons have been interpreted as living in turbulent shallow-water environments (Fortey 1979; Brezinski 1988).

4.2. MICROSTRUCTURES.

4.2a. Laminations

The organic matrix of trilobite exoskeletons is likely to have been a chitin-protein complex as in all other arthropods (Richards 1951). As horizontal laminations have been observed in the principal layer of trilobite cuticles (Plate 4.3b, c), it is also probable that the chitin fibrils were in helically arranged flat sheets according to the Bouligand model (1965). Laminae are occasionally more closely spaced at the top and bottom of the principal layer (Dalingwater and Miller 1977) which may be related to the rate of cuticle secretion (fastest in the central layers).

Sometimes the laminations are disturbed by canals and upturned to produce a 'Christmas tree' effect (Rolfe 1962, Dalingwater 1969, 1973; Størmer 1980) (Plate 4.6a). Under crossed polars this interferes with the extinction pattern and is useful in highlighting canal positions (Plate 4.6b).

4.2b. Reticulation

Some trilobite cuticles have a reticulate pattern on their external surfaces which may either be visible with the naked eye, as in some trinucleid glabellae, or several orders of magnitude smaller. By analogy with extant arthropods, the small polygons are thought to

represent the external expression of epidermal cells which secreted the cuticle (Chapter 1). The average cell size found on trilobite exoskeletons is 10-15μm diameter (Plates 6.1., 6.2a), comparable with that described for a Carboniferous crustacean (Briggs and Clarkson 1985). All proetide trilobites studied so far have much smaller cell polygons, approximately 5μm diameter (Chapter 5). Cell size reflects the amount of genetic material carried, although not necessarily the complexity of the organism, since radiolaria contain much more DNA than humans (S. Conway Morris, pers. comm.). Cell sizes in ostracodes are generally much larger than those of trilobites, reaching 60μm diameter (Okada 1981, 1982), whereas those of Cladocera are only 0,5-2μm across (Dahm 1976).

Cell polygons have been identified in most stages of the trilobite life cycle, from putative nauplius larvae (Fortey and Morris 1978) to holaspides. The size of the epidermal cells remains constant through ontogeny (Chapter 6), it is the total number that increases during growth. This is also found in some ostracodes, where the number of polygons doubles between each moult reflecting mitotic cell division (Okada 1981). Sometimes polygons are elongated in one direction reflecting active growth (Plate 4.5a, b).

The occurrence of cell polygons on the external surface of trilobite exoskeletons may be related to the absolute thickness of the prismatic layer. Cell polygons have been observed on the agnostines Agnostus pisiformis, Homagnostus obesus, and Ptychagnostus gibbus (Chapter 6); proetides Proetus (P.) concinnus, Warburgella (W.) scutterdinensis, W. (W.) stokesii, and Harpidella (H.) maura (Chapter 5); the olenid Olenus wahlenbergi, and the styginid Bumastus? phrix.

These trilobites, despite having very different total cuticle thicknesses (Appendix 3), all have thin prismatic layers (10μm or less). It is possible that the generation of cell polygons occurred early in the cuticle secretion process when new cuticle was only composed of prismatic layer and a thin principal layer (Miller and Clarkson 1980). Perhaps if the prismatic layer is thick, reticulation is not expressed externally.

Other, much larger scale reticulation clearly visible with the naked eye, may also occur on the external surfaces of trilobite exoskeletons, for example the cranidia of trinucleids such as Famatinolithis noticus Harrington and Leanza (Hughes et al. 1975, pl. 1, fig. 13), and the agnostine Trinodus aff. tardus (Barrande) (Owen and Bruton 1980, pl. 1, figs. 1-3; see Cech (1975) for discussion of cranidial reticulation in trinucleids). Such large scale features are not equivalent to cell polygons, being several orders of magnitude larger (Plate 4.5c), but may have been a means of strengthening the exoskeleton (Størmer 1930) as in true cell polygons (Chapter 7). Many trinucleids are reticulate as meraspides and small holaspides but are smooth when larger, although some retain reticulation throughout life (A. W. Owen, pers. comm.).

Unusual large-scale reticulation was documented by Palmer (1964, pl. 1, figs. 11, 15) for the olenellid Vanneria cf. V. walcottana. Here, a series of perforations on the visceral surface underly the ridges, creating lines of weakness. No comparable structures are known from other trilobites.

4.2c. Pore canals

Many different types of canal may occur within trilobite cuticles, but the most common are numerous small (1μm diameter or less) ducts that are probably analogous to the pore canals of other arthropods.

Although helicoidal pore canals have been documented in fossil crustaceans (Rolfe 1962; Neville and Berg 1971, Taylor 1973) there have been reports of both helicoidal (Dalingwater 1969, 1973) and non-twisted pore canals (Teigler and Towe 1975; Mutvei 1981) from trilobites. The appearance of twisted or straight pore canals rests largely on the state of preservation. Pore canals vary in concentration, but may be clearly seen in thin-sections of well preserved cuticle, especially under crossed polars.

Typical pore canals are absent from certain phacopide trilobites, however there is an abundance of 'Osmólska cavities' (Størmer 1980) first documented by Osmólska (1975). These are unusual fine canals with flared ends, interpreted by Størmer (1980) as having had a chemosensory function. He stated that Osmólska cavities are composed of regularly-sized pits (10-20μm diameter) located directly beneath the principal layer. Although the cavities are connected to canals in the principal layer, they did not appear to reach the external surface. If this were correct, Osmólska cavities are unlikely to have been chemosensory, as chemicals would have first had to diffuse through the calcitic prismatic layer. However, re-examination of Størmer's (1980) material and additional specimens of Phacops from the Devonian of New York has shown that his morphological description was incorrect.

In fact, the Osmólska cavities occur within the prismatic layer and open onto the external surface (Plate 4.4b-f). Størmer's 'prismatic

layer' is really a diagenetic overgrowth that occurs sporadically on only one specimen, and is a slightly different colour from the true cuticle (Plate 4.4a). It is therefore possible that such modified canals may have been chemoreceptors (or other kinds of sensory receptor) as they were open to the environment. However in extant arthropods, sensory receptors tend to occur in localised areas of the exoskeleton (Altner and Prillinger 1980), whereas Osmólska cavities are distributed all over the cuticle; even across other sensory structures such as pseudotubercles (Plate 4.6f) and socket pits (Plate 4.5f), and on the doublure. These facts, together with the absence of ordinary pore canals suggests that Osmólska cavities may have been modified pore canals involved in cuticle secretion.

4.2d. Arthropod sensory receptors

All arthropods are equipped with various sensory receptors with which they monitor the environment. These sense organs fall into several categories; photoreceptors, mechanoreceptors, chemoreceptors, equilibrium receptors, thermoreceptors, hygroreceptors and hydrostatic receptors. Each tend to be clustered on specific areas of the cuticle (Altner and Prillinger 1980).

Photoreceptors such as compound eyes may be the most prominent sensory structures, although eye spots may be especially significant in aquatic larval stages. Many arthropods also possess a general dermal light sensitivity which may be related to pigments or free nerve endings within the cuticle. For reviews of crustacean photoreceptors see Waterman (1961), and Shaw and Stowe (1982).

Other sensory receptors tend to be much smaller, but far more numerous; especially in the case of chemoreceptors and mechanoreceptors. Most work on arthropod sensory receptors has been performed on insects as they are easier to work with than marine groups. However knowledge of crustacean sense organs (which are most likely to resemble any that occurred on trilobites) is increasing, particularly in large forms such as crabs and lobsters.

The main difficulty involved in identifying specific sensory receptors is that there is no general correspondence between form and function. Some receptors may appear similar but have different internal structures and functions, whereas others differ in outward appearance and yet respond to the same stimuli (Altner and Prillinger 1980). As a result of this, each receptor has to be studied individually, which has proved very time consuming. The function of a receptor can only be truly known after several stages of investigation have been completed (Altner and Prillinger 1980). First of all behavioural tests have to be carried out to localise the main area of the response, followed by the collection of electrophysiological data to identify individual sensillae and ultimately, individual sensory cells.

Most sensillae are now classified according to their external and internal structure, such as presence of pores, the number of dendrites, and the type of nerve ending (Laverack 1987). For example perforated setae are usually chemosensory, although not all chemoreceptors are perforated (Laverack and Barrientos 1985). This is of course impossible to judge in fossil material. A summary of arthropod sensory receptors is given below, concentrating mainly on crustacean organs.

Mechanoreceptors are some of the most common sensory structures, and fall into several functional categories. For reviews of general arthropod mechanoreceptors see McIver (1975), Barth and Blickhan (1984); for crustaceans see Cohen and Dijkgraaf (1961), Lockwood (1968), Bush and Laverack (1982).

Proprioceptors are internal mechanoreceptors that monitor the relative positions of body parts. They are usually placed between joints or along muscles, and, being attached to soft tissue, are unlikely to be fossilised (Laverack and Barrientos 1985).

Several types of cuticular strain receptors have been identified from different arthropod groups, such as slit sensillae in spiders (Barth 1973). These tend to work on the principal of deflection of a membrane within the cuticle which enervates a mechanoreceptive dendrite. As the membrane has to be flexible, these have so far been found only in unmineralised or lightly mineralised cuticle (see review by Barth and Blickhan 1984). Crustacean campaniform organs were initially thought to be cuticular strain receptors (Shelton and Laverack 1968; Bush and Laverack 1982) but are now recognised as a combination of mechano- and chemoreceptors (Barth and Blickhan 1984), that is, 'taste' organs (Laverack 1988).

Crustacean cuticular articulated pegs (CAP's) are external mechanoreceptors that occur near joints and measure their displacements. Many setae are also mechanoreceptive and respond to changes in water flow, commonly occurring in sockets which facilitate articulation. Crustacean hair fan organs are very sensitive current monitors due to their larger surface area compared with single setae (Laverack and Barrientos 1985). However setae rarely operate singly but

occur in fields. Sometimes simple mechanoreceptors detect the direction of a steady current, whereas others respond to sudden agitations such as those produced by a predator or prey.

Mechanoreceptive setae are also present in balance and acceleration sensors. In large crustaceans this is performed by statocysts, usually located in appendages. These equilibrium-receptor organs are composed of a dense body (statolyth) surrounded by mechanoreceptors that monitor any displacement caused by changes in orientation or acceleration (Lockwood 1968; Budelmann 1988).

The most numerous sensory receptors are chemosensitive, and although they tend to occur in localised areas on insects, they may be found on almost all body regions of aquatic crustaceans (Laverack 1987, 1988).

The abundance of chemoreceptors is related to their great importance to the organism, since they determine so many behavioural responses (Kamil 1988). Chemoreception is involved in invertebrate feeding, escape responses, reproduction, settlement, and homing (Laverack 1974). Each type of chemoreceptor is sensitive to a different sort of chemical, which can induce or inhibit various behavioural responses (Carr 1988). Aquatic organisms begin feeding on detection of soluble metabolites from tissues; whereas secondary metabolites appear distasteful or poisonous. Secondary metabolites issued from predators (such as a slime trail) may induce predator avoidance behaviour. Alarm responses are also generated on detection of chemicals released from prey organisms being attacked. Some receptors are only sensistive to more specific chemical signals such as sex pheromones.

The two main groupings of chemoreceptors are those that smell (olfactory), or taste. In insects this distinction is dependent on whether the chemicals are airborne (smell) or soluble in water (taste); whereas with crustaceans, taste cells have to actually come into contact with the material, rather than just detect 'stray' molecules emitted from it (Laverack 1988). Hence crustacean taste receptors include a mechanoreceptive part to their structure, and are typically setae that articulate at the base but are chemosensitive at the tip, such as 'hedgehog hairs' (Altner et al. 1983). Other classifications have been based on the concentration of molecules needed to produce a response: a high concentration for taste, and a few molecules for smell (Laverack 1968), or alternatively on the type of behaviour induced (Atema 1977; Altner and Prillinger 1980). Hence local reflex actions generated in food localisation are classed as taste, and more complex behaviour such as mating is based on 'smell'.

Chemoreceptors either have terminal pores to receive chemicals, or take up molecules by diffusion through the setal wall (Altner and Prillinger 1980). However some pores are said to be involved in ecdysis rather than chemoreception (Ache 1982), so not all perforated setae are chemosensitive.

Thermoreceptors have been found in insects, and although not numerous, typically occur in association with two hygroreceptors (a moist and a dry air cell) (Altner and Prillinger 1980). Crustaceans tend to keep to preferred temperature regimes, though no specific thermoreceptors have yet been identified. Temperature may be monitored by the central nervous system rather than specific external receptors

(Ache 1982), as being cold-blooded (poikilothermic) organisms, the entire metabolic rate is determined by temperature.

4.2e. Trilobite sensory receptors

Most trilobites possessed compound eyes whose morphology and function have been the subject of detailed studies (see reviews by Clarkson 1975, 1979).

Less obvious sensory receptors must also have been present, including cuticular strain detectors and mechanoreceptors (including equivalents to crustacean CAP's likely to occur on coaptative devices, and monitoring of water currents). Chemoreceptors (both for 'taste' and 'smell'), and possibly equilibrium receptors and thermoreceptors may also have occurred. Differentiation between these different sense organs is almost impossible in fossilised material as soft-part morphology, so crucial in interpretation, is often not preserved. Exceptions are the remarkably preserved specimens of Agnostus pisiformis which still retain details of lightly sclerotised cuticle in addition to the dorsal exoskeleton (Müller and Walossek 1987). Those authors described sections of more pliable cuticle on the posterior of the second and third cephalic limbs (Müller and Walossek 1987, fig. 6; p. 16). Their flexibility and positioning indicates that these areas may represent cuticular strain detectors. Various surface microstructures may also be present and are likely to mark the positions of former sensory receptors, for example canals and tubercles.

4.2e(i). Canals and pits. Types of canals other than pore canals on trilobite exoskeletons range from 15-80μm diameter and occur either in isolation or associated with tubercles (Plate 4.6a, b, d, e). These probably represent gland ducts, or the positions of former sensory receptors containing setae. Some canals emerge from sockets (Plate 4.5d-f), and by analogy with extant arthropods it is likely that such 'socket pits' (Miller 1976) were mechanoreceptive at least in part. Canals are visible on the external surface as pits, however not all pits are caused by canals; for example those on Isotelus gigas (Teigler and Towe 1975, Pl. 3, fig. 5). Large pits on the free cheeks of Proetus are shallow depressions on the external surface of the cuticle, and are not associated with canals or any other microstructures (Section 5.2). Such structures are best referred to as dimples.

4.2e(ii). Pustules. Many different types of pustule occur on trilobite exoskeletons, which may be pierced by one or more canals, or capped by nodes (Plate 5.7). Two classification schemes have been devised to try and differentiate between them. Miller (1976) based his classification on the internal structure of pustules as seen in thin-sections. He distinguished 'domes', which involve a general raising of the entire cuticle (Plate 4.6c), from 'tubercles' which only have relief on the external surface (Plate 4.6a, b, d, e). Much larger pustular structures found on phacopid trilobites are termed 'pseudotubercles' (Plate 4.6f).

An alternative pustule classification by Størmer (1980) is based on the presence or absence of canals. His three main divisions are 'smooth tubercles', 'pitted tubercles', and large 'composite tubercles' (which include Miller's pseudotubercles). This classification is not as useful

for general use as that of Miller (1976) as it is so reliant on good preservation of the exoskeletons. Fine canals may often be obliterated after recrystallisation of the cuticle, or other destructive diagenetic processes (Chapter 3).

For this reason it is proposed that where possible, Miller's (1976) scheme should be adopted. When the internal structure is not known, the structures should be referred to as pustules, rather than tubercles. In addition, an extra term 'granules' should be added. These are small tubercles (10-15μm diameter) which may be pierced by a central canal and occur in high concentrations (approximately 10-15 per 100μm^2). Examples of such granulation are found on the exoskeleton of Proetus (P.) concinnus (Chapter 5).

The distinction of domes from tubercles does not necessarily necessitate the cutting of thin-sections (and hence damage to specimens). If the visceral surface of the cuticle is not visible, internal moulds can yield much information. Examples of domes are encrinurid and lichid 'tubercles' (Plate 4.6c), and the occipital 'tubercle' of proetids (Plate 5.8d).

Although all tubercles (by increasing the thickness of the exoskeleton), and domes (creating currugations) will have strengthened trilobite cuticle (Chapter 7), the main function of pustules was probably sensorial.

Cephalic and occipital pustules are common in trilobites but vary in position and structure. They have been allocated a variety of functions based either on functional morphology; for example photoreceptors (Fortey and Clarkson 1976) or analogy with extant

arthropod structures, such as the chemosensory and glandular complex in larval decapod crustaceans (Laverack and Barrientos 1985).

4.2e(iii). Terrace ridges. These are asymmetrical ridges that differ in morphology on the dorsal and ventral parts of the exoskeleton (Miller 1975). The size, structure, and distribution of terrace ridges varies greatly between different groups, and has led to several hypotheses for their function.

Miller (1975) first studied terrace ridges in depth and proposed that they acted as a current-monitoring system. This was based on the observation that canals opened out at the bases of ridge crests, and may have contained mechanosensitive setae.

Stitt (1976) inferred that the dorsal terrace ridges on the backwardly-burrowing trilobite Stenopilus were used as a frictional burrowing aid. This interpretation was followed by Schmalfuss (1981) who also suggested that terrace ridges on the doublure consolidated underlying sediment to enable construction of a respiratory and feeding chamber beneath the trilobite (Schmalfuss 1978b, 1981). These ideas were based on analogy with extant decapod crustaceans (Schmalfuss 1978a), and are supported by trace fossil evidence (Seilacher 1985). It has since been found that burrowing decapods use their terrace ridges to wedge themselves in their burrows during predatory attacks, rather than as an aid in the actual burrowing process (Savazzi 1985).

Fortey (1985) noted that although doublural terrace ridges may have consolidated sediment around feeding chambers in some trilobites, this cannot have been their function in pelagic species, or groups with very long pygidial doublures such as asaphids. It is much more likely that

terrace ridges performed a variety of functions depending on the ecological niches the various trilobites occupied. This is well illustrated by Symphysurus palpebrosus which has several different types of terrace ridge on the exoskeleton that can be assigned separate functions (Fortey 1986). In that species, terrace ridges on the cephalic and pygidial doublures interlocked during enrolment to act as an additional coaptative device. Monitoring of the degree of enrolment was probably carried out by receptors associated with long ridges on the margins of the thoracic facets, whereas those terraces on the petaloid thoracic facets permitted water circulation when the animal was completely enrolled. (Terrace ridges or granules on the thoracic facets of some phacopides and higher Asaphina may also have facilitated respiration during enrolment [Fortey and Chatterton 1988, text-fig. 13]). Coarse terraces on the anterior of the cephalic doublure and median body of the hypostome consolidated sediment around the top of the burrow when the animal had burrowed backwards. Other cephalic and thoracic terrace ridges remained exposed to the water surface and may have been involved in sensory reception.

Not only do terrace ridges vary greatly in size and distribution over the trilobite exoskeleton, they also differ in overall morphology. Miller (1975) stated that prismatic layer is discontinuous over the ridge crests, however this is not always so, for example in Paradoxides (Plate 4.7a). In addition, 'terrace canals' (Miller 1975) do not necessarily occur in association with ridge crests (Plate 4.7b, c). Osmólska (1975) noted that canals ended at ridge crests on proetide doublures (see Plate 7.1d), but as they appeared in every thin-section, they may represent central grooves running along the ridges rather than

individual canals. Examination of Silurian proetide species (Chapter 5) has not resolved this, as the terrace ridge crests were either broken or too poorly preserved to identify individual canal openings.

Miller (1975) described terrace ridges as escarpment-like features expressed on the external surface of the cuticle, however some have relief on both the external and visceral surfaces, as in certain Scutelluina. For example the cranidia of illaenids (Whittington 1963, pl. 17, fig. 6; pl. 18, figs. 9, 11-13; pl. 21, figs. 9, 10, 12; Whittington 1965, pl. 45, figs. 1-6, 19; pl. 50, figs. 1, 2, 4, 5, 7; pl. 51, fig. 9; Owen and Bruton 1980, pl. 2, figs. 4, 6); the hypostome of a styginid (Plate 4.7e); Stenopareia glaber rostral plate (Owen and Bruton 1980, pl.4, figs. 4, 8) and cephalon (Plate 4.7f); and the cephalon, pygidium and hypostome of the styginid Bumastus barriensis (Thomas 1978, pl. 2, figs. 1c, 7b, 11a, b, c) and the pygidial doublure of Cybantyx anaglyptos (Plate 4.7d). Other examples have been figured in the hypostomes of asaphids (Whittington 1965, pl. 26, figs. 6, 7; pl. 28, fig. 6; pl. 29, figs. 1-3); and the hypostome of the nileid Peraspis lineolata (Whittington 1965, pl. 35, figs. 6, 8). Such terrace ridges can be regarded structurally as folded plates, in contrast to the more typical terraces that act as T-beams (Chapter 7). All would have strengthened the exoskeleton mechanically.

4.2f. Muscle scars

Muscle scars are most common on the glabella, and may either be marked by a difference in exoskeletal colour (see discussion by Lane and Thomas p. 21, in Thomas 1978), for example Lonchodomas aff. pennatus (Owen and Bruton 1980, Fig. 4) or as areas lacking any form of surface

sculpture (Plate 5.1b). Phacopine muscle insertion structures and their significance in taxonomy were discussed by Eldredge (1971), and those of the Pseudoagnostidae by Shergold (1975).

Apodemes are protuberances on the visceral surface of the exoskeleton that formed muscle attachment areas. As they increase the thickness of the cuticle, they will also have strengthened the exoskeleton by acting as T-beams (Chapter 7).

4.2g. Caecae

Fine radiating ridges on trilobites, especially the cheeks are referred to as caecae and have been interpreted as reflecting an underlying alimentary system in agnostides (Opik 1960), and a respiratory system in polymerid trilobites (Jell 1978).

Jell (1978) proposed that caecae in polymerid trilobites with thin cuticles, such as olenids, were used as a dorsal respiratory system in addition to gills. In his hypothesis, oxygen diffused across the cuticle (as in some extant arthropods) into veins lying directly below the caecal ridges, ready for transportation to body organs. Although the morphology of the ridges is consistent with covering a respiratory circulatory system, it is unlikely that efficient gaseous exchange was possible through a highly calcified exoskeleton, especially when the ventral membrane was uncalcified.

Direct gaseous diffusion is only viable across *permeable* tissue less than 1mm thick (Wells 1980). It is unlikely that the thin trilobite cuticles described by Jell (1978) would have been sufficiently permeable for the necessary levels of oxygen uptake. Even specialised respiratory organs such as gills (composed of highly

permeable tissue with a very high surface area:volume ratio) also require good ventilation, either from natural water currents or generated by the organism itself (Green 1963; Lockwood 1968; Wells 1980). Therefore even if the exoskeleton of trilobites was permeable to oxygen, the animals would have had to have lived in turbulent waters or swum very fast to provide the necessary water circulation. This is inconsistent with morphological and geological evidence for olenids (Fortey 1974, 1985). In summary, it would seem that polymerid genal caecae overlay respiratory circulatory systems, but were not directly involved in gaseous exchange with the environment.

4.3. GLOSSARY OF TERMS APPLIED TO TRILOBITE EXOSKELETONS

APODEME - protuberance on the visceral surface of the exoskeleton that formed a muscle attachment area.

CAECAE - pattern of radiating and distally anastomosing raised ridges, occurring on the frontal area and genal field of the cephalon of polymerid trilobites. Radiating grooves and ridges (scrobiculae and rugae respectively) may occur on the cephalon, pygidium and thoracic segments of agnostine trilobites.

CELL POLYGONS - small reticulate structures (average 15μm diameter) expressed on the external surface of the cuticle, thought to represent the outlines of underlying epidermal cells.

CUTICLE - calcified portion of the integument that forms the dorsal exoskeleton.

DIMPLE - shallow depression on the external surface of the cuticle which is not associated with canals or other types of microstructure, for example the field of the free cheek of Proetus (Proetus) concinnus.

DOME - a pustule in which the entire cuticle arches, creating depressions on the visceral surface. Usually the cuticle thickness decreases markedly at the apex of the dome.

EPICUTICLE - thin, unmineralised outer layer of the cuticle. Rarely observed except as colour markings on the exterior, or as a diffuse residue after decalcification.

GRANULES - small tubercles 10-15μm diameter which may be pierced by a central canal. They often occur in high concentrations (10-15 per 100μm^2) for example Proetus (Proetus) concinnus.

LAMINATIONS - fine bands in the principal layer arranged parallel to the cuticle surface (syn. laminae).

MUSCLE SCARS - smooth, or depressed, or darker regions of the exoskeleton which may represent muscle attachment areas.

OSMÓLSKA CAVITIES - modified canals with flared ends (cavities) that occur in certain phacopide trilobites. The cavities (10-20μm diameter) occur within the prismatic layer and open onto the external surface. They are probably homologous with pore canals.

PORE CANALS - abundant, small canals (average 1μm diameter) that pierce the exoskeleton and are thought to be involved in cuticle secretion.

PRINCIPAL LAYER - inner layer of the exoskeleton which forms the bulk of the cuticle. The constituent crystals (average 0.5-1.5μm) are aligned parallel to the cuticle surface.

PRISMATIC LAYER - thin outer layer of the cuticle consisting of calcite crystals (average 1x10μm) orientated with their long c-axes perpendicular to the outer surface.

PROCUTICLE - calcified exoskeleton consisting of an outer prismatic layer and a thicker principal layer below.

PSEUDOTUBERCLE - large tubercle on phacopid trilobites with internal tubules.

PUSTULE - a general term for a small rounded prominence on the exterior of the exoskeleton (syn. boss, node).

SOCKET PIT - bowl-shaped depression on the external surface of the cuticle, with a central canal. It would have contained a mechanoreceptive seta.

TERRACE RIDGES - raised rigdes, usually asymmetrical in cross-section, which can be expresses either only on the external surface of the cuticle, or on both the external and visceral surfaces.

TUBERCLE - a pustule which involves a thickening of the cuticle and is only expressed on the external surface of the exoskeleton. May be pierced by one or more canals.

4.4. REFERENCES

ACHE, B. W. 1982. Chemoreception and thermoreception. In ATWOOD, H. L. and SANDEMAN, D. C. (eds.). The biology of Crustacea. Volume 3: Neurobiology: structure and function. 369-398. Academic Press, New York.

ALTNER, I., HATT, H. and ALTNER, H. 1983. Structural properties of bimodal chemo- and mechanosensitive setae on the pereiopod chelae of the crayfish, Austropotamobius torrentium. Cell Tissue Res., 228, 357-374.

ALTNER, H. and PRILLINGER, L. 1980. Ultrastructure of invertebrate chemo-, thermo-, and hygroreceptors and its functional significance. Inv. Rev. Cytol., 67, 69-139.

ATEMA, J. 1977. Functional separation of smell and taste in fish and Crustacea. Olfaction Taste Proc. Int. Symp., 6, 165-174.

BARTH, F. G. 1973. Microfibre reinforcement of an arthropod cuticle. Z. Zellforsch. mikrosk. Anat., 144, 409-433.

BARTH, F. G. and BLICKHAN, R. 1984. Mechanoreception. In BEREITER-HAHN, J., MATOLTSY, A. G. and SYLVIA RICHARDS, K. (eds.). Biology of the integument, Volume 1. 554-582. Springer-Verlag, Berlin.

BOULIGAND, Y. 1965. Sur une architecture torsadée répandue dans de nombreuses cuticules d'arthropodes. C. r. hebd. Séanc. Acad. Sci. Paris, 261, 3665-3668.

BREZINSKI, D. K. 1988. Trilobites of the Gilmore City Limestone (Mississippian) of Iowa. J. Paleont., 62, 241-245.

BRIGGS, D. E. G. and CLARKSON, E. N. K. 1985. The Lower Carboniferous shrimp Tealliocaris from Gullane, East Lothian, Scotland. Trans. R. Soc. Edinb., 76, 173-201.

BUDELMANN, B-U. 1988. Morphological diversity of equilibrium receptor systems in aquatic invertebrates. In ATEMA, J., FAY, R. R., POPPER, A. N. and TAVOLGA, W. N. (eds.). Sensory biology of aquatic animals 757-782. Springer-Verlag, New York.

BUSH, B. M. H. and LAVERACK, M. S. 1982. Mechanoreception. In ATWOOD, H. L. and SANDEMAN, D. C. (eds.). The biology of Crustacea 399-468. Academic Press, New York.

CARR, W. E. S. 1988. The molecular nature of chemical stimuli in the aquatic environment. In ATEMA, J., FAY, R. R., POPPER, A. N. and TAVOLGA, W. N. (eds.). Sensory biology of aquatic animals 3-27. Springer-Verlag, New York.

ČECH, S. 1975. Cranidial reticulation and functional morphology of the cephalic fringe in Trinucleidae (Trilobita). Věst. ústred. Úst. geol., 50, 173-177.

CLARKSON, E. N. K. 1975. The evolution of the eye in trilobites. Fossils Strata, 4, 7-31.

CLARKSON, E. N. K. 1979. The visual system of trilobites. Palaeontology, 22, 1-22, pl. 1.

COHEN, M. J. and DIJKGRAAF, S. 1961. Mechanoreception. In WATERMAN, T. H. (ed.). The physiology of Crustacea. Volume 2: Sense organs, integration and behaviour 65-108. Academic Press, New York.

DAHM, E. 1976. The carapace of Cladocera - a morphological comparison of Cladocera and Ostracoda. Abh. naturw. Ver. Hamburg. (N. F.), 18/19, 331-336.

DALINGWATER, J. E. 1969. Some aspects of the chemistry and fine structure of the trilobite cuticle. Ph.D. thesis (unpubl.), University of Manchester.

DALINGWATER, J. E. 1973. Trilobite cuticle microstructure and composition. Palaeontology, 16, 827-839, pls. 107-109.

DALINGWATER, J. E. and MILLER, J. 1977. The laminae and cuticular organisation of the trilobite Asaphus raniceps. Palaeontology, 20, 21-32, pls. 9-10.

ELDREDGE, N. 1971. Patterns of cephalic musculature in the Phacopina (Trilobita) and their phylogenetic significance. J. Paleont., 45, 52-67.

ESKER, G. C. 1968. Colour markings in Phacops and Greenops from the Devonian of New York. Palaeontology, 11, 498-499, pl. 96.

FORTEY, R. A. 1974. The Ordovician trilobites of Spitsbergen 1. Olenidae. Skr. norsk Polarinst., 160, 129pp. pls. 1-24.

FORTEY, R. A. 1979. Early Ordovician trilobites from the Catoche Formation (St. George Group), Western Newfoundland. Bull. geol. Surv. Can., 321, 61-114, pls. 23-37.

FORTEY, R. A. 1985. Pelagic trilobites as an example of deducing the life habits of extinct arthropods. Trans. R. Soc. Edinb., 76, 219-230.

FORTEY, R. A. 1986. The type species of the Ordovician trilobite Symphysurus: systematics, functional morphology and terrace ridges. Paläont. Z., 60, 3/4, 12 Abb. 255-275.

FORTEY, R. A. and CHATTERTON, B. D. E. 1988. Classification of the trilobite suborder Asaphina. Palaeontology, 31, 165-222, pls. 17-19.

FORTEY, R. A. and CLARKSON, E. N. K. 1976. The function of the glabellar 'tubercle' in Nileus and other trilobites. Lethaia, 9, 101-106.

FORTEY, R. A. and MORRIS, S. F. 1978. Discovery of nauplius-like trilobite larvae. Palaeontology, 21, 823-833, pl. 94.

GREEN, J. 1963. A biology of Crustacea 180pp. H. F. and G. Witherby Ltd., London.

HUGHES, C. P., INGHAM, J. K. and ADDISON, R. 1975. The morphology, classification and evolution of the Trinucleidae (Trilobita). Phil. Trans. R. Soc. Ser. B., 272, 537-607.

JELL, P. A. 1975. Australian Middle Cambrian eodiscoids with a review of the superfamily. Palaeontographica, Abt. A, 150, 1-97, figs. 1-3, 29 pls.

KAMIL, A. C. 1988. Behavioural ecology and sensory biology. In ATEMA, J., FAY, R. R., POPPER, A. N. and TAVOLGA, W. N. (eds.). Sensory biology of aquatic animals 189-201. Springer-Verlag, New York.

KRAMPITZ, G., DROLSHAGEN, H., HAUSLE, J. and HOF-IRMSCHER, K. 1983. Organic matrices of mollusc shells. In WESTBROEK, P. and DE JONG, E. W. (eds.). Biomineralisation and biological metal accumulation 231-247. D. Reidel Publishing Company, Dordrecht, Holland.

LAVERACK, M. S. 1968. On the receptors of marine invertebrates. Ocean. Mar. Biol. Ann. Rev., 6, 249-324.

LAVERACK, M. S. 1974. The structure and function of chemoreceptor cells. In GRANT, P. T. and MACKIE, A. M. (eds.). Chemoreception in marine organisms 1-48. Academis Press, London, New York.

LAVERACK, M. S. 1987. The nervous system of the Crustacea, with special reference to the organisation of the sensory system. In ALI, M. A. (ed.). Nervous systems in invertebrates. N.A.T.O. A.S.I. Series A, Volume 141 323-352. Plenum Press, New York, London.

LAVERACK, M. S. 1988. The diversity of chemoreceptors. In ATEMA, J., FAY, R. R., POPPER, A. N. and TAVOLGA, W. N. (eds.). Sensory biology of aquatic animals 287-312. Springer-Verlag, New York.

LAVERACK, M. S. and BARRIENTOS, Y. 1985. Sensory and other superficial structures in living marine Crustacea. Trans. R. Soc. Edinb., 76, 123-136.

LINDSTRÖM, G. 1901. Researches on the visual organs of the trilobites. K. Svensk. Vetensk. Akad. Handl., 34, 1-85.

LOCKWOOD, A. P. M. 1968. Aspects of the physiology of Crustacea 328pp. Oliver and Boyd, Edinburgh.

McIVER, S. 1975. Structure of cuticular mechanoreceptors of arthropods. Ann. Rev. Entomol., 20, 381-397.

MILLER, J. 1975. Structure and function of trilobite terrace lines. Fossils Strata, 4, 155-178.

MILLER, J. 1976. The sensory fields and life mode of Phacops rana (Green, 1832) (Trilobita). Trans. R. Soc. Edinb., 69, 337-367, pls. 1-4.

MILLER, J. and CLARKSON, E. N. K. 1980. The post-ecdysial development of the cuticle and the eye of the Devonian trilobite Phacops rana milleri Stewart 1927. Phil. Trans. R. Soc. Ser.B., 288, 461-480, pls. 1-7.

MÜLLER, K. J. and WALOSSEK, D. 1987. Morphology, ontogeny, and life habit of Agnostus pisiformis from the Upper Cambrian of Sweden. Fossils Strata, 19, 1-124, pls. 1-33.

MUTVEI, H. 1981. Exoskeletal structure in the Ordovician trilobite Flexicalymene. Lethaia, 14, 225-234.

NEVILLE, A. C. and BERG, C. W. 1971. Cuticle ultrastructure of a Jurassic crustacean (Eryma stricklandi). Palaeontology, 14, 201-205.

OKADA, Y. 1981. Development of cell arrangement in ostracod carapaces. Paleobiology, 7, 276-280.

OKADA, Y. 1982. Structure and cuticle formation of the reticulated carapace of the ostracode Bicornucythere bisanensis. Lethaia, 15, 85-101.

OPIK, A. 1960. Alimentary caeca of agnostid and other trilobites. Palaeontology, 3, 410-438.

OSMÓLSKA, H. 1975. Fine morphological characters of some Upper Palaeozoic trilobites. Fossils Strata, 4, 201-207.

OWEN, A. W. and BRUTON, D. L. 1980. Late Caradoc - early Ashgill trilobites of the central Oslo Region, Norway. Paleont. Contrib. Univ. Oslo, 245, 63pp. pls. 1-10.

PALMER, A. R. 1964. An unusual Lower Cambrian trilobite fauna from Nevada. Prof. Pap. U. S. geol. Surv., 483-F, 1-13, pls. 1-3.

RAYMOND, P. E. 1922. A trilobite retaining color markings. Am. J. Sci. Ser. 5, 4, 461-464, fig. 1.

RICHARDS, A. G. 1951. The integument of arthropods xvi + 411 pp. University of Minnesota Press, Minneapolis.

ROLFE, W. D. I. 1962. The cuticle of some Middle Silurian ceratocaridid Crustacea from Scotland. Palaeontology, 5, 30-51.

ROSENFELD, A. 1979. Structure and secretion of the carapace in some living ostracodes. Lethaia, 12, 353-360.

ROSENFELD, A. 1982. The secretion process of the ostracod carapace. In BATE, R. H., ROBINSON, E. and SHEPPARD, L. M. (eds.). Fossil and Recent ostracods 12-24. Published for the British Micropalaeontological Society by Ellis Horwood Ltd.

SAVAZZI, E. 1985. Functional morphology of the cuticular terraces in burrowing terrestrial brachyuran decapods. Lethaia, 18, 147-154.

SCHMALFUSS, H. 1978a. Structure, patterns and function of cuticular terraces in Recent and fossil arthropods. 1. Decapod crustaceans. Zoomorphologie, 90, 19-40.

SCHMALFUSS, H. 1978b. Constructional morphology of cuticular terraces in trilobites, with conclusions on synecolgical evolution. Neues. Jb. Geol. Paläont. Abh., 157, 164-168.

SCHMALFUSS, H. 1981. Structure, patterns and function of cuticular terraces in trilobites. Lethaia, 14, 331-341.

SEILACHER, A. 1985. Trilobite palaeobiology and substrate relationships. Trans. R. Soc. Edinb., 76, 231-237.

SHAW, S. R. and STOWE, S. 1982. Photoreception. In ATWOOD, H. L. and SANDEMAN, D. C. (eds.). The biology of Crustacea. Volume 3: Neurobiology: structure and function. 291-367. Academic Press. New York.

SHELTON, R. G. J. and LAVERACK, M. S. 1968. Observations on a redescribed crustacean cuticular sense organ. Comp. Biochem. Physiol., 25, 1049-1059.

SHERGOLD, J. H. 1975. Late Cambrian and early Ordovician trilobites from the Burke River Structural Belt, western Queensland. Bull. Bur. Miner. Resour. Geol. Geophys. Aust., 153, 251pp. 58 pls. (2 Vols).

STITT, J. H. 1976. Functional morphology and life habits of the Late Cambrian trilobite Stenopilus pronus Raymond. J. Paleont., 50, 561-576.

STØRMER, L. 1930. Scandinavian Trinucleidae, with special reference to Norwegian species and varieties. Norsk Vidensk. -Akad. Oslo Mat. Naturv. Kl., 4, 1-111.

STØRMER, L. 1980. Sculpture and microstructure of the exoskeleton in chasmopinid and phacopid trilobites. Palaeontology, 23, 237-271, pls. 25-34.

TAYLOR, B. J. 1973. The cuticle of Cretaceous macrurous Decapoda from Alexander and James Ross Islands. Br. Antarct. Surv. Bull., 35, 91-100.

TEICHERT, C. 1944. Permian trilobites from western Australia. J. Paleont., 18, 445-465.

TEIGLER, D. J. and TOWE, K. M. 1975. Microstructure and composition of the trilobite exoskeleton. Fossils Strata, 4, 137-149, pls. 1-9.

THOMAS, A. T. 1978. British Wenlock trilobites (Part 1). Palaeontogr. Soc. Monogr., 1, 1-56, pls. 1-14.

WATERMAN, T. H. 1961. Light sensitivity and vision. In WATERMAN, T. H. (ed.). The physiology of Crustacea. Volume 2. Sense organs, integration, and behaviour. 1-64. Acadenic Press, New York.

WELLS, J. W. 1942. Supposed color markings in Ordovician trilobites from Ohio. Am. J. Sci. Ser 5, 240, 710-713.

WELLS, R. M. G. 1980. Invertebrate respiration. Institution of Biology. Studies in Biology 127. iii + 72pp. Edward Arnold Limited, London.

WHITTINGTON, H. B. 1963. Middle Ordovician trilobites from Lower Head, Western Newfoundland. Bull. Mus. comp. Zool. Harv., 129, 1-118, 36 pls.

WHITTINGTON, H. B. 1965. Trilobites of the Ordovician Table Head Formation, Western Newfoundland. Bull. Mus. comp. Zool. Harv., 132, 275-442, 68 pls.

WILLIAMS, J. S. 1930. A color pattern on a new Mississipian trilobite. Am. J. Sci. Ser. 5, 20, 61-64.

Plate 4.1. Spotted exoskeleton of *Greenops boothi* (Green, 1837).

a, Greenops boothi Hamilton Shale, Alden, New York (Middle Devonian). (LSU) 8270. Dorsal view of thorax and pygidium with dark spots on the cuticle. Anterior to right hand side. Figured by Esker (1968, Pl. 96, fig. 2). x5.
b, Greenops boothi Hamilton Shale, Alden, New York (Middle Devonian). (LSU) 8270. Dark spots on the cuticle are in fact pillars that penetrate the entire cuticle thickness, visible on broken edges. Figured by Esker (1968, Pl. 96, fig. 2). x15.

Plate 4.2. Colour markings on *Phacops rana* Green, 1832.

a, Phacops rana Hamilton Shale, Alden, New York (Middle Devonian). (LSU) 8269.3. Dorsal view of complete specimen. Figured by Esker (1968, Pl. 96, figs. 1, 4). x2.5.
b, Phacops rana Hamilton Shale, Alden, New York (Middle Devonian). (LSU) 8269.3. Dark spots of variable size on the dorsal surface of thoracic segments. Figured by Esker (1968, Pl. 96, figs. 1, 4). x6.
c, Phacops rana Hamilton Shale, Alden, New York (Middle Devonian). (LSU) 8269.3. Colour markings around the eye and on the eye lenses. Figured by Esker (1968, Pl. 96, figs. 1, 4). x12.
d, Phacops rana Hamilton Shale, Alden, New York (Middle Devonian). (LSU) 8271. Colour markings on an enrolled specimen (dorsal view). Figured by Esker (1968, Pl. 96, figs. 3, 5). x3.

PLATE 4.2

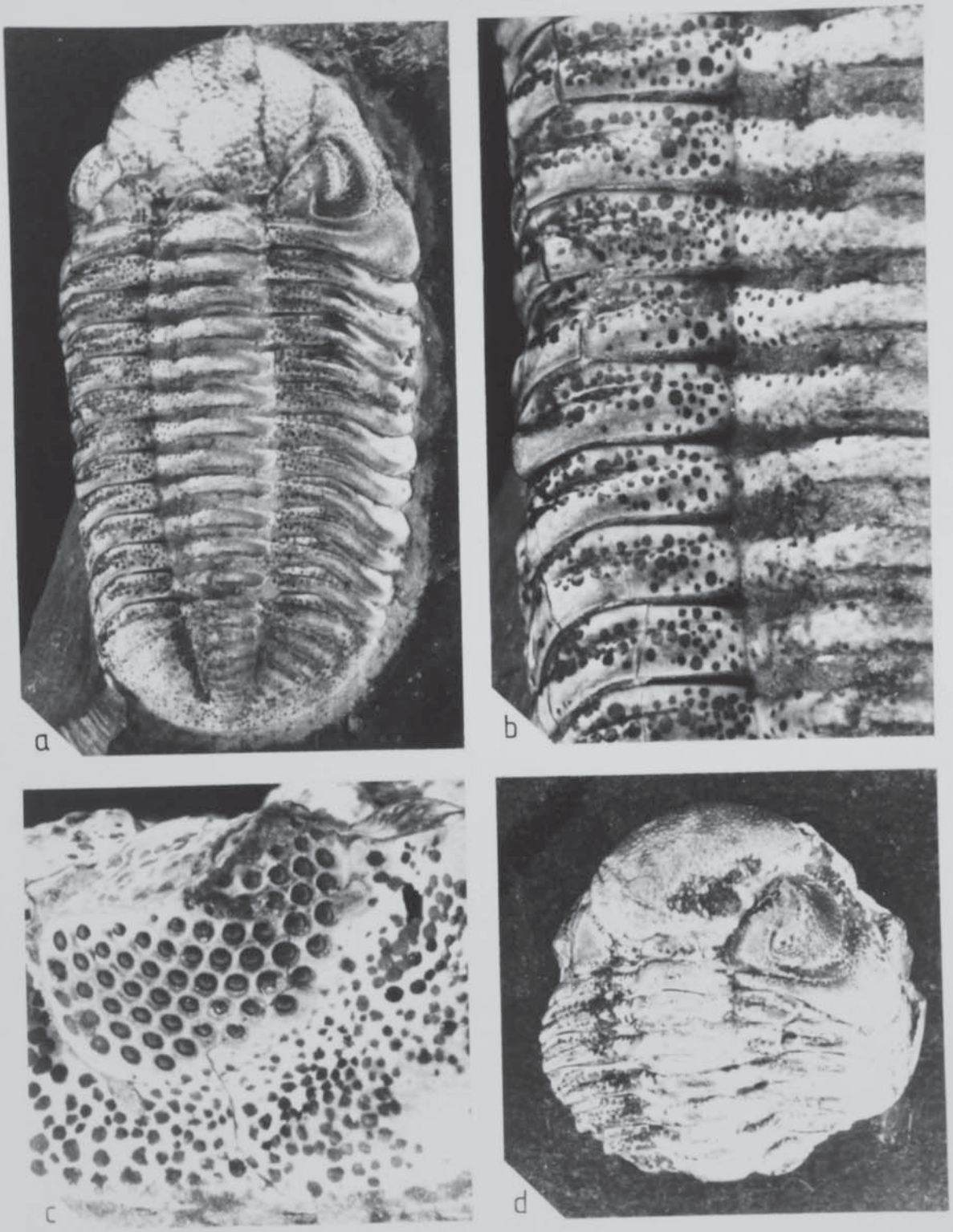

Plate 4.3. Ultrastructure of trilobite exoskeletons.

a, Carcinus sp. (Recent) (JED). Thin-section through the cuticle, showing division into layers and laminations. Epicuticle (ep), Exocuticle (ex), Endocuticle (en). x135.
b, Asaphus raniceps Dalman. Lower 'raniceps' Limestone, Öland (Llanvirn). (JED)01. A37.1. Thin-section through the exoskeleton containing laminations (l). x40.
c, Asaphus sp. Asaphus Limestone, Norway (Ordovician). NW1. Thin-section through the exoskeleton, revealing laminations (l). x60.
d, Phacops rana milleri Stewart. Silica Shale, Silica, Ohio (Middle Devonian). NE7.3. The zones of extinction 'sweep' along the specimen as the stage is rotated. x50
e, Phacops rana crassituberculata Stumm. Silica Shale, Silica, Ohio (Middle Devonian). NE4.C. Scanning electron micrograph of prismatic layer with calcite crystals (1x10μm) orientated with their c-axes perpendicular to the surface. x1250.
f, Phacops rana crassituberculata Stumm. Silica Shale, Silica, Ohio (Middle Devonian). NE4.C. Scanning electron micrograph of the principal layer, with calcite crystals aligned parallel to the surface. x1250.

PLATE 4.3

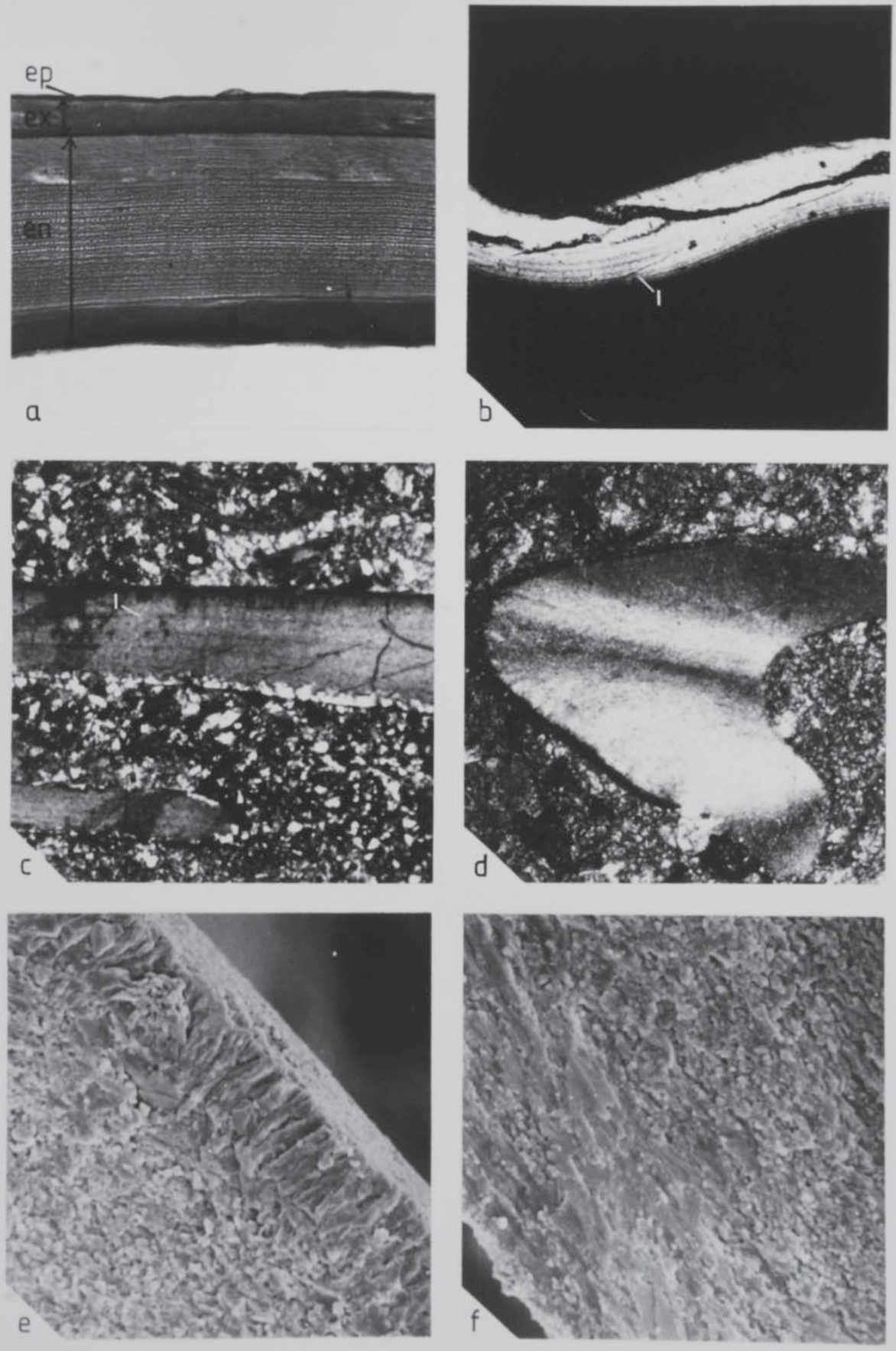

Plate 4.4. Osmólska cavities.

a, Phacops granulatus (Münster). Poland (Devonian). (PMO)A38817.1. Thin-section through a pseudotubercle, with Osmólska cavities overlain by a diagenetic 'prismatic' layer. Figured by Størmer (1980, Pl. 30, figs. 1-7; Pl. 31, figs. 1-5). x140.
b, Phacops rana crassituberculata Stumm. Silica Shale, Silica, Ohio (Middle Devonian). NE4.A. Scanning electron micrograph of the dorsal surface of the glabella, with numerous Osmólska cavities. x500.
c, Phacops rana crassituberculata Stumm. Silica Shale, Silica, Ohio (Middle Devonian). NE4.2. Transverse section through the cephalon, showing Osmólska cavities within the true prismatic layer connected to fine canals (c) in the principal layer. x70.
d, Phacops rana crassituberculata Stumm. Silica Shale, Silica, Ohio (Middle Devonian). NE3.3. Longitudinal section through thoracic segments, showing Osmólska cavities within the prismatic layer. x140.
e, Phacops rana crassituberculata Stumm. Silica Shale, Silica, Ohio (Middle Devonian). NE4.C. Scanning electron micrograph of infilled Osmólska cavities (Oc) within the prismatic layer. x1500.
f, Phacops rana crassituberculata Stumm. Silica Shale, Silica, Ohio (Middle Devonian). NE4.C. Scanning electron micrograph of an Osmólska cavity within the prismatic layer. x3000.

PLATE 4.4

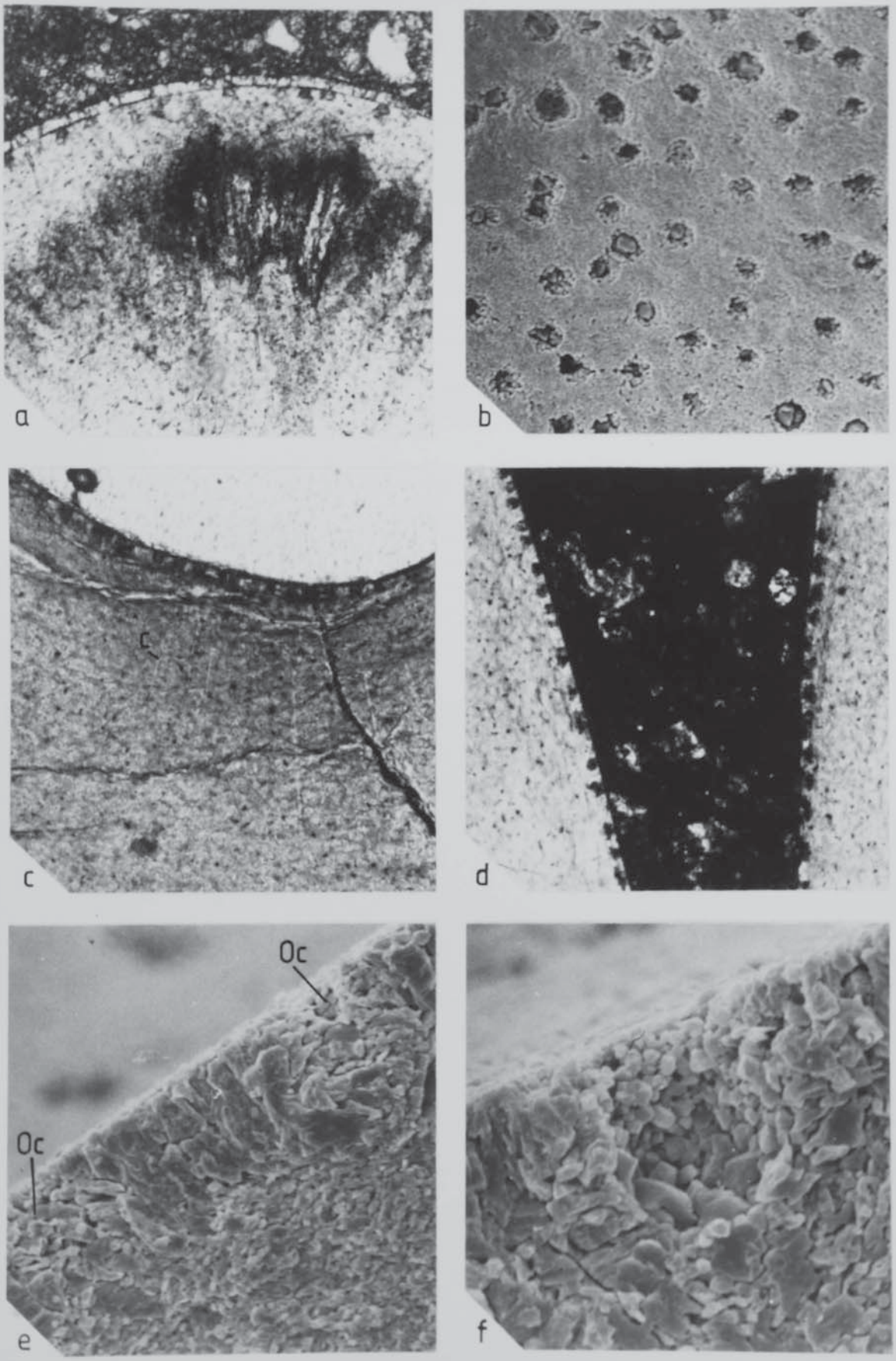

Plate 4.5. Scanning electron micrographs of trilobite surface reticulation and canals.

a, Olenus wahlenbergi Westergård. Andrarum, Skåne, Sweden (Upper Cambrian). Ow.23. Cell polygons on the occipital ring. Note more elongated polygons in the occipital furrow. x400.
b, Olenus wahlenbergi Westergård. Andrarum, Skåne, Sweden (Upper Cambrian). Ow.13. External mould of a genal spine showing impressions of tubercles and highly elongated cell polygons (10x30µm). x1000.
c, Bonnia sp. Peary Land, Greenland (Cambrian). NW6.A. Large scale reticulation (125µm diameter) on the cranidium. x150.
d, Phacops rana crassituberculata Stumm. Silica Shale, Silica, Ohio (Middle Devonian). NE6.A. Socket pits (approximately 70µm diameter) and Osmólska cavities on the eye socle. x150.
e, Ellipsocephalus sp. Bornholm, Öland (Cambrian). NW11. Socket pits on the dip slopes of shallow terrace ridges, anterior border of the cranidium. x300.
f, Phacops rana crassituberculata Stumm. Silica Shale, Silica, Ohio (middle Devonian). NE4.A. Large socket pit (approximately 150µm diameter) at the base of a glabellar pseudotubercle. Note the abundance of Osmólska cavities on the surface, even within the socket. x150.

PLATE 4.5

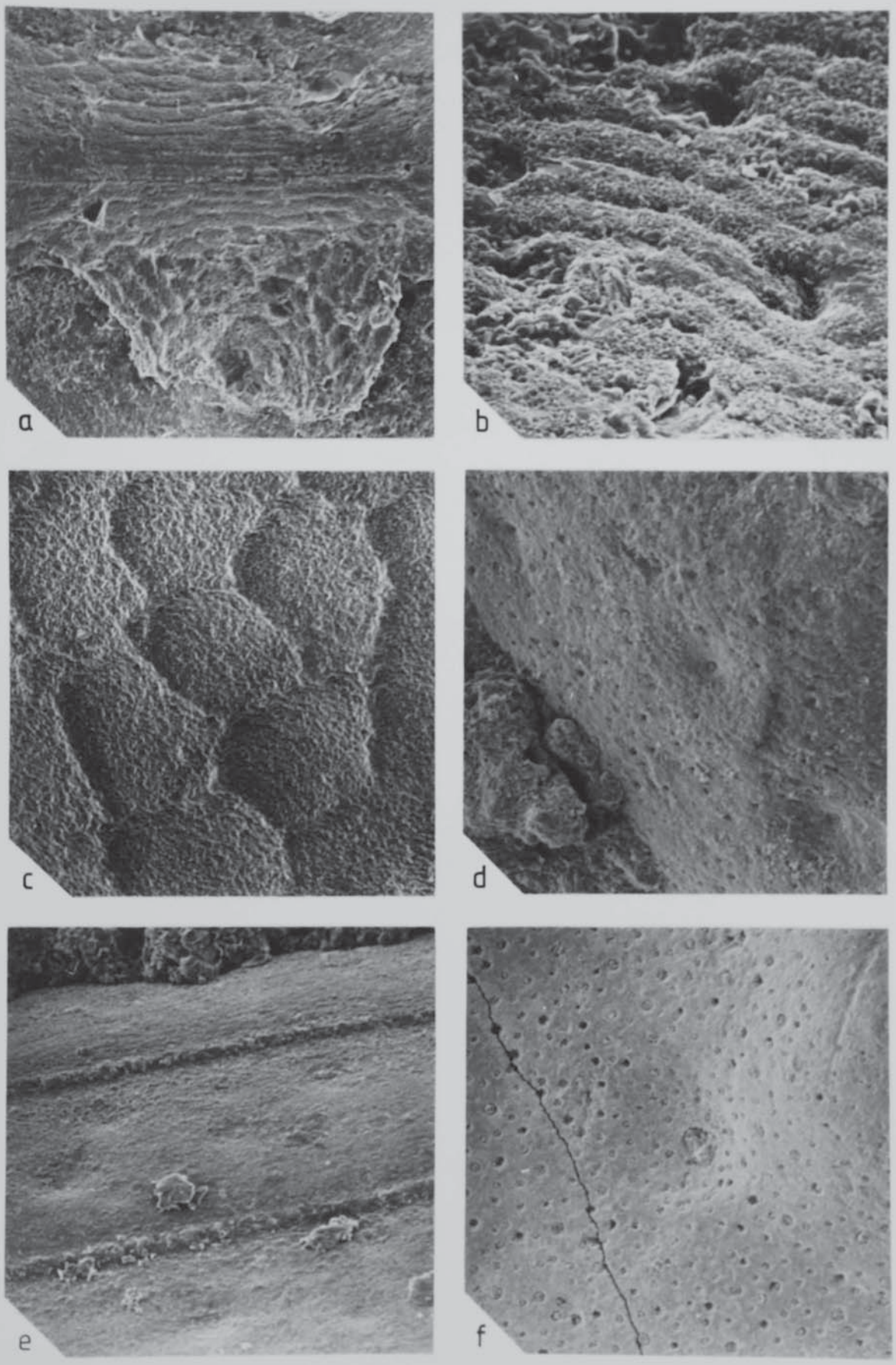

Plate 4.6. Pustules on trilobite cuticles.

a, Chasmops sp. Oslo Fjord, Norway (Middle Ordovician). (PMO)94398. Thin-section of tubercles with central canals and upturned laminations, producing a 'Christmas tree' effect. Also note the Osmólska cavities (Oc) within the thin prismatic layer. x150.
b, Dalmanites myops (König). Much Wenlock Limestone Formation, Wren's Nest, Dudley (Wenlock). D24.2. Thin-section through a pygidium viewed under crossed polars, emphasising numerous small tubercles with central canals. x60.
c, Hemiarges bucklandii (Milne Edwards). Much Wenlock Limestone Formation, Wren's Nest, Dudley (Wenlock). D33.3. Longitudinal section through cranidial domes. x45.
d, Cyphoproetus depressus (Barrande). Dolyhir and Nash Scar Limestone Formation, near Dolyhir Bridge SO 2403 5825 (Wenlock). NW10.1. Thin-section through a cranidium containing tubercles with central canals. x60.
e, Calymene sp. Much Wenlock Limestone Formation, Wren's Nest, Dudley (Wenlock). D14.1. Small true tubercles with central canals, seen on a longitudinal section of the cranidium. Note possible Osmólska cavities within the prismatic layer (arrowed). x140.
f, Phacops granulatus (Münster). Poland (Devonian). (PMO)A38817.1. Thin-section through pseudotubercles containing internal tubules, and Osmólska cavities (Oc) within the prismatic layer. Figured by Størmer (1980, Pl. 30, figs. 1-7; Pl. 31, figs. 1-5). x40.

PLATE 4.6

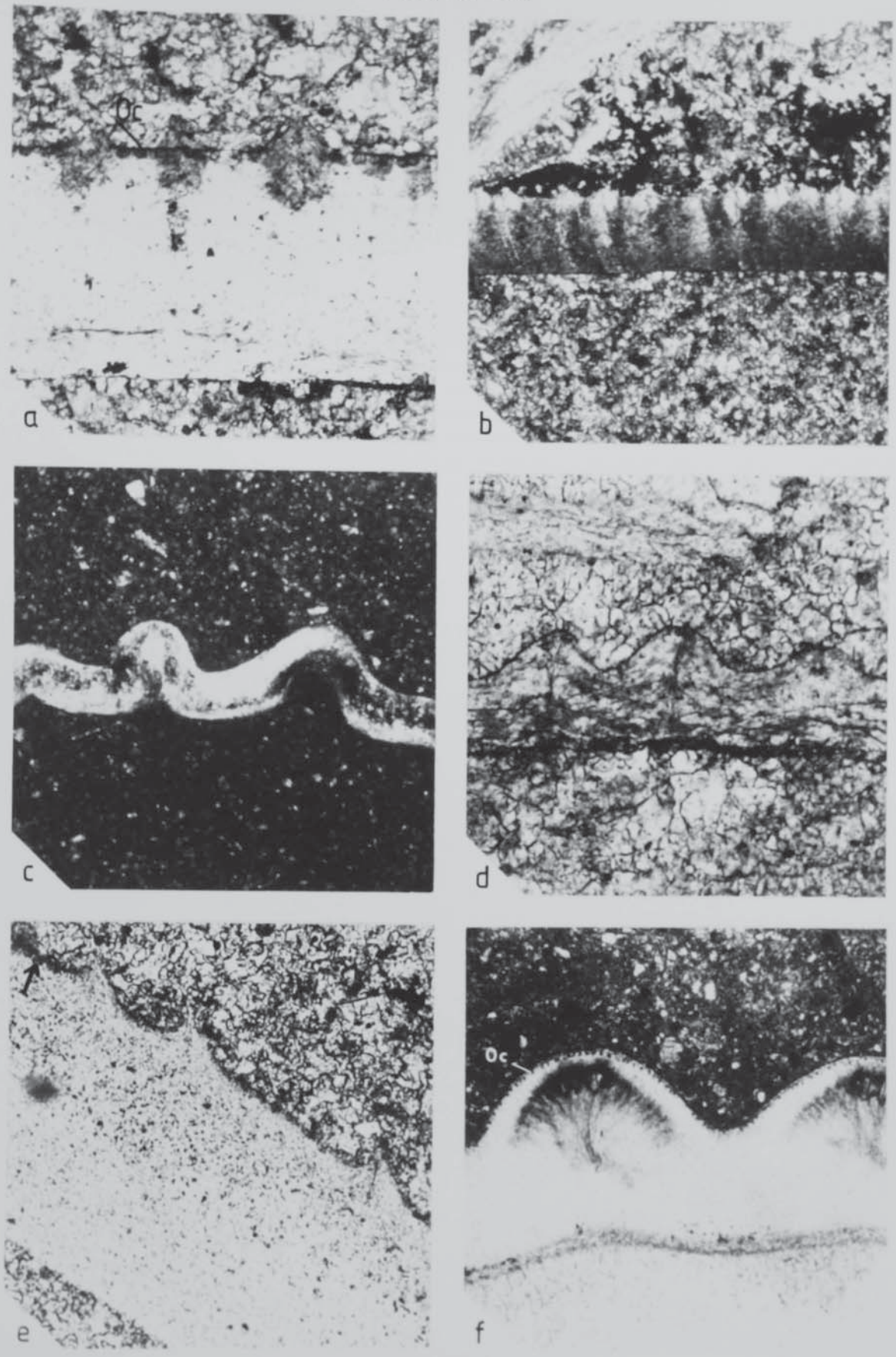

Plate 4.7. Terrace ridges.

a, Paradoxides sp. Slemmestad, Oslo Fjord, Norway (Middle Cambrian). NW4.2. Thin-section through terrace ridges with continuous prismatic layer (p). x75.
b, Bumastus? phrix Lane and Thomas. Dolyhir and Nash Scar Limestone Formation, near Dolyhir Bridge SO 2403 5825 (Wenlock). NW10.4. Scanning electron micrograph of terrace ridges on the free cheek doublure. Canal (c) distribution is not associated with the ridge crests. x200.
c, Cybantyx anaglyptos Lane and Thomas. Much Wenlock Limestone Formation, Wren's Nest, Dudley (Wenlock). D37.A. Scanning electron micrograph of the doublure of the free cheek, with infilled canals opening towards the bases of the ridge crests. x70.
d, Cybantyx anaglyptos Lane and Thomas. Much Wenlock Limestone Formation, Wren's Nest, Dudley (Wenlock). NW43. Dorsal view of a pygidium, prepared to show the visceral surface of the doublure with terrace ridges. Also note the openings of canals visible as on the dorsal surface. The specimen was lightly coated with ammonium chloride. x15.
e, Styginid hypostome, Lansa, Gotland (Silurian). (NRS)Ar.46992a. Dorsal view with impressions of terrace ridges on the internal mould. The specimen was lightly coated with ammonium chloride. Figured by Lindström (1901, Pl. 2, figs. 28-30). x5.
f, Stenopareia glaber (Kjerulf). Central Oslo Region, Norway (Ordovician). NW13. Anterior view of an enrolled specimen, preserved as internal mould. Note the faint impressions of terrace ridges on the cephalon. The specimen was lightly coated with ammonium chloride. x1.7.

PLATE 4.7

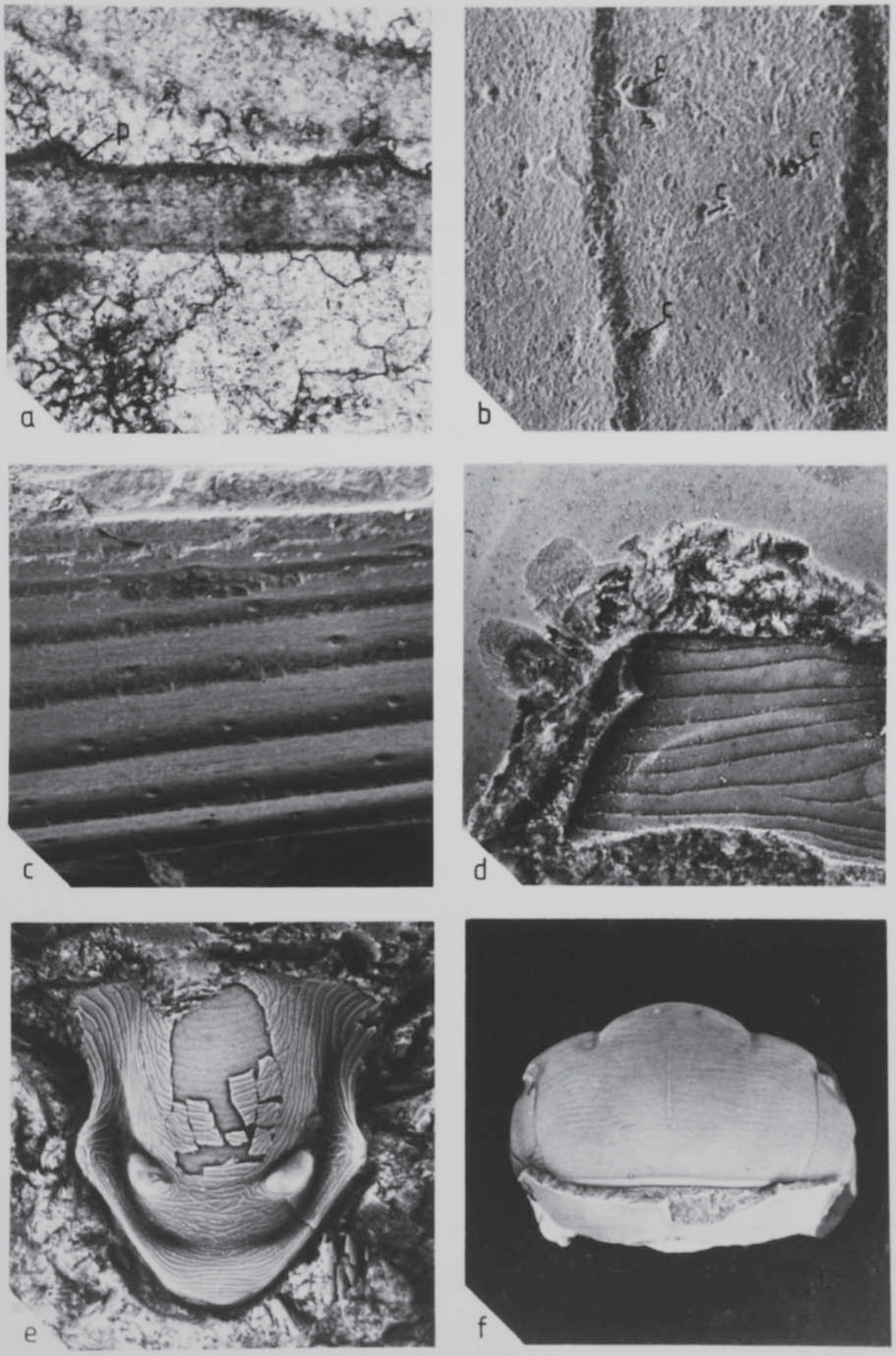

CHAPTER 5

SENSORY FIELD MAPS IN PROETIDE TRILOBITES

ABSTRACT. The sensory fields of the four Wenlock trilobites Proetus (Proetus) concinnus, Warburgella (Warburgella) stokesii, Warburgella (Warburgella) scutterdinensis, and Harpidella (Harpidella) maura are described and found to be species-specific. Certain features, such as cell size, and relative thickness of the prismatic layer are characteristic of the Order Proetida. Intraspecific variation is related to ontogenetic development, most markedly in the field of the free cheek of P. (P.) concinnus. The proetid occipital pustule may have functioned as a light-sensitive organ. The tropidium of W. (W.) stokesii is a ridge with a central canal or groove, rather than a tube-like structure, and probably contained a sensory receptor rather than a circulatory system. Despite microstructural distribution being species-specific, it is of limited practical value in taxonomy as the fine details are easily lost during diagenesis

5.1. Introduction

WORK on the pore distribution of Recent crustaceans has shown that although some genera show pore pattern species-specifity, such as the copepod Eucalanus (Fleminger 1973), this is not true for all Crustacea (Mauchline 1977). In those studies, the positions of gland ducts and sensillae were documented and found to occur in areas of high and low density over the exoskeleton (Mauchline 1977), typically in a bilaterally symmetrical pattern which is serially homologous (Fleminger 1973). Fleminger (1973) found that closely related Eucalanus species have the most similar sensory field maps, and that some pore positions are characteristic of the whole genus. Three types of pore were

distinguished, each maintaining a constant number and distribution. ("designated sites"), so intraspecific variation is negligible. Interspecific variation is concentrated in only nine sites out of a total of thirty-seven.

Variation in large-scale trilobite cuticular structures is already known, for example tuberculation in the Encrinuridae. Study of cephalic pustules in particular, has shown that the number and position of pustules in encrinurids is species-specific (Tripp 1957; Evitt and Tripp 1977). Pygidial surface structures have been used to distinguish between Lower Devonian odontochilid species (Šnajdr 1987).

Miller (1976) was the first to identify regions from the whole trilobite exoskeleton containing specific cuticular structures (some only a few microns in diameter), which were likely to have had a sensory function, and plotted their distributions to produce a "sensory field map". However, he only studied the phacopid species Phacops rana, and the present research demonstrates that trilobite microstructural "sensory fields" are species-specific, and hence an aid in taxonomy.

This study has concentrated on four proetide species of Wenlock age: Proetus (Proetus) concinnus (Proetidae), Warburgella (Warburgella) stokesii (Brachymetopidae), W. (W.) scutterdinensis (Brachymetopidae) and Harpidella (Harpidella) maura (Aulacopleuridae). Cuticular microstructures have been examined from numerous exoskeletal fragments, either as thin-sections (TS) of known orientation for transmitted light microscopy, or with a scanning electron microscope (SEM). All these species are relatively small, typical cranidial length usually being 6mm for P. (P.) concinnus and W (W.) stokesii species, and less than this for H. (H.) maura and W. (W.) scutterdinensis. In the following sections, sensory fields are described for each species and the data summarised as sensory field maps.

5.2. PROETUS (PROETUS) CONCINNUS (DALMAN, 1827).

5.2a. Material

The specimens examined (thin-sections (TS) PRO 1-47, SEM stubs (SEM) PRO 1-48) were collected from the Much Wenlock Limestone Formation (Homerian) at Wren's Nest, Dudley, West Midlands; and from localities 43 and 64 of Thomas (1978). Additional material was loaned by the Sedgwick Museum, Cambridge (specimens A95471a, A95512, A95524, A95612a, A95631, A95649a, A95657, A95681a, A95845a), and the National Museum of Wales, Cardiff (specimen NMW 76.6G.297).

5.2b. Cuticular structure

For detailed descriptions of this species, see Owens (1973), p. 12-15, pl. 2, figs. 14, 15; pl. 3, figs. 1-9; and Thomas (1978), p. 36-37, pl. 9, figs. 1-9.

Proetus (Proetus) concinnus is the type species of the genus Proetus, the members of which commonly appear to have a surface sculpture of fine pitting on the field of the free cheek (Owens 1973). Thomas (1978) also recognised the presence of a fine granular sculpture on the exoskeleton of some specimens of P. (P.) concinnus but did not regard it as of taxonomic significance. Typical specimen sizes are given in Owens (1973), and cuticle thickness varies from 65-160µm depending on the size of the individual. In all, the prismatic layer forms a tenth of the total cuticle thickness.

This study shows that P. (P.) concinnus is characterised by a granular surface microstructure covering the whole of the dorsal exoskeleton, apart from the eye socle, the posterior border of the free cheek, and within furrows. The granules each have a central canal (Plate 5.9a) and occur in densities of 13-15 per 100µm^2 (Plate 5.1a, b). Although the size of the granules is constant for a particular

specimen, there is some intraspecific variation, with granule sizes ranging from 10-15μm diameter. Lack of granulation is a result of poor preservation: such specimens are seen to be recrystallised when examined by SEM. On the margins of the cephalon, between the ridges, the concentration of granules diminishes to approximately 7 per 100μm² (Plate 5.1a, c). In one specimen, granules and socket pits (both 10μm diameter) were present between ridges (Plate 5.1d), at a joint concentration of 6 per 100μm². The field of the free cheek in small specimens may also have a lower concentration of granules. Here, as in areas between marginal ridges, cell polygons (5μm diameter) are commonly present (Plate 5.1c, Plate 5.2a, b).

More consistent intraspecific variation involves the surface features of the field of the free cheek. This is related to the size of the individual, and hence stage of ontogenetic development. The smaller specimens have granules at densities of approximately 5 per 100μm² with no indication of "pitting" (Plate 5.2a). Larger individuals develop circular areas (50μm diameter) devoid of granulation which resemble dimples (Plate 5.2c). Sometimes these dimples are genuinely depressed areas of cuticle, and together with their lack of granules, this creates the impression of pitting (Owens 1973). These structures are better described as dimples as they are areas lacking other surface sculpture and do not contain canals (Plate 5.2d). One large holaspid appeared to have much more pronounced dimples. When examined by SEM the effect was found to be caused by the arrangement of 20μm diameter tubercles with central canals, encircling slightly depressed areas of cuticle (150μm diameter) lacking other surface features (Plate 5.2e, f).

The eye socle lacks granulation but contains canals 5μm diameter at a concentration of 4 per 100μm², for example (SEM)PRO 35. Granules are

also absent from the posterior border of the free cheek. There, pits approximately 4-8μm in diameter, occur at densities of 15 per 100μm². The cuticular microstructure of the thoracic segments is unknown. The dorsal surface of the pygidium is covered by granules except within furrows. On the axis these increase in size to 20μm diameter, for example in (SEM)PRO 42.

The occipital pustule in the Proetidae is a domed structure (Miller 1976) in which the thickness of the cuticle decreases substantially on the visceral surface till just the prismatic layer remains (Plate 5.8d). No canals have been observed on the exterior.

Several hypostomes of P. (P.) concinnus have been examined by SEM, and also found to contain possible sensory structures. The most distinctive features are the terrace ridges on the margins, and especially the median body (Plate 5.3a). These terrace ridges have a height (h) of 10μm with a dip slope width (λ) of 70μm, and although always present, the exact pattern they form varies between specimens. The lateral parts of the median body are covered by tubercles (10μm diameter) at densities of 10 per 100μm², possibly containing central canals (Plate 5.3b). Canals (4μm diameter) are also present on the posterior wings (Plate 5.3c).

A sensory field map for the dorsal surface of P. (P.) concinnus is shown in Fig. 5.1A.

5.3. WARBURGELLA (WARBURGELLA) STOKESII (MURCHISON, 1839)

5.3a. Material

The specimens examined (thin-sections (TS) WAR 1-42, SEM stubs (SEM) WAR 1-26) came from the Much Wenlock Limestone Formation (Homerian), Wren's Nest, Dudley, and localities 43 and 64 of Thomas (1978).

Additional material was loaned by the Sedgwick Museum, Cambridge (specimens A95208, A95217a, A95332a, A95335, A95341a, A95348a, A95352a, A95353a, A95358a, A95382a, A95396, A95397a, A95399a, A95400a, A95401a, A95403, A95409, A95424, A95433, A95439a, A95450), and the National Museum of Wales, Cardiff (specimen NMW.83.2G.2).

5.3b. Cuticular structure

Detailed descriptions of this species can be found in Owens (1973), p. 67-70, pl. 13, figs. 5-13; pl. 14, fig. 2; and Thomas (1978), p. 50-51, pl. 13, figs. 1-10.

One of the most diagnostic features of W. (W.) stokesii is the presence of a preglabellar field, containing a bulbous preglabellar ridge and a thinner tropidium (Plate 5.4a). The preglabellar ridge does not appear to have canals or tubercles on its surface, however this may be due to loss of detail during diagenesis. Thin-sections show it to be a thickening of the cuticle on the dorsal surface. The tropidium, in thin-section, may sometimes be seen to have a canal running through to the crest (Plate 5.9b). However, surface preservation was never sufficiently good to determine whether these were true canals or just a single groove, as the crest of the ridge was always broken off (Plate 5.4b).

The cuticle thickness of W. (W.) stokesii varies from 40-160μm depending on the size of the specimen. The prismatic layer forms a tenth of the total cuticle thickness. Typical size ranges for this species are given in Owens (1973). As in P. (P.) concinnus, the cephalon of W. (W.) stokesii is mostly covered by a granular surface microstructure, but the granules, although 10μm in diameter are shallower than those of P. (P.) concinnus and present in sparser concentrations (10 per 100μm^2). (Plate 5.4a)

Due to the granulation of W. (W.) stokesii being less pronounced, cell polygons (5μm diameter) are more commonly visible, for example on the glabella (Plate 5.4c), the pygidial axis (SEM.WAR 13), the lateral border of the free cheek (A95450) and on thoracic segments (A95332a, A95424). On larger individuals, the glabellar granules grade into small, discontinuous ridges, most prominent towards the posterior (see Owens 1973, pl. 13, fig. 13b; and Thomas 1978, pl. 13, fig. 4). Both granulation and ridges are absent from furrows and muscle scars.

The surface microstructures on the pygidium of W. (W.) stokesii vary through ontogeny. Early meraspides, such as (SEM)WAR 1 are covered by granules (apart from within furrows) which become more concentrated (10 per 100μm²) on the margins. The axis has larger tubercles 20μm diameter, at densities of 5 per 100μm². In slightly larger specimens, for example (SEM)WAR 13, the fine granulation on the pleural fields has been replaced by 15μm diameter tubercles at densities of 5 per 100μm². Holaspides, such as (SEM)WAR 15 have pleural fields with even larger tubercles of 40μm diameter, 3 per 100μm².

The cuticular microstructures of thoracic segments are poorly known due to lack of sufficiently well-preserved specimens, however cell polygons have been identified. Thomas (1978) noted the presence of fine terrace ridges on the articulating facets. These may have acted as part of a ventilation system when the animal was enrolled, as suggested for similar structures in Symphysurus (Fortey 1986).

Terrace ridges on the hypostome of W. (W.) stokesii are in a similar position to those of P. (P.) concinnus, that is, confined to the central area of the median body and margins (Thomas 1978, pl. 13, fig. 10a). Relatively poor preservation prevented identification of further structures.

A sensory field map for W. (W.) stokesii is shown in Fig. 5.1B.

5.4. WARBURGELLA (WARBURGELLA) SCUTTERDINENSIS OWENS, 1973

5.4a. Material

The following account of cuticular microstructures are based on SEM examination of specimens War.scutt.1-4, collected from the Woolhope Limestone Formation (Sheinwoodian), at locality 38 of Thomas (1978).

5.4b. Cuticular structure

This species is described in Owens (1973), p. 70-71, pl. 14, figs, 4-7, text-fig. 9; and Thomas (1978), p. 52, pl. 13, figs. 11-15, 19.

Cuticle thickness of *W. (W.) scutterdinensis* is approximately 80μm with a prismatic layer 6μm thick, similar to that of *W. (W.) stokesii* specimens of similar size. This species is characterised by the presence of tropidial ridges rather than a tropidium, and lack of a preglabellar ridge.

The anterior border of the cranidium has terrace ridges (h=6μm) between which are 5μm diameter cell polygons (Plate 5.5a). The preglabellar field is covered by pores (presumably the openings of canals through the cuticle) 9μm diameter, at a concentration of 20 per 100μm^2 (Plate 5.5b). Tropidial ridges (h=5μm) lie to the margins of the preglabellar field (Plate 5.5b) and in the anterior half of the field of the free cheek. No canals were visible on the tropidial ridges but this may have been due to slight recrystallisation of the cuticle. The glabella, except within furrows, is covered by granules similar to those of *W. (W.) stokesii*.

One specimen of a free cheek (War.scutt.2) has a raised ridge covered in tubercles up to 30μm in diameter, rather than true tropidial ridges (Plate 5.5e). The rest of the field of the free cheek is composed of granules (10μm diameter) at a density of 10 per 100μm^2 (Plate 5.5e, f). Towards the genal spine, the granules grade into fine,

discontinuous anastomosing ridges (Plate 5.5d) similar to those from the glabella and palpebral lobes of W. (W.) stokesii. The posterior border of the free cheek is devoid of granulation and ridges, but no pitting is discernable either (Plate 5.5f), which may be a result of recrystallisation.

Cuticular microstructures on the thoracic segments and pygidia of W. (W.) scutterdinensis remain unknown, but the first example of a hypostome has been found (Plate 5.5c). Although fine surface detail has been lost, terrace ridges on the median body are seen to be much more abundant than those of P. (P.) concinnus (Plate 5.3a) or W. (W.) stokesii, extending to the margins of the median body. Scattered tubercles (15μm diameter) are present on the posterior margin.

A cephalic sensory field map of W. (W.) scutterdinensis can be seen in Fig. 5.2A.

5.5. HARPIDELLA (HARPIDELLA) MAURA ALBERTI, 1967

5.5a. Material

The following account of cuticular microstructure is based on specimens (TS)HAR 1-32, and (SEM)HAR 1-34, collected from the Farley Member of the Coalbrookdale Formation (Homerian) at locality 14 of Thomas (1978).

5.5b. Cuticular structure

British material of this species was described by Thomas (1978), p. 33-34, pl. 8, figs. 11, 12, 15, 17.

H. (H.) maura is a small species (typical cranidial sagittal length 3mm), and consequently has a thinner cuticle (25-75μm) than the proetides described above. The prismatic layer forms approximately one tenth of the total cuticle thickness. In transverse section, the

cranidium is highly convex (see Thomas 1978, pl. 8, fig. 17a), with relatively large tubercles on the preglabellar field, glabella, and field of the free cheek.

The margin of the anterior border is covered solely by granules (10μm diameter, 20 per 100μm²) rather than terrace ridges (Plate 5.6a). However in some specimens the granules are arranged in rows to give the impression of ridges (Plate 5.6b). This trend is also seen on the lateral border of the free cheek, where granules become more aligned towards the genal spine (Plate 5.6c). Granules (15μm diameter) also occur on pygidia at concentrations of 15 per 100μm², for example (SEM)HAR 15.

Cell polygons (5μm diameter) occur over all the cranidium, and the lateral margin and field of the free cheek. They tend to be more pronounced around the glabellar tubercles (Plate 5.7a).

Large tubercles occur on the preglabellar field, the posterior third of the glabella, the glabella lobes, and the posterior edge of the occipital ring. The size and number of tubercles is variable (20-90μm diameter; average 60μm diameter). Larger specimens have bigger tubercles. Some specimens only have tubercles on the preglabellar field, such as (SEM)HAR 1. Smaller tubercles (20-25μm diameter) occur on the field of the free cheek at densities of 1 per 100μm², for example (SEM)HAR 21.

In thin-section the tubercles are seen to be pierced by a central canal (Plate 5.8c). Sometimes the tubercles are topped by several nodes, the larger ones having more (Plate 5.7a, b). For example glabellar tubercles, 60μm diameter, have 3-5 nodes (10μm diameter) (Plate 5.7a) whereas preglabellar field tubercles (50-80μm diameter) have 6-8 nodes (Plate 5.7b). The occipital tubercle also appears to have a central canal (Plate 5.8c), however no canal openings were ever

Figure 5.1. Sensory field maps for the dorsal exoskeletons of two Homerian proetide trilobites.

A. Proetus (Proetus) concinnus (Dalman, 1827)

Outline based on specimen A10248, Sedgwick Museum, Cambridge. x4.

B. Warburgella (Warburgella) stokesii (Murchison, 1839)

Outline based on specimen A28256, Sedgwick Museum, Cambridge. x6.

Figure 5.2. Sensory field maps for the cranidia of two Wenlock proetide trilobites.

A. Warburgella (Warburgella) scutterdinensis Owens, 1973 (Sheinwoodian).

Outline based on Owens (1973), text-fig. 9A. x12.5.

B. Harpidella (Harpidella) maura Alberti, 1967 (Homerian).

Outline based on specimens (SEM)HAR 3A, (SEM)HAR 21. x30.

visible on the surface. A cephalic sensory field map is shown in Fig. 5.2B.

5.6. DISCUSSION

The above descriptions demonstrate the gross similarity of cuticular features within proetide trilobites. They all have prismatic layers which form approximately one tenth of the total cuticle thickness, and relatively small cell polygons of 5μm diameter. Cell polygons of other trilobite groups are typically 15-20μm across (Section 4.2b). The cephalic doublures form tube-like structures which are mechanically strong (Chapter 7), and all possess an occipital pustule.

The internal organisation of the proetid occipital dome is very similar to that of the glabellar 'tubercle' in Nileus, which, from its position and internal structure is thought to have been a light-sensitive organ (Fortey and Clarkson 1976). The Proetus occipital pustule is likely to have had a similar function despite its domed appearance as the internal morphology is the same. A photoreceptor in such a highly elevated position is not an unreasonable assumption. The occipital pustule in W. (W.) stokesii is also domed, but it was not possible to determine the exact internal morphology. By contrast, the H. (H.) maura occipital pustule is a tubercle with a central canal, so although the occurrence of an occipital pustule is common to all proetides, the internal structure varies within the Order. This is also true of the pre-occipital glabellar pustule in the Asaphina (as defined by Fortey and Chatterton [1988]).

The sensory fields identified in the proetide species, although being species-specific, have some broad similarities. None appears to

have conventional pore canals, yet granules with pores are widespread. It is not possible to determine whether these structures were secretory or sensorial (or indeed both) in function. The cephalic margins have a narrow field containing either a dense concentration of granules, rows of aligned granules, or ridges with sparse granulation. Most of the cuticular structures are concentrated towards the anterior or on elevated parts of the exoskeleton, for example the preglabellar field, the posterior of the glabella, and the pygidial axis. These are the best situations for sense organs, especially chemoreceptors. Perhaps this is one reason for the development of more pronounced posterior glabellar ridges on W. (W.) stokesii compared to the earlier species W. (W.) scutterdinensis.

The tropidium of W. (W.) stokesii has been interpreted as comprising a tube (half made of chitin, and half of a more fleshy substance) that could have distributed vital fluids across the cephalon (Přibyl and Vaněk, 1987). This interpretation seems unlikely in view of thin-section data. The tropidium is not tube-like in structure, and had the same calcitic composition throughout (Chapter2). The presence of either canals or a central groove opening to the exterior suggests that the tropidium was some form of sensory structure rather than part of a circulatory system.

The eye socle of the proetides studied is lacking in much surface microstructure. Simple canals normal to the outer surface may be present in low concentrations, but the surface is essentially smooth. This is in contrast to Clarkson's (1975) observations of the eye socles of Paladin eichwaldi (King) and Cummingella brevicauda (Goldring) which have distinct ridges and grooves, possibly leading to canals.

The two proetide species P. (P.) concinnus and W. (W.) stokesii are the two most numerous trilobites in the Much Wenlock Limestone

Formation (Thomas 1979). Although V. (W.) stokesii may have preferred slightly deeper water (Thomas 1979), the two species inhabited broadly the same environment; that is, a warm, shallow-water shelf sea which contained much carbonate mud (Ratcliffe 1987). Contrasts in cuticular surface features may have aided species recognition, or more likely, indicates that they inhabited separate ecological niches within this environment.

Despite the species-specifity of trilobite cuticular microstructure highlighted by this research, such features are of limited use in taxonomy due to their great vulnerability to destruction during diagenesis. In many of the specimens examined, recrystallisation of the exoskeleton has obliterated fine surface details.

Some proetides have been found in possible life positions, partially burrowed in subtidal deposits (Brezinski 1986, 1988). Similar life positions have been reported in illaenimorphs (Stitt 1976; Westrop 1983), the phacopid Phacops rana (Zell 1988), and inferred for the nileid Symphysurus palpebrosus (Fortey 1986). Other, small spiny proetides have been suggested as having been planktic organisms (Cisne 1970).

Tuberculate proetide species have been interpreted as needing thicker exoskeletons for added strength (Fortey 1979; McNamara and Fordham 1981), or as a means of camouflage in coarse sediments (Brezinski 1988). These suggestions are unlikely to be valid for the Wenlock proetides Cyphoproetus depressus and H. (H.) maura which occur in pure sparry algal limestones, and deep water shelf limestones respectively (Thomas 1979).

The large number of wide and narrow (exsag.) thoracic segments of some aulacopleurids may be an adaptation to low oxygen environments (Fortey and Chatterton 1988, p. 197), as with olenids (Fortey 1985). H.

(H.) maura is most commonly found in somewhat deeper water sediments of the shelf slope than the other species studied (Thomas 1979), which may have been less well oxygenated. This may also account for the small size of H. (H.) maura, since small animals have a greater relative surface area for oxygen uptake. Reduced illumination near the base of the palaeoslope may have caused this species to place more emphasis on chemoreception; a possible function of the numerous tubercles on the dorsal surface.

5.7. REFERENCES

ALBERTI, G. K. 1967. Neue obersilurische sowie unter-und mitteldevonische Trilobiten aus Marokko, Deutschland und einigen anderen europäischen Gebieten. 2. Senckenberg. leth., 48, 481-509, 1pl.

BREZINSKI, D. K. 1986. Trilobite associations from the Chouteau Formation (Kinderhookian) of central Missouri. J. Paleont., 60, 870-881.

BREZINSKI, D. K. 1988. Trilobites of the Gilmore City Limestone (Mississippian) of Iowa. J. Paleont., 62, 241-245.

CISNE, J. L. 1970. Constantina pulcra: an unusual proetid trilobite from the Devonian of Pennsylvania. J. Paleont., 44, 522-523.

CLARKSON, E. N. K. 1975. The evolution of the eye in trilobites. Fossils Strata, 4, 7-31.

DALMAN, J. W. 1827. Om Palaederna, eller de så kallade Trilobiterna. K. svenska Ventensk Akad. Handl. (for 1826), 113-152, 226-294, pls. 1-6.

EVITT, W. R. and TRIPP, R. P. 1977. Silicified middle Ordovician trilobites from the families Encrinuridae and Staurocephalidae. Palaeontograghica, Abt A, 157, Lfg. 4-6, 109-174, 24 pls.

FORTEY, R. A. 1979. Early Ordovician trilobites from the Catoche Formation (St. George Group), Western Newfoundland. Bull. geol. Surv. Can., 321, 61-114, pls. 23-37.

FORTEY, R. A. 1985. Pelagic trilobites as an example of deducing the life habits of extinct arthropods. Trans. R. Soc. Edinb., 76, 219-230.

FORTEY, R. A. 1986. The type species of the Ordovician trilobite Symphysurus: systematics, functional morphology and terrace ridges. Paläont. Z. 60, 3/4, 12 Abb. 255-275.

FORTEY, R. A. and CHATTERTON, B. D. E. 1988. Classification of the trilobite suborder Asaphina. Palaeontology, 31, 165-222, pls. 17-19.

FORTEY, R. A. and CLARKSON, E. N. K. 1976. The function of the glabellar "tubercle" in Nileus and other trilobites. Lethaia, 9, 101-106.

McNAMARA, K. J. and FORDHAM, B. G. 1981. Mid-Cautleyan (Ashgill Series) trilobites and facies in the English Lake District. Palaeogeog. Palaeoclimatol. Palaeoecol., 34, 137-161.

MILLER, J. 1976. The sensory fields and mode of life of Phacops rana (Green, 1832) (Trilobita). Trans. R. Soc. Edinb. 69, 337-367, pls. 1-4.

MURCHISON, R. I. 1839. The Silurian System, founded on geological researches in the counties of Salop, Hereford, Radnor, Montgomery, Caermarthen, Brecon, Pembroke, Monmouth, Gloucester, Worcester, and Stafford; with descriptions of the coalfields and overlying formations. xxxii +768pp., 37pls. London.

PŘIBYL, A, and VANĚK, J. 1987. Phylogeny of several lineages of the trilobite family Tropidocoryphidae (Proetacea). In POKORNÝ, V. (ed.). Contribution of Czechoslovak Palaeontology to evolutionary science, 1945-1985. 62-72, 1 pl. Prague.

OWENS, R. M. 1973. British Ordovician and Silurian Proetidae (Trilobita). Palaeontogr. Soc. [Monogr.]. 98pp., pls. 1-15.

RATCLIFFE, K. T. 1987. Sedimentology, palaeontology and diagenesis of the Much Wenlock Limestone Formation. Ph.D thesis (unpubl.), Aston University.

ŠNAJDR, M. 1987. Bohemian Lower Devonian Odontochilinae. Sbor. geol. ved. Palaeont., 28, 9-60, 20 pls.

STITT, J. H. 1976. Functional morphology and life habits of the Late Cambrian trilobite Stenopilus pronus Raymond. J. Paleont., 50, 561-576.

THOMAS, A.T. 1978. British Wenlock trilobites (Part 1). Palaeontogr. Soc. [Monogr.]. 1, 1-56, pls. 1-14.

THOMAS, A. T. 1979. Trilobite associations in the British Wenlock. In HARRIS, A. L., HOLLAND, C. H. and LEAKE, B. E. (eds.). Geol. Soc. Sp. Pub. 8: The Caledonides of the British Isles -reviewed. 447-451. Published for The Geological Society by Scottish Academic Press.

TRIPP, R. P. 1957. The trilobite Encrinurus multisegmentatus (Portlock) and allied Middle and Upper Ordovician species. Palaeontology, 1, 60-72, pls. 11, 12.

WESTROP, S. R. 1983. The life habits of the Ordovician illaenine trilobite Bumastoides. Lethaia, 16, 15-24.

ZELL, P. D. 1988. Burrowed Phacops rana from the Moscow Formation of New York. J. Paleont., 62, 311-312.

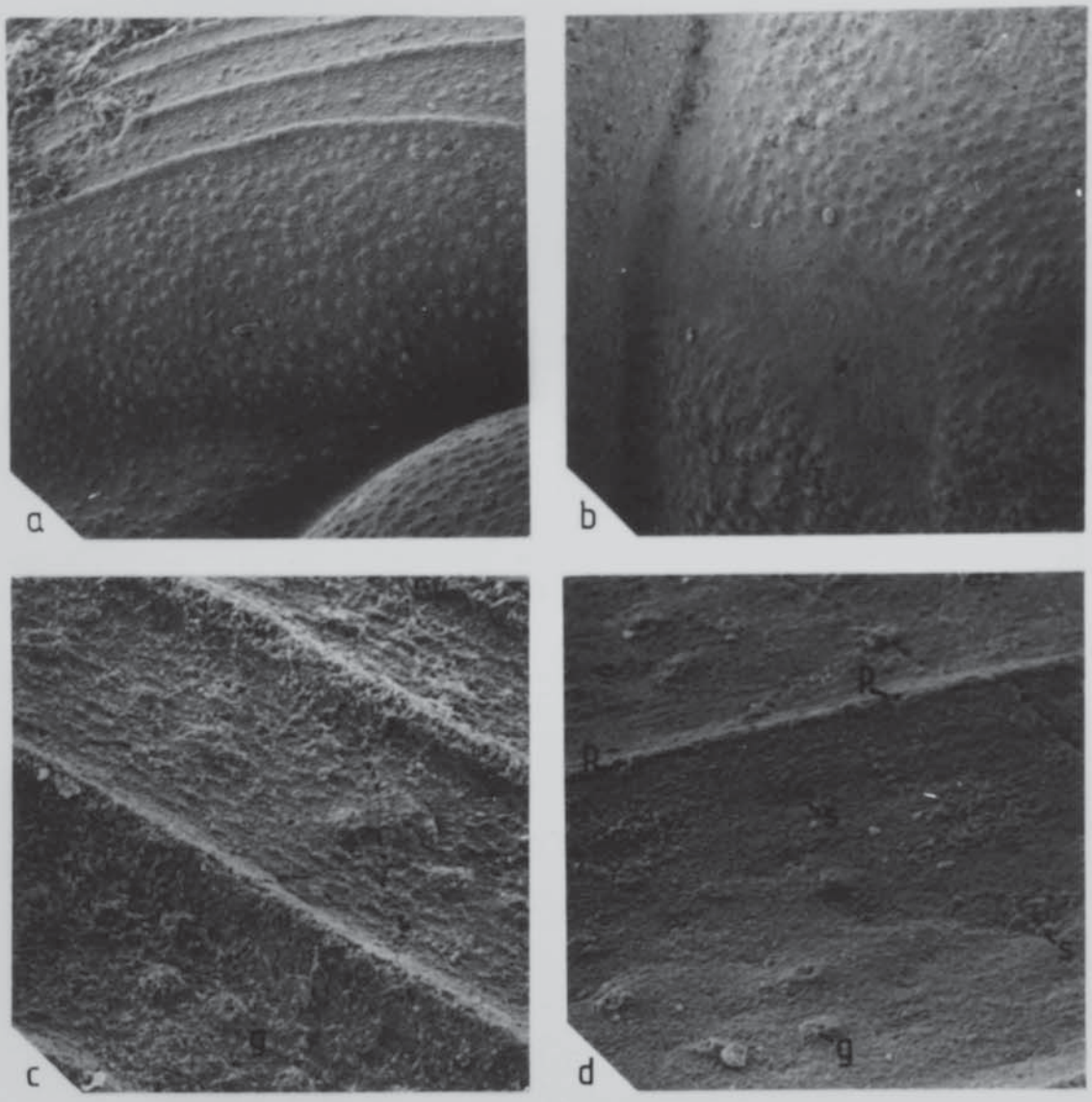

Plate 5.1. Surface granulation on *Proetus (Proetus) concinnus* (Dalman).

a, P. (P.) concinnus Locality 43 of Thomas (1978), Homerian. (SEM)PRO.5. Anterior border and glabella with granulation. x100.
b, P. (P.) concinnus Locality 43 of Thomas (1978), Homerian. (SEM)PRO.6. Glabella and palpebral lobe. Note the absence of granulation within furrows. x100.
c, P. (P.) concinnus Locality 43 of Thomas (1978), Homerian. (SEM)PRO.7. Lateral border of free cheek. Note the presence of granules with central pores 4µm diameter (g) between the ridges, and cell polygons on the surface. x500
d, P. (P.) concinnus Locality 64 of Thomas (1978), Homerian. (SEM)PRO.33. Lateral border of free cheek with granules (g) and socket pits (s), both 10µm diameter, between the ridges. Note two pores 4µm diameter (p) on the crest of the ridge. x500.

Plate 5.2. Surface microstructure of the free cheek of *Proetus (Proetus) concinnus* (Dalman).

a, P. (P.) concinnus Locality 43 of Thomas (1978), Homerian. (SEM)PRO 11. Granules (12μm diameter) and cell polygons on the field of the free cheek. No "dimples" are present. x500.
b, P. (P.) concinnus Locality 43 of Thomas (1978), Homerian. (SEM)PRO 11. Cell polygons (5μm diameter) on the field of the free cheek. Note also the crystals (c), 1μm diameter, of the prismatic layer. x3000.
c, P. (P.) concinnus Locality 43 of Thomas (1978), Homerian. (SEM)PRO 13. Field of free cheek with circular areas, devoid of granulation, which give a "dimpled" effect. x100.
d, P. (P.) concinnus Locality 43 of Thomas (1978), Homerian. (SEM)PRO 12. Field of free cheek. Circular areas lacking granulation are slightly depressed, creating a stronger dimpled effect. x100.
e, P. (P.) concinnus Locality 64 of Thomas (1978), Homerian. (SM)A95612a. General view of lateral border and field of free cheek. Ordinary granulation present on the lateral border, but rings of tubercles (20μm diameter) occur on the field of the free cheek. x50.
f, P. (P.) concinnus Locality 64 of Thomas (1978), Homerian. (SM)A95612a. Ring of tubercles on the free cheek surrounding an area (150μm diameter) lacking other surface sculpture. x400.

PLATE 5.2

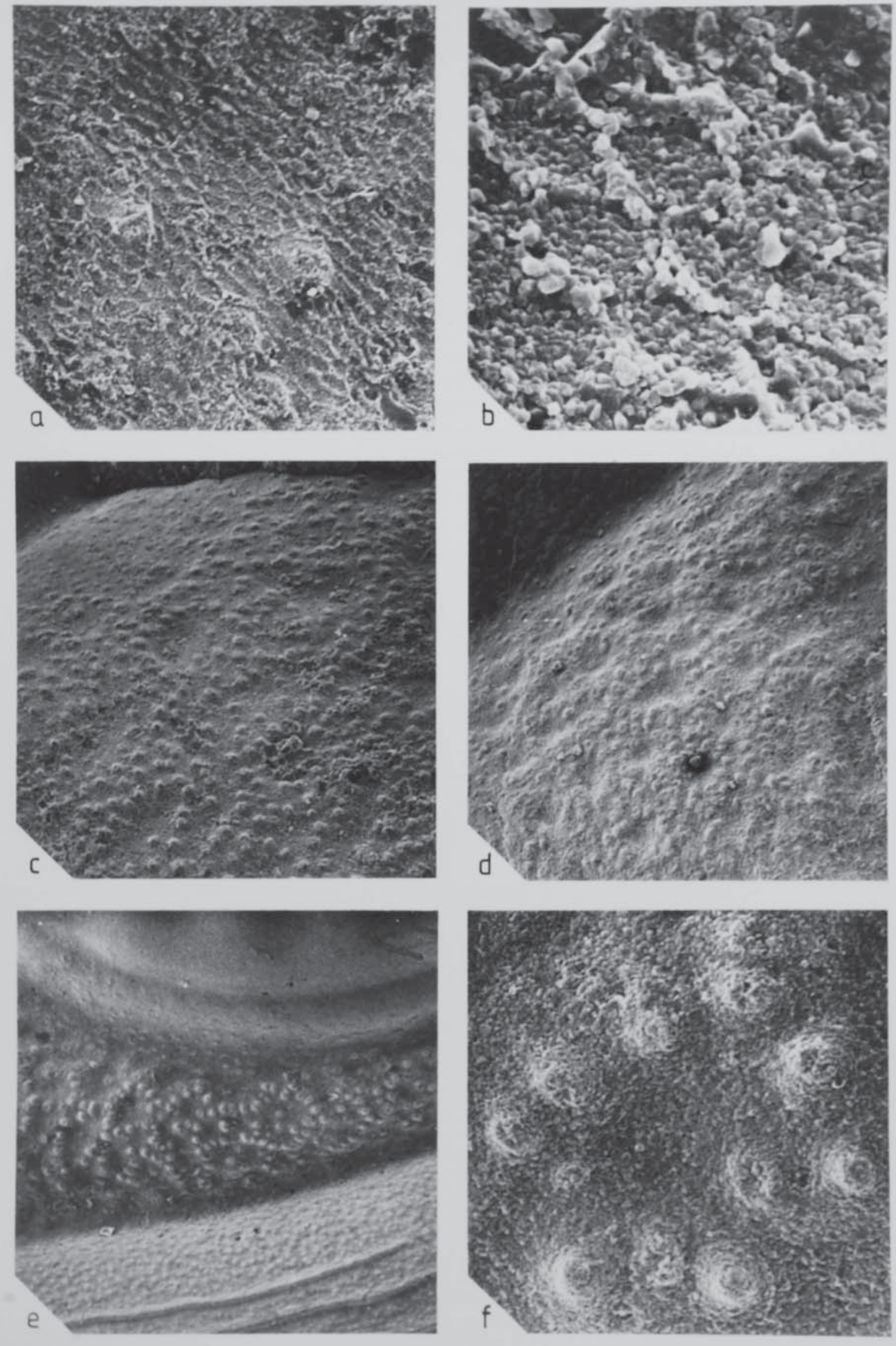

Plate 5.3. Surface microstructure of the hypostome of *Proetus (Proetus) concinnus* (Dalman).

a, P. (P.) concinnus Locality 64 of Thomas (1978), Homerian. (SEM)PRO 17. General view of hypostome, anterior on right hand side. x30.

b, P. (P.) concinnus Locality 64 of Thomas 1978), Homerian. (SEM)PRO 17. Median body of hypostome with central terrace ridges (h=10μm, λ=70μm), and low pustules (10μm diameter) towards the border furrow. x100.

c, P. (P.) concinnus Locality 64 of Thomas (1978), Homerian. (SEM)PRO 17. Posterior wing of hypostome with canal openings, 4μm diameter. x300.

PLATE 5.3

a

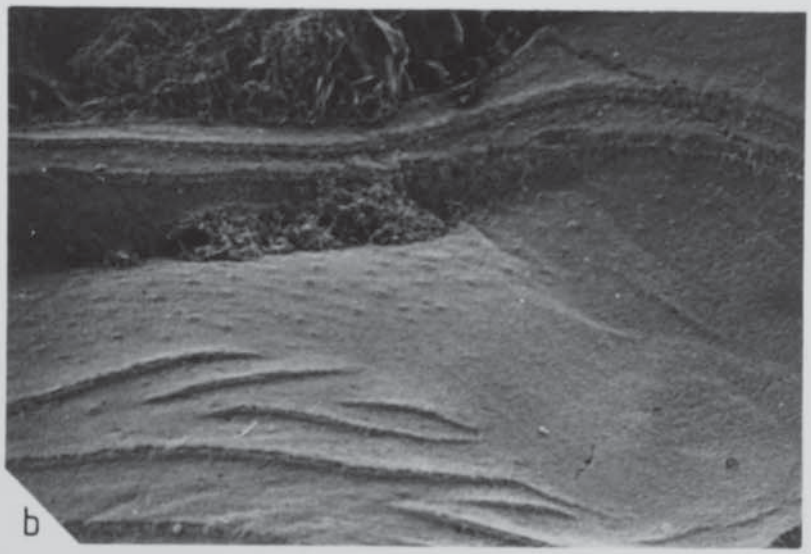

b

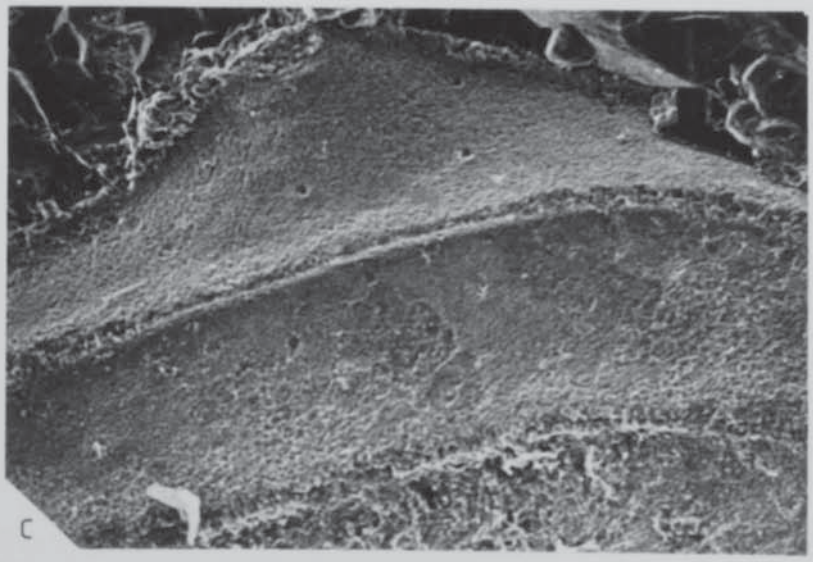

c

Plate 5.4. Scanning electron micrographs of *Warburgella (Warburgella) stokesii* (Murchison).

a, W. (W.) stokesii Locality 64 of Thomas (1978), Homerian. (SEM)WAR 23. Anterior of cranidium, with bulbous preglabellar ridge (r), and tropidium (t). Note granulation (g) on glabella which is less distinct than that of P. (P.) concinnus, x50.

b, W. (W.) stokesii Locality 39 of Thomas (1978), Homerian. (SM)A95382a. Typical preservation of a tropidium on a free cheek, with broken off crest. x300.

c, W. (W.) stokesii Locality 64 of Thomas (1978), Homerian. (SEM)WAR 12. Cell polygons (5μm diameter) on the glabella. x500.

PLATE 5.4

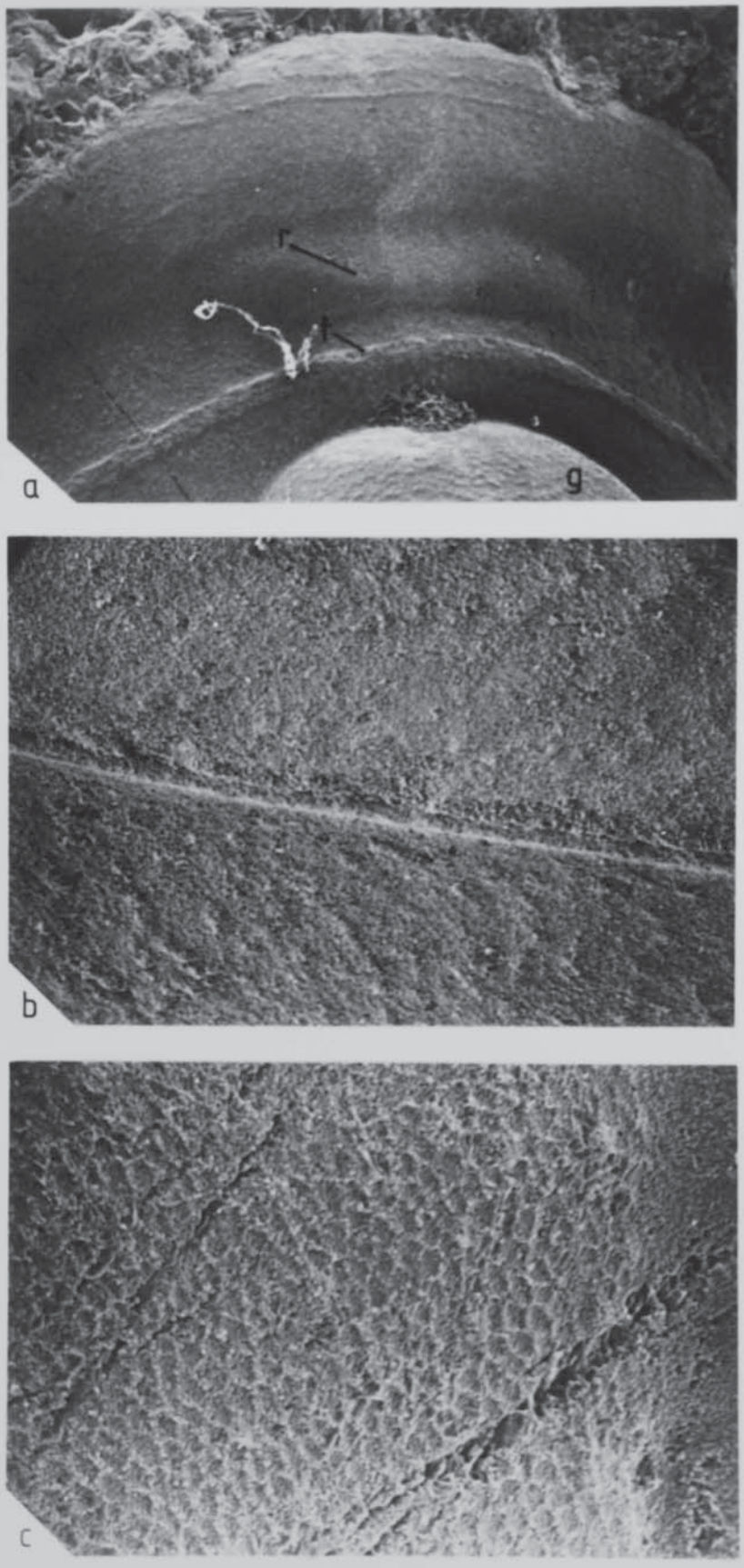

Plate 5.5. Surface cuticular structure on *Warburgella (Warburgella) scutterdinensis* Owens.

a, W. (W.) scutterdinensis Locality 38 of Thomas (1978), Sheinwoodian. War.scutt.3. Anterior border of cranidium with ridges (h=6μm) and cell polygons (5μm diameter. x350.
b, W. (W.) scutterdinensis Locality 38 of Thomas (1978), Sheinwoodian. War.scutt.3. Tropidial ridges (h=5μm) on preglabellar field. The rest of the field is covered by canals (9μm diameter). x350.
c, W. (W.) scutterdinensis Locality 38 of Thomas (1978), Sheinwoodian. War.scutt.4. Only known example of a hypostome, anterior to right hand side. x350.
d, W. (W.) scutterdinensis Locality 38 of Thomas (1978), Sheinwoodian. War.scutt.2. Surface microstructure on genal spine, with terrace ridges on the borders and small, anastomosing ridges in the centre. x75.
e, W. (W.) scutterdinensis Locality 38 of Thomas (1978), Sheinwoodian. War.scutt.2. "Tropidial ridges" of free cheek consisting of an alignment of closely packed tubercles, up to 30μm diameter. The rest of the field of the free cheek is covered by granules (10μm diameter) at a density of 10 per 100μm^2. x70.
f, W. (W.) scutterdinensis Locality 38 of Thomas (1978), Sheinwoodian. War.scutt.2. Field of free cheek with granulation, and posterior border lacking surface sculpture. x70.

PLATE 5.5

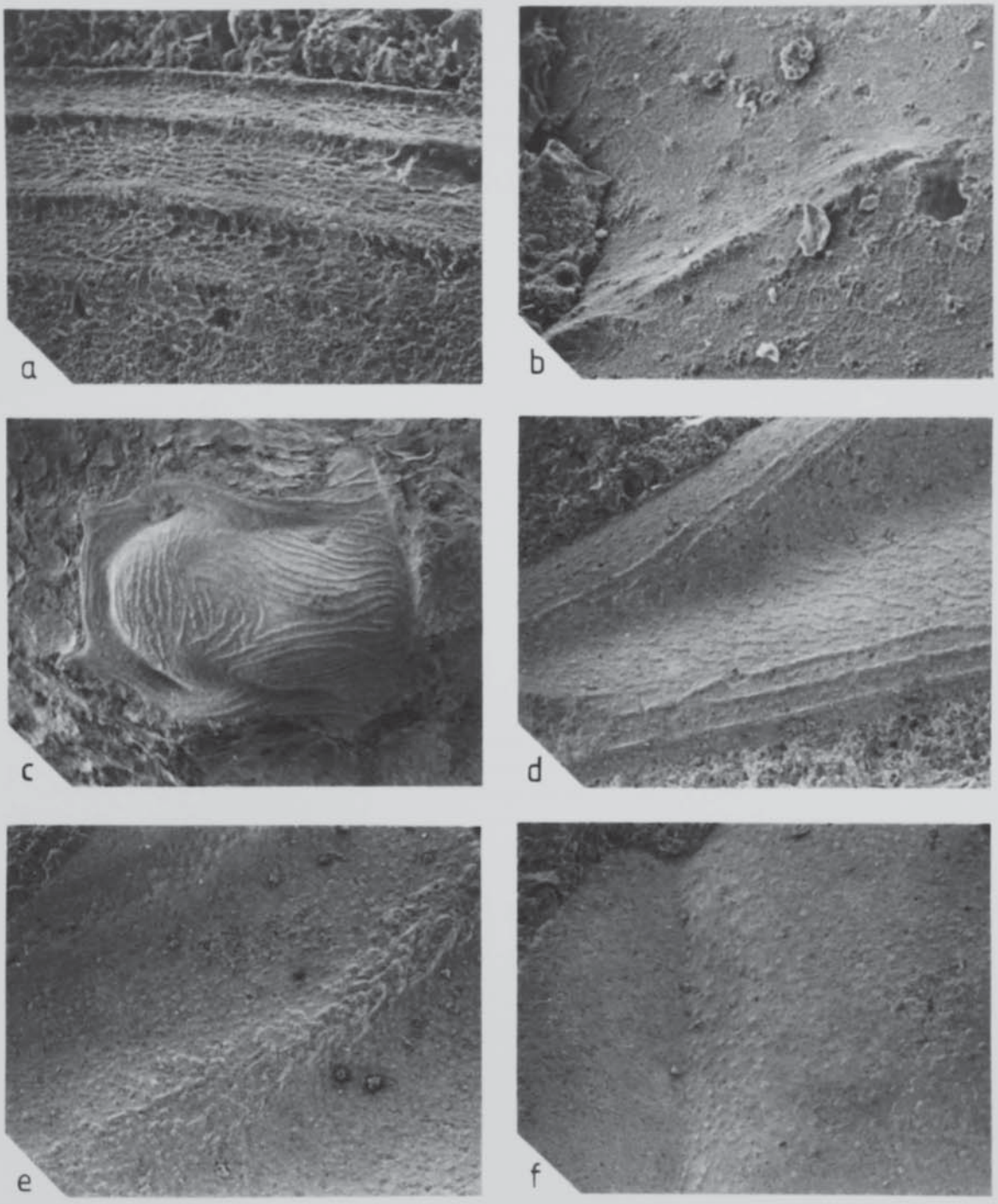

Plate 5.6. Surface microstructure on *Harpidella (Harpidella) maura* Alberti.

a, H. (H.) maura Locality 14 of Thomas (1978), Homerian. (SEM)HAR 8. Anterior border of cranidium with granules (10μm diameter) at a density of 20 per 100μm². x200.

b, H. (H.) maura Locality 14 of Thomas (1978), Homerian. (SEM)HAR 11. Anterior border of cranidium. Granules are arranged in rows to produce ridges. x200.

c, H. (H.) maura Locality 14 of Thomas (1978), Homerian. (SEM)HAR 13. General view of free cheek. Lateral border with granules grading into ridges towards the genal spine. Coarse tuberculation is present on the field of the free cheek, which has a pitted internal mould. x30.

PLATE 5.6

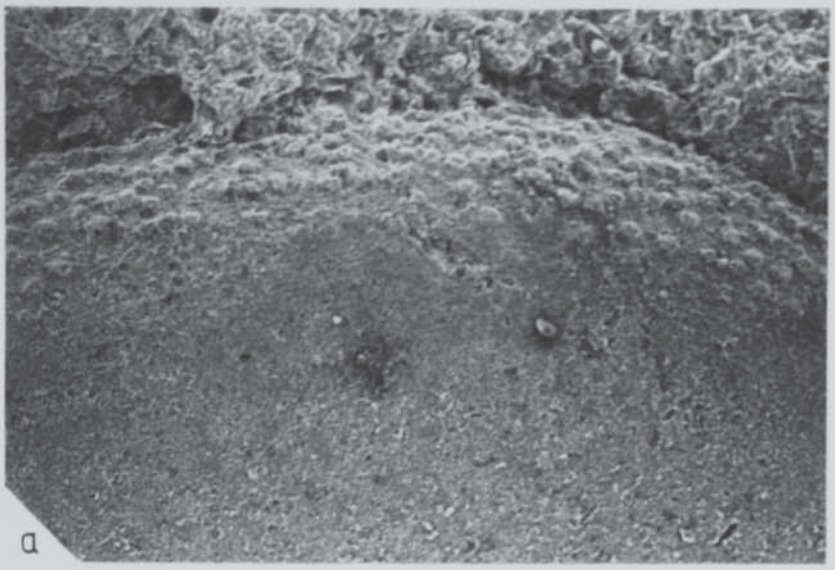

a

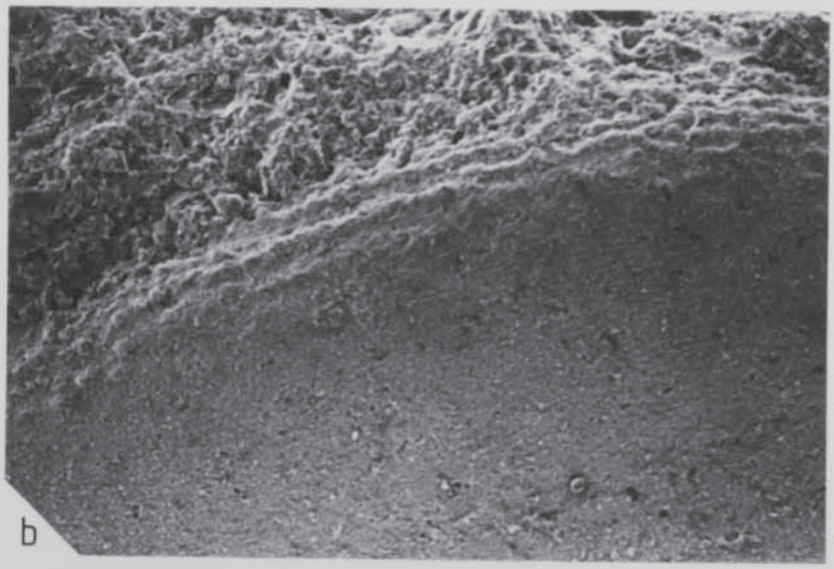

b

c

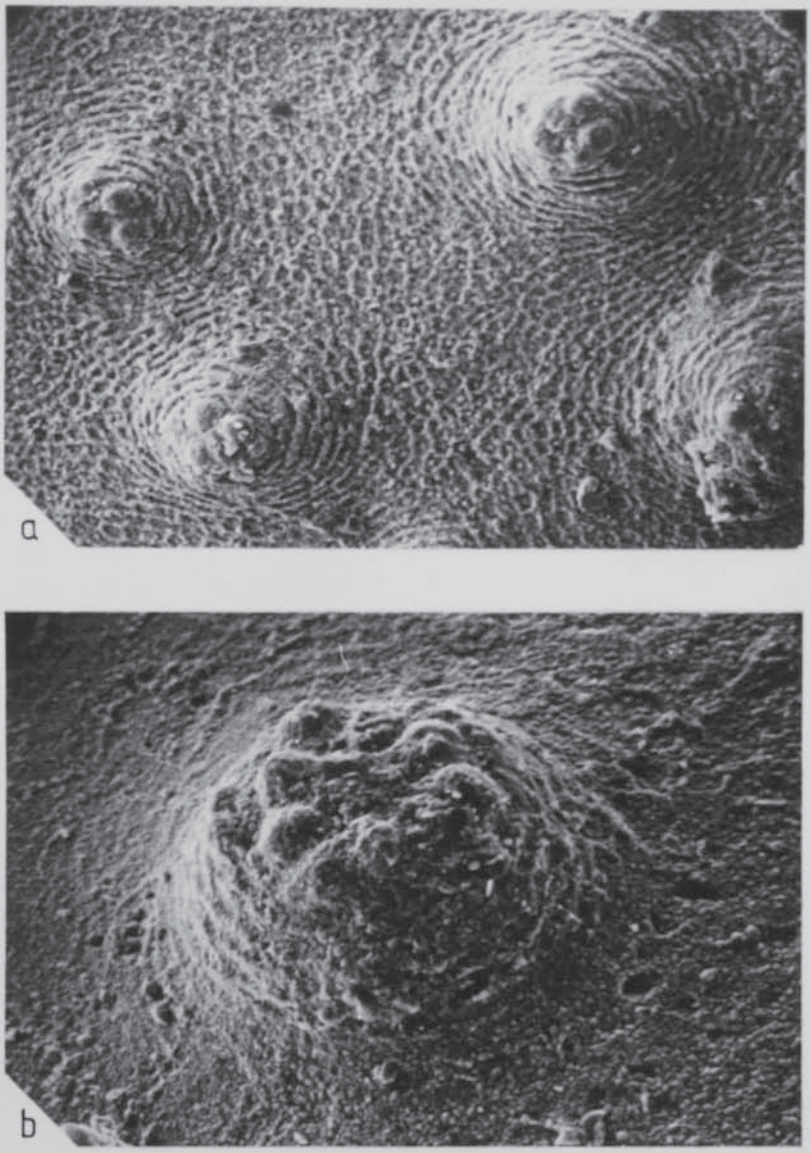

Plate 5.7. Tubercles on *Harpidella (Harpidella) maura* Alberti.

a, H. (H.) maura Locality 14 of Thomas (1978), Homerian. (SEM)HAR 29. Scanning electron micrograph of glabella tubercles with nodes, and cell polygons 5µm diameter. x400.
b, H. (H.) maura Locality 14 of Thomas (1978), Homerian. (SEM)HAR 29. Scanning electron micrograph of a tubercle on the preglabellar field, 80µm diameter. x800.

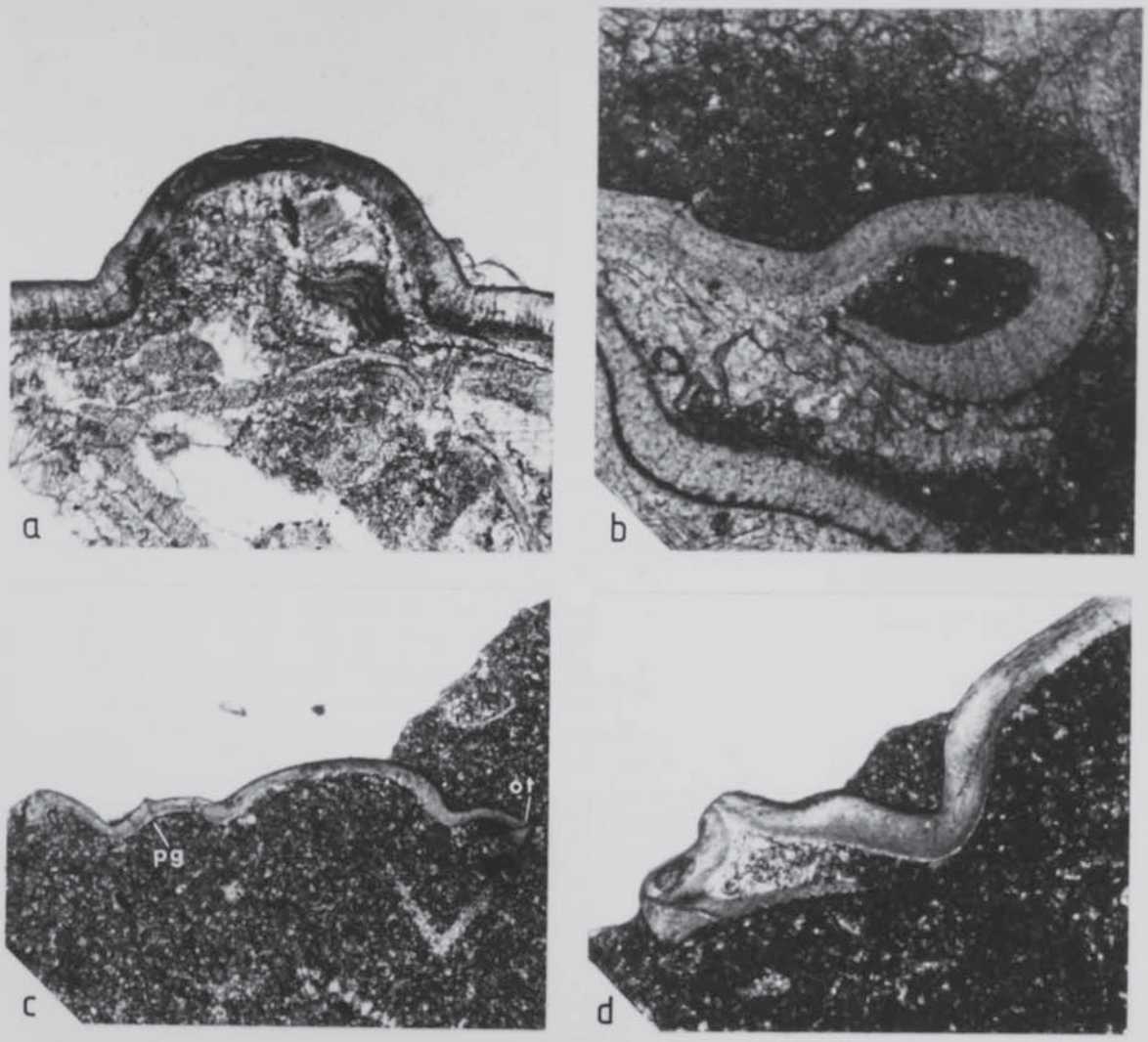

Plate 5.8. Photomicrographs of thin-sections through Wenlock proetide trilobites.

a, Proetus (Proetus) concinnus (Dalman). Locality 64 of Thomas (1978), Homerian. (TS)PRO 12. Transverse section through a pygidium revealing numerous fine canals (1µm diameter). x35.
b, Warburgella (Warburgella) stokesii (Murchison). Wren's Nest, Dudley, West Midlands (Homerian). (TS)14.10. Transverse section through a free cheek showing the tropidium with a central canal, and the tube-like doublure which has canals running to the ridge crests. x65.
c, Harpidella (Harpidella) maura Alberti. Locality 14 of Thomas (1978), Homerian. (TS)HAR 7. Longitudinal section through a cranidium, showing a canal running through a preglabellar field tubercle (pg), and also through the occipital tubercle (ot). x25.
d, Proetus (Proetus) concinnus (Dalman). Locality 14 of Thomas (1978), Homerian. A95512. Sagittal section through the occipital tubercle. Note the dramatic thinning of the cuticle on the visceral surface. x40.

CHAPTER 6

CUTICULAR STRUCTURE OF THE AGNOSTINE TRILOBITE *HOMAGNOSTUS OBESUS*

ABSTRACT. Study of the exoskeletal surface microstructure of *Homagnostus obesus* has yielded information about the structure of agnostine cuticle. It is likely that the very thin agnostine cuticle (5-15μm), unlike that of polymerid trilobites, was constructed only from prismatic layer. The exoskeletons were strengthened by reticulation on the external surface, which forms up to 15% of the total cuticle thickness. Pits occurring on the visceral surface of the exoskeleton of *H. obesus* may have contained photoreceptors as their morphology is similar to that of the *Nileus* glabellar 'tubercle'. This would have allowed the animal to monitor changes in light intensity. Possible sensory receptors in other agnostine trilobites are reviewed. Most sense organs were positioned on the unmineralised ventral surface of the organism.

6.1. Introduction

AGNOSTINA (informal agnostine) are some of the most distinctive trilobites, due to their small size, possession of only two thoracic segments, and extremely thin cuticles (only 5-15μm thick, see Appendix 3). Yet despite being well known taxonomically, the life habits of agnostines remain the subject of controversy. Cuticular studies can aid these discussions by identifying possible sensory structures; such research has been carried out recently (Müller and Walossek 1987) on

exceptionally preserved specimens of Agnostus pisiformis (Wahlenberg, 1818). That study, together with additional data on Homagnostus obesus (Belt, 1967) are used to discuss the extent of sensory perception in the Agnostina.

6.2. CUTICULAR STRUCTURE OF HOMAGNOSTUS OBESUS.

6.2a. Material and preservation

The cuticular structure of Homagnostus obesus (Belt, 1867) has been studied using well-preserved specimens from Andrarum, Skåne, Sweden (Upper Cambrian). The material consists of many disarticulated ontogenetic stages (see Rushton 1983, text-fig. 4 for illustration of some instars) which have been made into thin-sections O.w.1-4, and SEM stubs O.w.1-33. Only approximately one tenth of the specimens were sufficiently well preserved to reveal any fine detail. Those that did were most commonly early meraspides, larger specimens tended to be more coarsely recrystallised. This is similar to the phenomenon described by Müller and Walossek (1987), where exceptional preservation of Agnostus pisiformis (Wahlenberg, 1818) through phosphate replacement is restricted to specimens less than 1-2mm long.

6.2b. Cuticular structures

The cuticle of H. obesus is very thin, being only 5-10μm thick, but may retain fine surface details despite being recrystallised internally. Often the outlines of calcite crystals (1-2μm diameter) forming the prismatic layer are visible on the external surface (Plate 6.1b, c) or external mould (Plate 6.1d, e). On one specimen, both the external mould and visceral surface of the cuticle appeared to retain

impressions of prismatic layer crystals (Plate 6.1f), suggesting that the exoskeleton was composed only of prismatic layer. This is consistent with the thinness of the cuticle, which is comparable or less to just the prismatic layer of polymerid trilobites.

The most distinctive feature of the calcitic exoskeleton of H. obesus is the well defined reticulation on the dorsal surface (Plate 6.1). Polygonal structures 10-15μm diameter (cell polygons) probably represent the surface expression of epidermal cells which secreted the cuticle (see Section 4.2b). The cell polygons are the same size in all the specimens, they are just more numerous in larger individuals. Similar cell polygons 10-20μm diameter are also present on the agnostines Ptychagnostus gibbus (Plate 6.2a) and Agnostus pisiformis (Müller and Walossek 1987, pl. 1, fig. 2; pl. 7, figs. 2-8; pl. 8, figs. 1, 5) but are less pronounced. The reticulation is delimited by an interconnected network of raised ridges (the tops of interprismatic septa) which surround each polygon. These ridges may form as much as 15% of the total cuticle thickness.

The cuticle fragments of H. obesus appear to lack canals and pustules. The lack of external sensory receptors on the dorsal exoskeleton indicates that the animal gained most of its information about the environment from receptors located on the unmineralised ventral surface. Indeed, many setae, bristles, and other possible sense organs have been documented from the appendages and ventral membrane of Agnostus pisiformis (Müller and Walosek 1987). However, the visceral surface of the dorsal exoskeleton of H. obesus is uniformly covered by a series of pits 3-6μm diameter, at a density of 36 per 100μm^2 (Plate 6.1f). They have no expression on the dorsal surface and do not

correspond to the positions of overlying cell polygons. On internal moulds these pits take the form of domed structures (Plate 6.1a). No such structures have been observed in any other agnostine.

6.2c. Discussion

The distribution of the pits is inconsistent with them having been muscle insertion areas, and they cannot have been the sites of external mechanoreceptors or chemoreceptors since they are not connected to the exterior. However it is possible that they may have contained photoreceptors and functioned rather like primitive trilobite eyes, in the manner of the Nileus glabellar 'tubercle' (Fortey and Clarkson 1976). Light could have been directed through the c-axes of the calcite crystals in the prismatic layer, onto the cavities below. Sensory neurons within the pits stimulated by the light rays, would then have transmitted the information to the central nervous system.

Behavioural tests have shown that many crustaceans exhibit a general dermal light sensitivity after their compound eyes have been covered or removed (Waterman 1961), so it is possible that 'blind' H. obesus was also able to monitor changes in light intensity. The general photoreceptors in crustaceans are thought to give rise to the 'shadow response' in predator avoidance behaviour. Many agnostines are thought to have been planktic (Robison 1972), and small extant planktic organisms are sensitive to light in order to keep to a constant light intensity throughout the day. This is achieved by migrating up and down the water column (Tait 1981). Planktic agnostines with dermal photosensitivity may have used enrolment to regulate their position in the water column; enrolling to sink. Certainly agnostids are well

adapted for enrolment (see discussions by Robison 1972; Müller and Valossek 1987) and many are found fossilised in this state.

6.3. POSSIBLE SENSORY RECEPTORS AND MODE OF LIFE OF OTHER AGNOSTINES

Inferred life positions and geographical distributions have been used to suggest possible ecological niches for agnostine trilobites. There is still no consensus of opinion. Almost every possible marine habitat has been proposed for agnostines, ranging from planktic to benthic and shallow to deep water (see review by Robison 1972). Suggestions have also included parasitism (Bergström 1973), attachment to algal strands (Pek 1977), and a more benthic habit as indicated from facies-related distributions (Jago 1973; Fortey 1980). Evidence supporting individual cases can be quite strong, and it is likely that agnostines as a group were sucessful in several ecological niches, rather than just one. Study and interpretation of cuticular microstructures can lend support to hypotheses of possible life modes, but detailed microstructural studies are rare.

Agnostine trilobites have the thinnest exoskeletons in the Class Trilobita, ranging from just 5-15μm (see Appendix 3). Although all the agnostines examined have been recrystalised internally, such as Peronopsis interstricta (Plate 6.2b), it is possible that unlike polymerid trilobites, all agnostine cuticles were composed only of prismatic layer, and lacked an underlying principal layer. This will have affected the mechanical properties of the exoskeleton (Chapter 7). Although prismatic layer is strong under evenly distributed compressive forces (such as water pressure) it has extremely poor crack-stopping abilities when subjected to localised sudden impacts. However, due to

the small size of agnostines, impact damage was probably unimportant as predators were most likely to swallow them whole rather than first cracking them open. This would also be true of small polymerid trilobites and meraspides.

Large scale cuticular features of agnostines are well known; radiating ridges and furrows (rugae and scrobiculae respectively) on agnostine acrolobes probably represent the surface expression of alimentary systems (Opik 1960). Surface sculpture also includes coarse tuberculation, for example Ptychagnostus (Ptychagnostus) aculeatus (Angelin) (Westergård 1946, pl. 12, figs. 8-11) which is relatively rare, or large scale reticulation such as that on Trinodus aff. tardus (Barrande) (Owen and Bruton 1980, pl. 1, figs. 1-4). Such structures dramatically increased the thickness of the cuticle and therefore strengthened the exoskeleton. The ridges of cell polygons also strengthen the cuticle as they act mechanically as T-beams which are structurally very strong (Chapter 7). Together they form a strengthening meshwork over the external surface of the exoskeleton, which is particularly important for trilobites with such thin cuticles. In H. obesus the reticulation is usually most pronounced on the borders, probably because it is advantageous to have extra strength here where the greatest internal strains occur (Chapter 7). Most trilobite doublures increase in thickness where the cuticle changes direction (Appendix 4), a mechanically strong arrangement. However Peronopsis interstricta (Plate 6.2b) shows no increase in cuticle thickness across the doublure, so other forms of reinforcement such as reticulation are necessary.

Obvious agnostine cuticular sense organs are few. Except for Oculagnostus frici (Ahlberg 1988), agnostines lack eyes and so presumably had to rely mainly on mechano- and chemoreceptors to monitor the external environment. The axial glabellar node commonly contains pores and has been regarded as a median eye to give some indication of light intensities (Shergold 1977), as in naupliar eye spots. An alternative hypothesis based on analogy with the dorsal median organ of larval decapod crustaceans, is that such structures (especially those of trinucleids) were joint chemosensory and glandular complexes (Barrientos and Laverack 1986).

The exceptional preservation of Agnostus pisiformis (Wahlenberg, 1818) through phosphatisation has generated the only previous detailed description of fine surface sculpture of an agnostine species (Müller and Walossek 1987). Pores are present on the external surface of the exoskeleton including the doublure, but not on the ventral surface. Several different types of pore have been identified, some of which may well have been sensorial in function, although no setae have been recovered. This apparent lack of external setation, however, may be a result of the preservation and extraction processess. All bristles and fine hairs that have been retained occur within enrolled specimens; that is, in relatively sheltered areas that supported the necessary microenvironment for such fine replacement. It is also likely that if any fine setae were preserved on the external surface, they were dislodged during extraction of the fossils from the rock matrix, whereas thin membranes at or below the exoskeletal surface remain intact.

The remarkable A. pisiformis material reveals that most sensory structures are situated on the ventral surface of the organism, especially on the appendages (see Section 4.2e. for discussion of possible cuticular strain detectors). Müller and Walossek (1987) suggested that the prominent hypostome may have been photosensitive; an idea based on the theory that polymerid hypostomal maculae were ventral eye structures (Lindström 1901). However this is inconsistent with Müller and Walossek's (1987) proposal that A. pisiformis spent life in an enrolled state and was unable to fully outstretch.

The articulation of agnostine exoskeletons is unusual, due to the lack of an articulating half-ring on the first thoracic segment. This generates an opening (cephalothoracic aperture) between the cephalon and the thoracic segment upon enrolment (Whittington 1963; Robison 1964; Pek 1971). Müller and Walossek (1987) documented the presence of a thin membrane across the cephalothoracic aperture which is pierced by two ducts. They thought it unlikely that these ducts were sensorial in nature, but did not suggest any other possible function. It is possible that they formed respiration holes when the animal was tightly enrolled. Gill ventilation during enrolment has been achieved in several ways by polymerid trilobites. In some, the cephalon and pygidium do not completely interlock producing a cavity between the two, such as those described in encrinurids (Clarkson and Henry 1973) and dalmanitids (Campbell 1977, p. 75-79). Others such as Symphysurus, have terrace ridges on the pleural facets which cross over each other during enrolment to create fine passages for water circulation (Fortey 1986). Therefore it is not implausible that agnostids had similar structures, especially if they spent much of their time enrolled.

However the cephalothoracic aperture is not well positioned for such a purpose; water currents would not have had easy access to the gills. An alternative possibility is that the membrane ducts led to glands which secreted adhesive substances used for attachment purposes. This would support Pek's (1977) theory of attachment to algal strands, where aligned enrolled agnostines appear to be fixed at this point (Pek 1977, pl. 10).

6.4. REFERENCES

AHLBERG, P. 1988. Ocular structures in an Ordovician agnostid trilobite. Lethaia, 21, 115-120.

BARRIENTOS, Y. and LAVERACK, M. S. 1986. The larval crustacean dorsal organ and its relationship to the trilobite median tubercle. Lethaia, 19, 309-313.

BELT, T. 1867. On some new trilobites from the Upper Cambrian rocks of North Wales. Geol. Mag. 4, 294-295, pl. 12, figs. 3-5.

BERGSTRÖM, J. 1973. Organisation, life and systematics of trilobites. Fossils Strata, 2, 1-69, pls. 1-5.

CAMPBELL, K. S. W. 1977. Trilobites of the Haragan, Bois d'Arc and Frisco Formation (Early Devonian) Arbuckle Mountains Region, Oklahoma. Bull. Oklahoma geol. Surv., 123, vi + 227pp., 40 pls.

CLARKSON, E. N. K. and HENRY, J-L. 1973. Structures coaptatives et enroulememt chez quelques Trilobites ordoviciens et siluriens. Lethaia, 6, 105-132.

FORTEY, R. A. 1980. The Ordovician trilobites of Spitsbergen III. Remaining trilobites of the Valhallfonna Formation. Skr. norsk. Polarinst., 171, 1-113, pls. 1-25.

FORTEY, R. A. 1986. The type species of the Ordovician trilobite Symphysurus: systematics, functional morphology and terrace ridges. Paläont. Z. 60, 3/4, 12 Abb., 255-275.

FORTEY, R. A. and CLARKSON, E. N. K. 1976. The function of the glabellar 'tubercle' in Nileus and other trilobites. Lethaia, 9, 101-106.

JAGO, J. B. 1973. Cambrian agnostid communities in Tasmania. Lethaia, 6, 405-421.

LINDSTRÖM, G. 1901. Researches on the visual organs of the trilobites. K. Svensk. Vidensk. Akad. Handl. 34, 1-85.

MÜLLER, K. J. and WALOSSEK, D. 1987. Morphology, ontogeny, and life habit of Agnostus pisiformis from the Upper Cambrian of Sweden. Fossils Strata, 19, 1-124, pls. 1-33.

OPIK, A. 1960. Alimentary caeca of agnostid and other trilobites. Palaeontology, 3, 410-438.

OWEN, A. W. and BRUTON, D. L. 1980. Late Caradoc-early Ashgill trilobites of the central Oslo region, Norway. Paleontological contrib. Univ. Oslo, 245, 1-62, pls. 1-10.

PEK, I. 1971. Articulation in Condylopyge rex (Barrande, 1846) (Trilobita). Acta Universitatis palackianae olomucensis Facultas Rerum Naturalium. 38, 139-140, 1 pl.

PEK, I. 1977. Agnostid trilobites of the central Bohemian Ordovician. Czech. J. Geol. Sci. Palaeont. 19, 7-43, 12 pls.

ROBISON, R. A. 1964. Late Middle Cambrian faunas from western Utah. J. Paleont., 38, 510-566, pls. 79-92.

ROBISON, R. A. 1972. Mode of life of agnostid trilobites. Proc. Intn. geol. Congr. 7, 33-40. Montreal.

RUSHTON, A. W. A. 1983. Trilobites from the Upper Cambrian Olenus Zone in Central England. In BRIGGS, D. E. G. and LANE, P. D. (eds.). Trilobites and other early arthropods: papers in honour of Professor H. B. Whittington, F.R.S. Spec. Pap. Palaeont., 30, 107-139, pls. 14-19.

SHERGOLD, J. H. 1977. Classification of the trilobite Pseudagnostus. Palaeontology, 20, 69-100.

TAIT, R. V. 1981. Elements of marine ecology (third edition). 356pp. Butterworths, London.

WAHLENBERG, G. 1818. Petrificata Telluris Svecanae. Nova Acta Regiae Societatis Scientiatum Upsaliensis, 8, 1-116, pls. 1-4.

WATERMAN, T. H. 1961. Light sensitivity and vision. In WATERMAN, T. H. (ed.). The physiology of Crustacea. Volume 2: Sense organs, integration, and behaviour. 1-64. Academic Press, New York.

WESTERGÅRD, A. H. 1946. Agnostidae of the Middle Cambrian of Sweden. 140pp. Sver. geol. Unders. Afh. C, 477. Stockholm.

WHITTINGTON, H. B. 1963. Middle Ordovician trilobites from Lower Head, Western Newfoundland. Bull. Mus. comp. Zool. Harv. 129, 1-118, 36 pls.

Plate 6.1. Reticulation on the dorsal cuticle surface of *Homagnostus obesus* (Belt).

a, H. obesus Andrarum, Sweden (Upper Cambrian). O.w.23. Lateral border and acrolobe of cephalon showing marked reticulation (cell polygons) on the external surface of the cuticle, and domed structures on the internal mould. x400.

b, H. obesus Andrarum, Sweden (Upper Cambrian). O.w.7. Cell polygons on the pygidial axis. x2000.

c, H. obesus Andrarum, Sweden (Upper Cambrian). O.w.13. Cell polygons on the acrolobe of the pygidium (10-12μm diameter). Note also the outlines of crystals (1-1½μm diameter) in the prismatic layer. x3000.

d, H.obesus Andrarum, Sweden (Upper Cambrian). O.w.13. External mould of pygidium with impressions of cuticular reticulation and prismatic layer crystals. x3000.

e, H. obesus Andrarum, Sweden (Upper Cambrian). O.w.5. Cell polygons (approximately 10μm diameter) on the external mould of the cephalic border. Note the impressions of crystals (1-2μm diameter) in the prismatic layer. x3000.

f, H. obesus Andrarum, Sweden (Upper Cambrian). O.w. 21. Visceral surface of pygidial cuticle (c) with pits 3-6μm diameter, and external mould (m) with reticulation. Note the impression of prismatic layer crystals on both sides of the cuticle. The exoskeleton is now recrystallised internally. x1000.

PLATE 6.1

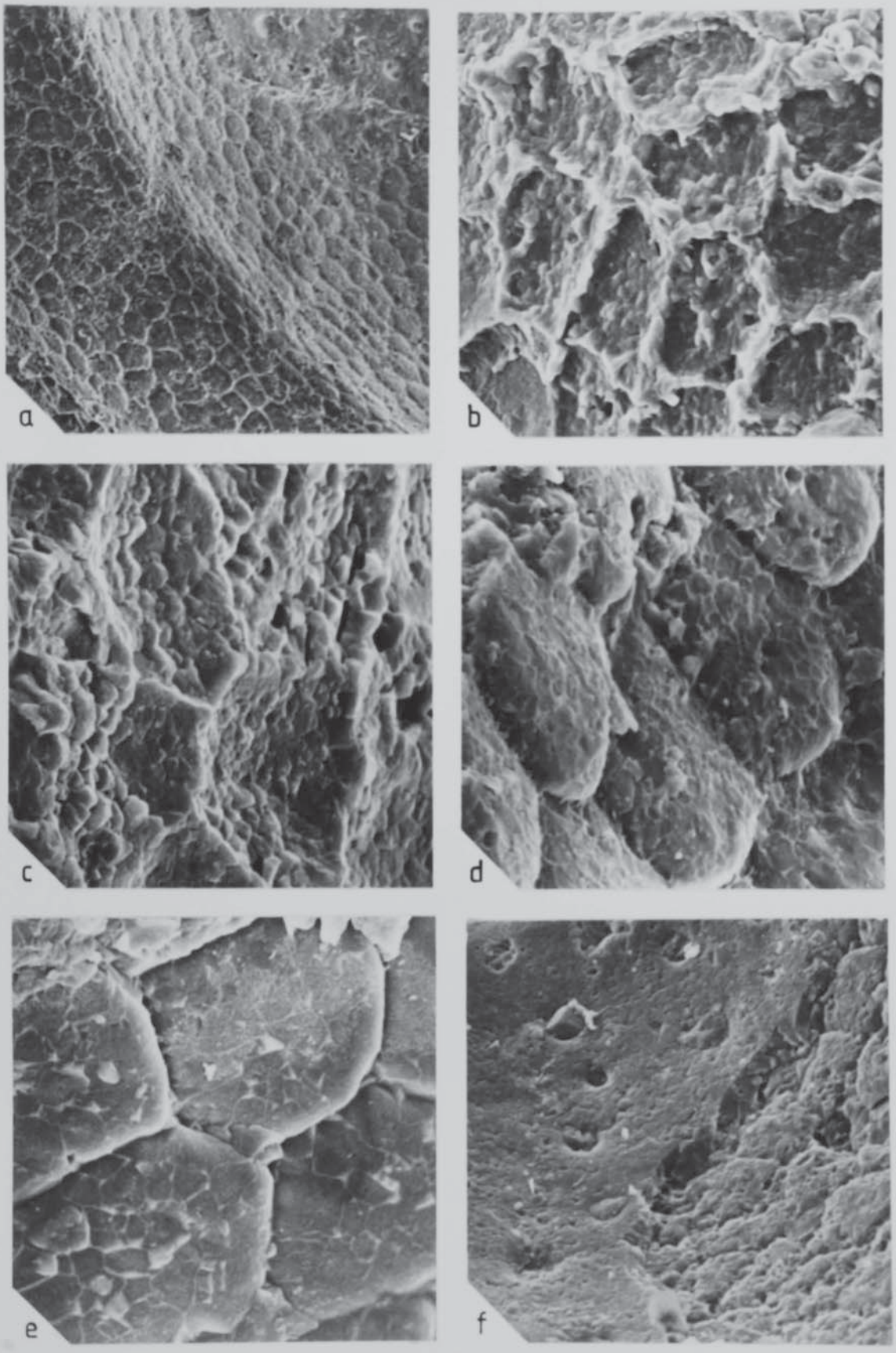

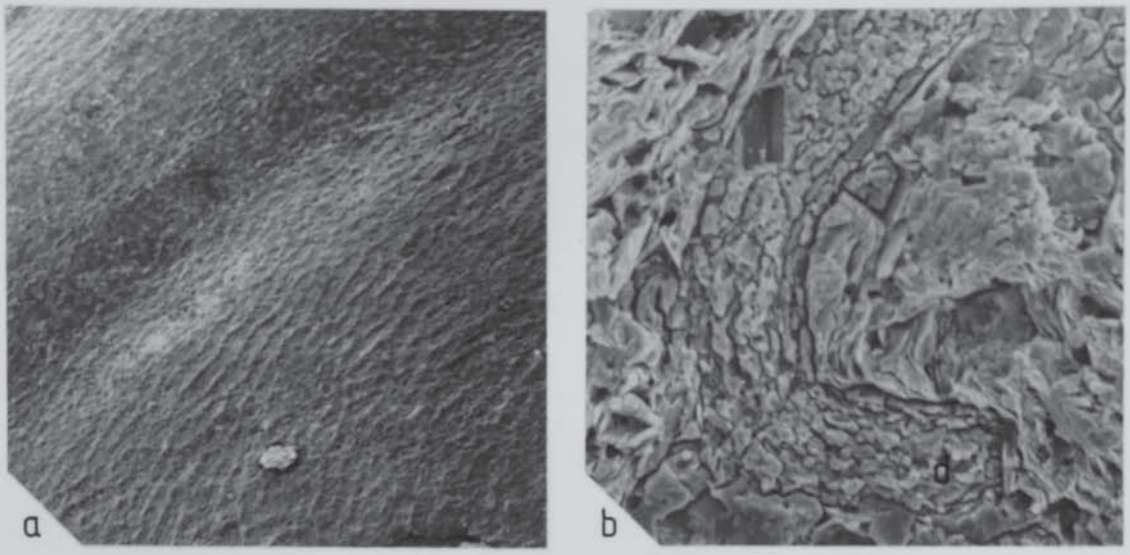

Plate 6.2. Scanning electron micrographs of agnostid cuticle.

a, Ptychagnostus gibbus Robison. Locality unknown (Middle Cambrian). (BGS)FOR 2393. Reticulation on the external surface of the cuticle. x150.

b, Peronopsis interstricta (White). Utah, U.S.A. (Middle Cambrian). NW 31B. Etched transverse section through a pygidium (15µm thick) showing the doublure (d). All internal structure has been lost during recrystallisation. x1000.

CHAPTER 7

BIOMECHANICS OF TRILOBITE EXOSKELETONS

ABSTRACT. The study of the mechanical properties of biological materials is known as biomechanics. Most skeletal materials, such as bone and insect cuticle are viscoelastic, though heavily mineralised structures such as mollusc shell, are linearly elastic. The type of microstructure used is related to required mechanical strength and the metabolic cost involved in constructing it. The effects of composition, microstructure, and architecture on mechanical properties are discussed, and then related to trilobite exoskeltons. Due to their composition and internal organisation, trilobite cuticles can be regarded as ceramics that behaved in a linearly elastic manner. The small size of the calcite crystals, and the presence of an organic framework reduced the risk of crack formation and slowed the progress of fractures. Due to its crystal arrangement, the thin outer prismatic layer would have had good compressive strength, but only poor crack-stopping abilities, whereas the underlying principal layer added bulk to the cuticle. Structurally, trilobite exoskeletons are analogous to monocoque shells, that is, they are strong 'thin shells' with the same composition throughout and behave as a 'stressed skin'. The overall architecture of the cephalon and pygidium is of a series of modified domes, strengthened by the presence of the doublure; whereas thoracic segments are compromise structures which have to facilitate articulation as well as confer mechanical strength.

7.1. Introduction

THE mechanical properties of materials reflect the way in which they respond to forces acting upon them. Accommodation of the resulting strains is a function of the composition, microstructural organisation. and overall form (or architecture) of the specimen. The study of the mechanical characteristics of biological materials is known as biomechanics; a relatively new field with most research occurring from the 1970's onwards. Such research has concentrated on determining the biomechanics of Recent skeletal materials such as bone (Currey 1969, 1975, 1979), insect cuticle (Hepburn et al. 1975; Vincent 1980), and mollusc shell (Taylor and Layman 1972; Currey and Taylor 1974; Currey 1976, 1980) in order to compare their competencies. Various mechanical tests have been developed to measure the tensile, compressive, bending, and hardness characteristics of these materials by modification of standard engineering procedures. However although the tests were basically the same, authors each followed their own individual techniques. Currey (1980) argued that sample preparation, size, and shape, would all have a bearing on the results obtained, and so demonstrated the need for a standard methodology.

These studies have demonstrated that not only do materials with the same composition have different mechanical properties, but also that biomechanics may not be the most important factor in their design: the metabolic cost involved in constructing a skeleton is also very important (Currey 1980). Some of the common terms used in biomechanical studies are explained at the end of this section.

The mechanical properties of biological materials have generally been related to composition and microstructure. The significance of the

form of the organism has only been studied in depth for the Ostracoda (Benson 1974, 1975, 1981, 1982). Most testing of arthropod exoskeletons has been on insect cuticle, mainly because they are the most common arthropods today (see Vincent 1980 for review). However such cuticles are all uncalcified and behave as viscoelastic materials; in contrast to heavily mineralised exoskeletons which behave as ceramics and are linearly elastic. Consequently the biomechanics of trilobite exoskeletons which were strongly calcified, are better compared with other mineralised skeletons such as mollusc shells, rather than insect cuticle. In the following sections the effects of composition, ultrastructure, and architecture on mechanical properties are discussed in turn, and the principles involved then related to trilobite cuticles.

7.2. Terminology

STRESS (σ), force applied to the specimen.

STRAIN (ϵ), deformation created within the specimen after being subjected to stress.

STIFFNESS is a measure of the resistance of the material to deformation. This is defined as the force required to double (or halve) the length (or thickness, or width) of a sample (Vincent and Hillerton 1979). It is measured by performing tensile tests (Currey and Taylor 1974; Joffe *et al.* 1975; Ker 1980), or compression tests (Taylor and Layman 1972; Currey 1976), both of which have to be repeatable, that is, not incurring permanent damage to the specimen such as fracture.

HARDNESS measures the ease with which the material flows under a stress, and is related to the stiffness of the material, and its

plasticity i.e. its ductility. For details of tests see Taylor and Layman 1972; Craig and Vaughan 1981; and Hillerton et al. 1982. It is useful for comparing viscoelastic materials, or ceramics with grain sizes of about 100μm.

LINEARLY ELASTIC materials such as ceramics, react immediately to the application of a stress, for as long as it is present; and on its removal immediately revert back to their pre-stressed state (Fig. 7.1A[i]).

Strain is directly proportional to stress

$$\epsilon = \sigma / E$$

where E is a constant (Young's Modulus) and is a measure of the stiffness of the material.

VISCOELASTIC materials, such as insect cuticle increasingly deform the longer a force is applied. Once the stress is removed, recovery is also gradual, so that any measurement of strain is time-dependent (Fig. 7.1A[ii]).

See Wainwright et al. (1976), Dorrington (1980), Gordon (1980), and Vincent (1980, 1982) for more details about linearly elastic and viscoelastic materials.

7.3. COMPOSITION

Every material has a unique response to both tension and compression, which is largely due to its composition and the strength of the bonds that maintain its atomic structure. For example, metals are weak under

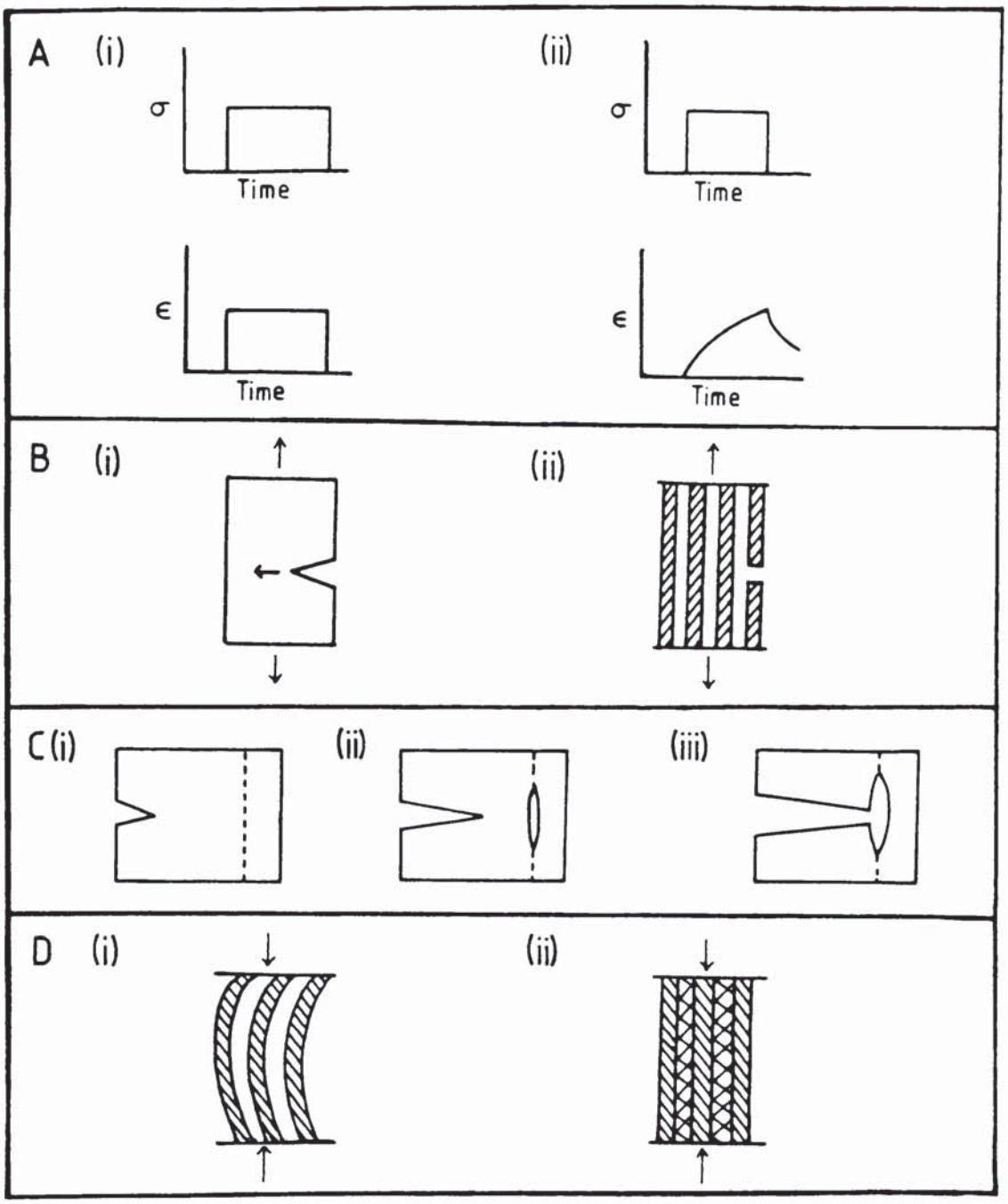

Figure 7.1. Responses of different materials to stress.
Based on Wainwright et al. (1976) fig.2.12., and Gordon (1980) figs.6,7.
A[i]. Linearly elastic materials.
A[ii]. Viscoelastic materials.
B[i]. Continuous material is weak in tension, as cracks can advance unimpeded.
B[ii]. Isolated elements are stronger in tension as cracks are unable to spread once the first element has broken.
C. Weak interfaces prevent the spread of cracks (Cook-Gordon mechanism)
[i]. Crack formation begins.
[ii]. Weak interface opens out in advance of the crack.
[iii]. Progression of the crack is stopped.
D. Weak lateral bonds increase compressive strength.
[i]. Isolated elements bend under compression.
[ii]. Weak lateral bonds restrict movement.

tension as planes of atoms can slip past one another; ceramics, characterised by ionic or covalent bonding have great compressive strength.

As organisms are subject to both tensile and compressive forces, their skeletons usually comprise a mixture of components, that is, they are composites. In this way a compromise is achieved whereby the skeleton benefits from the different properties of each phase. Tensile forces are usually inherent within the structure of the skeleton, or created by support of the viscera; whereas compressive forces can be induced by walking, the surrounding water pressure, or predation.

Insect cuticle is one of the most efficiently constructed naturally occurring composites, being composed of chitin fibrils weakly bonded to a protein matrix. Chitin is very strong when subject to tensile forces whereas the protein matrix resists compression. The arrangement of these two components is also important (see 7.4). Stiff and pliant cuticles owe their differences to their protein matrix compositions; the properties of the chitin fibrils are always the same (Hillerton 1984). Additional hardening can be generated by sclerotisation, for example in locust incisors (Hillerton 1980). This involves the incorporation of phenols which become tightly bound within the cuticle, coupled with some loss of water (Vincent and Hillerton 1979).

Some marine arthropods harden their exoskeletons by reducing the amount of protein present and mineralising their exoskeletons with calcium salts. It has been demonstrated for crustaceans that the greater the proportion of calcium salts, the harder the cuticle becomes (Welinder 1974; Abby-Kalio 1982). The type of mineralisation is also important, for example the cuticle of the mantid shrimp Gonodactylus is

mainly composed of calcium carbonate, however the harder outer surface of the smashing limb is predominantly calcium phosphate (Currey et al. 1982).

Sometimes organic matter is incorporated within the actual crystal lattices and alters the way in which the mineral fractures, such as proteins within the calcite crystals of echinoderm plates (Berman et al. 1988). Although the concentration of protein is very small (only approximately ten molecules per 1 x 10^6 unit cells) these crystals are less brittle than inorganic calcite.

7.4. MICROSTRUCTURE

The size and arrangement of skeletal materials are of fundamental importance to the mechanical behaviour of the structure as a whole. In general, composites are stronger than pure materials. Cracks, generated in tensile conditions, are unable to propagate between isolated elements (Fig. 7.1B), hence chitin fibrils are extremely strong as they are composed of individual long chains of chitin molecules. If one chain is broken, the fracture does not spread to the others.

Weak interfaces within a material can also give strength due to the Cook-Gordon mechanism (Cook and Gordon 1964). As a crack propagates through a material, the weak interface opens up in advance. When the crack reaches the hole, its energy is dissipated and so is unable to continue (Fig. 7.1C). Wood behaves in this manner. Weak bonds between components can also increase compressive strength by creating greater resistance to bending (Fig. 7.1D).

Arthropod cuticle is a very efficient composite as it has alternating layers of tension and compression-resistant members. The

chitin fibrils are arranged in sheets parallel to the cuticle surface. Each sheet contains fibrils orientated in the same direction, but successive layers are rotated by a few degrees to produce a helicoidal structure. The typical laminated appearance of arthropod cuticle is due to this internal arrangement; each unit of 180° rotation of the helicoid corresponding to a single lamina (Bouligand 1965; Neville and Luke 1969; Neville 1970; Livolant et al. 1978). Consequently the cuticle is extremely strong in tension along any plane parallel to the surface. Sometimes the sheets show preferred orientation along the direction of greatest stress (Wainwright et al. 1976), for example in the walking legs of spiders (Barth 1973), the hind limbs of coleopterans (Dennel 1978), and the legs of the Carboniferous eurypterid Mycterops (Dalingwater 1985).

The organic matrix of heavily mineralised skeletons is one of the most important factors in determining its mechanical properties. Most biomineralisation is an 'organic matrix-mediated' process (Lowenstam 1981) where the organic matter not only forms a framework to control the nucleation, size, and orientation of the inorganic crystals, but also the physical behaviour of the shell (Krampitz et al. 1983). The organic matrix of crustaceans is a chitin-protein complex, and the proteins can be subdivided into water insoluble, and soluble fractions (Richards 1951) which are species-specific (Hackman 1974). This is also true of other marine invertebrates such as molluscs. Weiner et al. (1983) demonstrated that molluscan insoluble matrix (including chitin fibrils) forms a framework to limit the size and orientation of the crystals, which is very important mechanically; and also supports the

soluble matrix that controls nucleation sites. See also review by Mann 1988 concerning organic matrices.

The quantity and mechanical characteristics of the organic framework compared with the crystalline component can greatly influence the strength of a 'stony' (Wainwright et al. 1976) skeleton. As the matrix is much less brittle than the crystals it encloses, when sufficiently thick it can absorb some of the energy involved in crack propagation by plastic flow. If the organic matrix is only thin, fractures are prevented from developing mainly by deflecting cracks as they reach crystal boundaries.

The size of the crystalline component of a stony skeleton (as controlled by the organic framework) is also very important. The larger the object, the more likely it is to contain flaws such as internal deformations or cracks. For linearly elastic solids at a given stress level, there is a critical crack length or defect size at which fracture rapidly occurs. Therefore it is advantageous for a ceramic to be constructed from small components to reduce the chances of containing defects. For calcium carbonate minerals in tension, the critical crack length is 2-8μm (Wainwright et al. 1976). In general, heavily mineralised skeletal materials have grain sizes with one dimension smaller than 3μm to increase the fracture strength. Uniformity in size is also advantageous, to prevent weak links. The less organic matrix present, the more important it is for the crystal sizes to be small, so that if cracks do form, they frequently have to change direction at crystal boundaries, requiring more energy. Hence fine-grained ceramic skeletons that contain only a small amount of organic matrix, are much stronger than a large inorganic crystal. This

has been demonstrated for mollusc shells, which only contain 0.1-5% matrix (Currey 1980) and yet are stronger than inorganically precipitated calcite (Taylor and Layman 1972). Currey (1980, fig.5) has illustrated the extremely good crack-stopping capabilities of molluscan nacre, which is composed of many thin sheets of aragonite separated by thin organic layers. A crack has to proceed along a very tortuous path in order to cross this type of microstructure. Therefore it is not surprising that most ceramic skeletons are fine grained and contain very few voids. When voids do occur, such as ducts, their function outweighs the structural weaknesses they induce (Wainwright et al. 1976).

It can therefore be seen that the type of microstructure used to construct a skeleton will influence its mechanical characteristics. Mollusc microstructural types (described by Watabe 1984) have been found to exhibit different mechanical properties despite all being constructed from calcium carbonate. For example nacre is the strongest, and crossed lamellar structure the hardest. However, mechanical strength may not be the most important factor involved in the design of a skeleton. Although nacre is the strongest of all types of molluscan microstructure and occurred first in the fossil record, weaker structural units are more commonly used today (Currey and Taylor 1974). The metabolic cost involved in secreting the material is likely to be more important than its overall strength (Currey 1980). A metabolically cheaper type of microstructure to construct, although of inferior quality to nacre, may be adequate for a particular lifestyle. Indeed, there is a general correspondance between molluscan microstructure and mode of life (Taylor and Layman 1972; Currey and Taylor 1974; Currey

1976). Oyster shells for example, are constructed from relatively weak microstructures (foliated structure and chalky deposits) and are prone to attacks from boring organisms, however they can grow very quickly, which suits their particular mode of life (Currey 1980).

7.5. ARCHITECTURE

The general shape of a structure will also influence the way in which it responds to stresses. Structural mechanics have only been applied in any depth to the design of ostracode carapaces, where exoskeletal features have been discussed in relation to common engineering or architectural structures (Benson 1974, 1975, 1981, 1982). Impact and compression testing of ostracode carapaces (Whatley et al. 1982) did not reveal any one factor that had overiding importance in conferring strength, though the architecture of cirripede exoskeletons is more important than microstructure in this respect (Murdock and Currey 1978).

The importance of shape to the overall mechanical strength of a structure is best explained with reference to common architectural structures. The concept of 'strength through form' (Nervi 1951) has been successfully exploited in architecture from the 1950's. The various man-made constructional forms which have been developed abide with well understood engineering principles, and have many analogies with biological designs. For an introduction to structural mechanics see Buckle (1977) and Cowan (1980).

The type of material to be used usually determines the type of structure that is produced. Due to their different mechanical properties, materials lend themselves to be used in certain ways; for

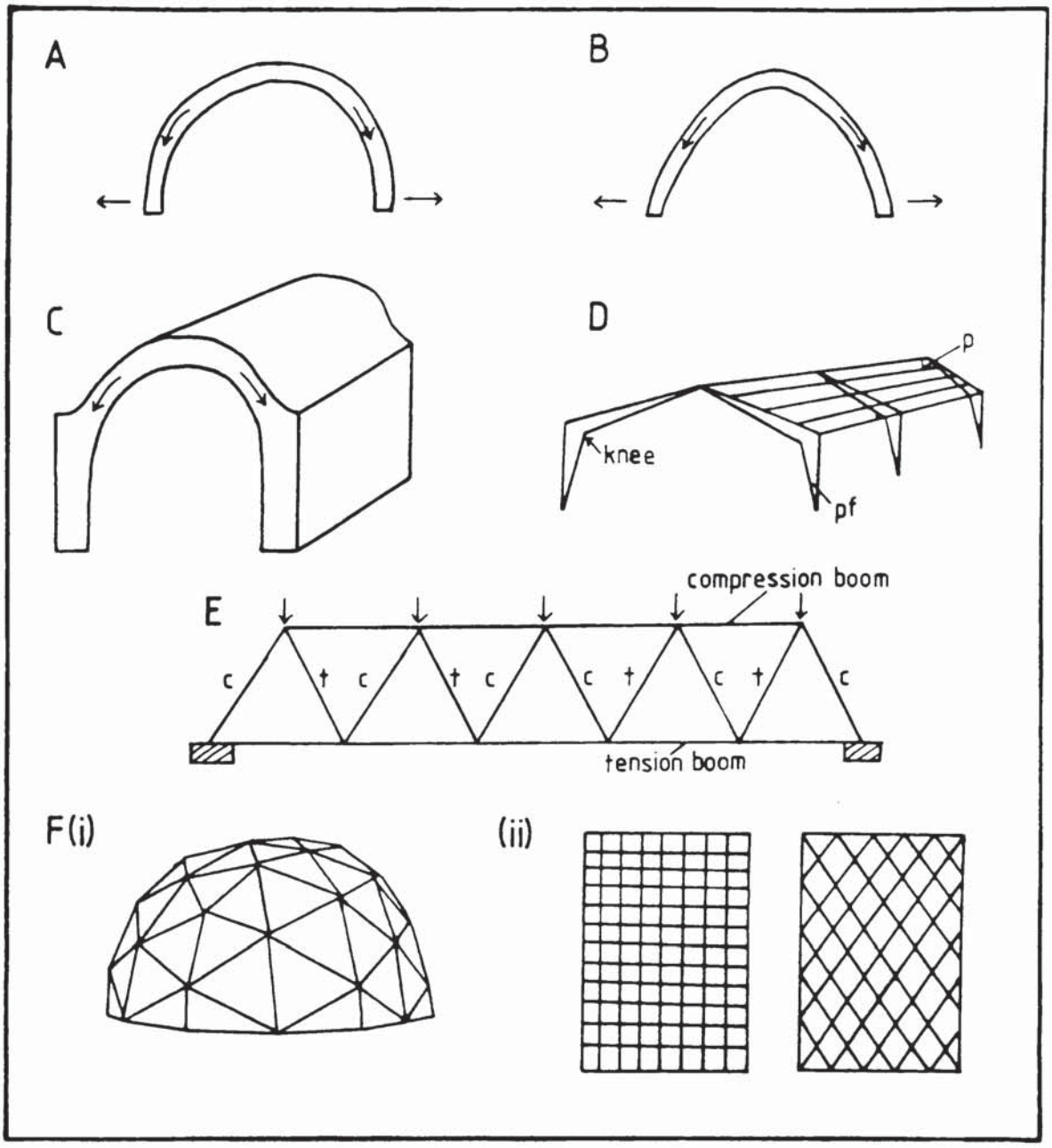

Figure 7.2. Space-spanning structures.
A. Hemisphere.
B. Dome.
C. Stone vault. Thick walls counteract outward thrusts from the arch and ensure that the forces are deflected to the ground within the structural form (or else the building would collapse).
D. Portal frames (pf) and purlins (p). Portal frames always have a shallow pitch, and the knee is strengthened by increased thickness or reinforcement. The weight and outward thrusts are absorbed by the foundations.
E. Truss. The girders of the truss act either in tension (T) or compression (C) to take up the load, and have flexible joints. Based on Buckle (1977) Fig. 8.1.
F. Space frames.
[i]. Geodesic dome. Based on triangular or diamond-shaped grids with flexible joints. (From Buckle 1977, Fig. 15.3).
[ii]. Lamellar roofs of various shapes are based on horizontal or diagonal grids with rigid joints.

example, stone is relatively weak in tension but possesses great compressive strength.

Some of the more common three-dimensional architectural structures are illustrated in Fig. 7.2. A catenary is the shape a cable takes when suspended equally at both ends, and can be expressed mathematically as

$$y = a/2\ (e^{x} + e^{-x})$$

where x and y are coordinates

e = exponential constant 2.71

a = variable

When inverted, this form is a catenary arch, on which vertical loads are directed evenly over the whole length. Its three-dimensional extension is the dome (Fig. 7.2B). Although a hemisphere (Fig. 7.2A) encloses a given volume with less surface area than a catenary-shaped dome, the dome is structurally superior at resisting forces directed normally, or horizontally to the crown. In both structures, the weight of the material is directed downwards, generating horizontal thrusts at the margins. These have to be counteracted either by ring beams, or some other sort of reinforcement such as increased thickness, which confines outward movement of the base.

A vault is another three-dimensional version of an arch, and also has outward thrusts at its base. For stone vaults (Fig. 7.2C), thick adjoining walls are necessary to counteract these horizontal moments and ensure that the thrusts are directed to the foundations within the building structure. This buttressing is essential to prevent collapse. Steel, reinforced concrete, and timber are all stronger than stone and so can be used to construct thinner arches. Portal frames are space-spanning structures composed of straight members (Fig. 7.2D). The

greatest shear and bending moments occur at the joint between the beam and the column, so the 'knee' is usually strengthened, either by thickening or adding reinforcing material. As with arches, shallower frames are subject to greater horizontal thrusts, and ties can be introduced between the supports to attain equilibrium. Purlins are beams that span between portal frames, and on which additional material can be placed such as roofing tiles. The load acts on the joints between the purlins and the portal frames.

Folded plates and corrugated sheets (Fig. 7.3) are more economical in material than flat plates spanning the same area, as their shape imparts strength and so they can be thinner. A vertical load acting on corrugations is divided into two components; a force R acting at right-angles to the slab surface, and a force P acting parallel to it. P forces are resisted by 'skin stresses' within the slab, so only force R will cause bending. Consequently much greater forces can be withstood than by a horizontal slab of the same thickness, on which all the force is directed perpendicularly to the surface. A corrugated sheet can withstand up to a hundred times its own weight in load (Cowan 1980), and its strength is a function of its sinusoidal cross-section, and its overall depth (moment of resistance).

As a method of spanning space, a truss (Fig. 7.2E) is more economical in material than a solid beam, and there are many different types. Simply, the stresses from a vertically acting load are taken up by a series of members which act either in tension or compression. Space frames (Fig. 7.2F) can be likened to three-dimensional trusses. Variously shaped strong, and lightweight lattices provide the necessary support for thin coverings. As in trusses, the members of the grid act

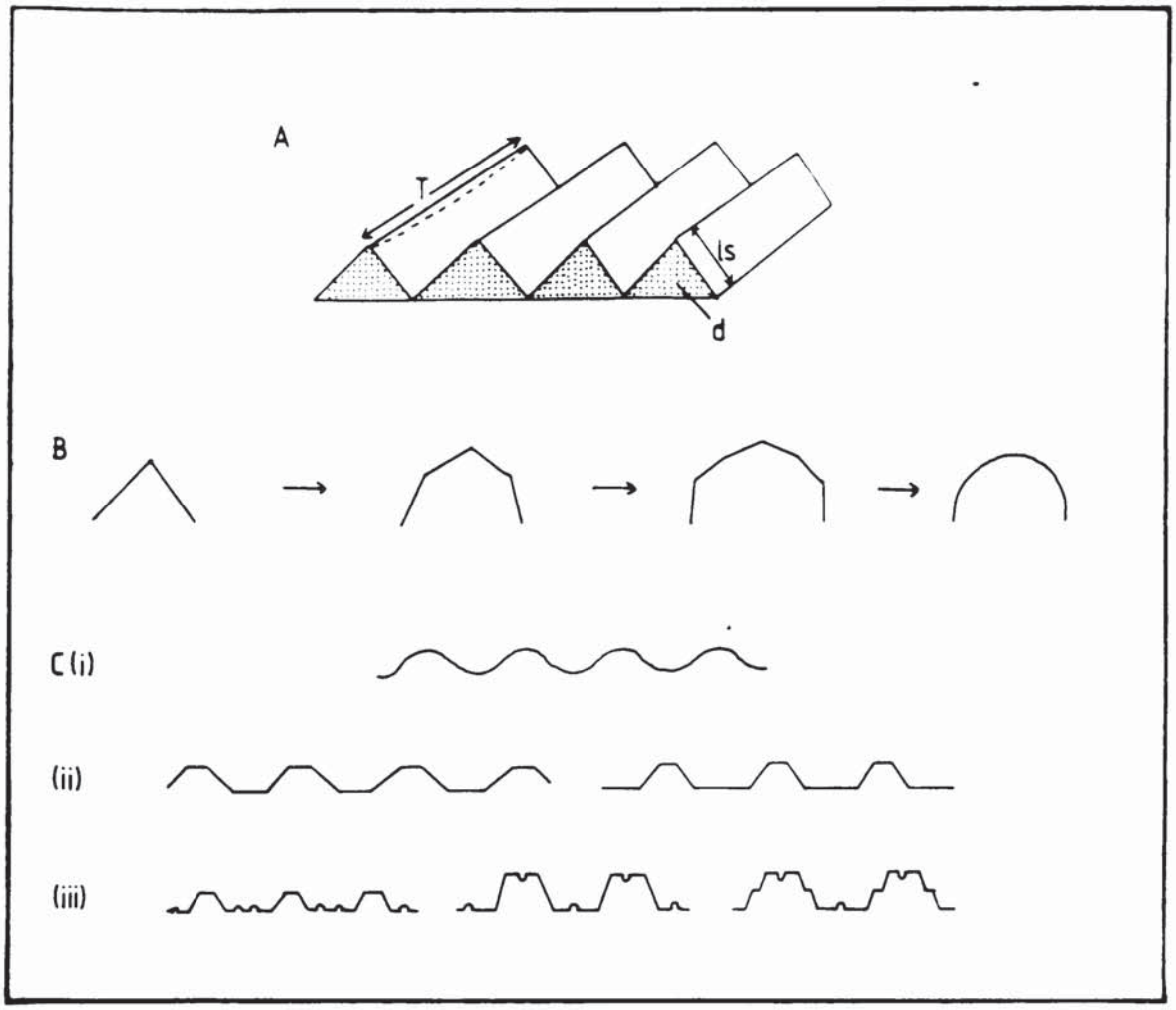

Figure 7.3. Corrugations.

A. Folded sheet. There is only a small local span (ls) so only thin slabs are necessary to resist the R and P forces. Thin end diaphragms (d) resist the thrusts (T) from the whole roof. (Based on Buckle 1977, Fig. 14.7).

B. The more folds in the folded sheet, the less local bending, enabling thinner slabs to be used. Therefore sinusoidal corrugations are the strongest.

C. Examples of various profiles of corrugations used in buildings.

[i]. Sinusoidal.

[ii]. Trapezoidal (symmetrical and asymmetrical).

[iii]. Stiffened trapezoidal.

either in tension or compression to transmit the stresses acting on the structure. The covering 'membrane' or 'skin' just lies passively between the struts. An alternative type of space frame is the monocoque shell (Benson 1974, 1975) which does not have an internal grid. It is composed of the same material throughout to produce a strong thin shell, and all the load is transmitted through this thin 'stressed skin'.

7.6. INFLUENCES OF TRILOBITE CUTICLE COMPOSITION AND MICROSTRUCTURE ON MECHANICAL BEHAVIOUR

Since the organic matrix has so much influence on the mechanical behaviour of heavily mineralised exoskeletons, no mechanical tests were performed in this study on fossil material, as any remaining organic matter will have been degraded. This has been proved by compression and impact tests on fossil and Recent ostracodes of the same species (Whatley et al. 1982), which were found to have different strengths. However, knowledge of trilobite microstructure (Chapter 4) can still provide much information on the likely mechanical properties of the exoskeleton.

Trilobite exoskeletons were heavily calcified, composed predominantly of low-magnesian calcite (Chapter 2) with only a small proportion of organic matter. In this respect they can be categorised with other stony skeletons as behaving as ceramics. Remnants of the organic matrix have been obtained by decalcifying the cuticles in EDTA (Dalingwater 1969, 1973; Teigler and Towe 1975; Miller 1976; Dalingwater and Miller 1977). Although the composition remains

uncertain, it is likely to have consisted of proteins and chitin fibrils as in all other arthropods.

Like all exoskeletons, trilobite cuticles were used both for protecting and supporting the viscera, and would have been subject to both tensile and compressive forces. Tensile forces parallel to the surface would have been inherent within the domed structure of the skeleton as well as being generated by the suspension of the viscera. The surrounding water would have imposed compressive forces perpendicular to the surface, in addition to compressive stress from water currents or predators. To resist these, the exoskeleton contained tension elements, probably long chitin fibrils orientated parallel to the cuticle surface, and short calcite crystals strong under compression.

Unmineralised insect cuticle is stronger and stiffer than calcified crustacean cuticle; crustacean exoskeletons have to be thicker to compensate. However calcification is very common in the marine environment as calcium ions are readily available for use. Hence it is much more economical for a marine invertebrate to construct an exoskeleton consisting of less protein and more calcium carbonate in comparison to its terrestrial counterpart (Wainwright et al. 1976). This is most probably the reason why trilobite exoskeletons were heavily calcified.

Apart from agnostine exoskeletons which may have been constructed from only a thin, prismatic layer (Chapter 6), all calcified trilobite cuticles comprise an outer prismatic layer with a thicker principal layer below. The prismatic layer is a relatively thin layer of calcite crystals, approximately 1μm diam. orientated with their longer c-axes

perpendicular to the outer surface. It is not analogous to molluscan prismatic layer which can have crystals up to several millimetres long, with each surrounded by a thick (5μm) layer of organic matrix (Currey 1980). Trilobite principal layer forms 85-95% of the total cuticle thickness. It is finer grained, and has a much less regular crystal arrangement. Parallel laminations are sometimes preserved within this layer which may mark the former positions of long chitin fibrils within the organic matrix. The amount of organic matrix was low, with much less than 1μm thickness between crystals. As in mollusc shells, fracture of trilobite exoskeletons mainly occurred through the thin layers of organic matter rather than through individual calcite crystals. Except for eye lenses which were necessarily always of extremely high quality calcite, none of the cuticular crystals have two axes more than 3μm long, so the risks of dangerously large internal defects are minimised.

It has been demonstrated that the type of microstructure used is a compromise between the mechanical properties necessary for a particular mode of life, and the metabolic price that has to be paid in order to construct it. Trilobites, like other arthropods, regularly had to shed their exoskeletons in order to grow. Immediately after moulting, the organism would have been unable to move or feed properly, as well as being very vulnerable to predation, and so it would have been advantageous to construct a new mineralised cuticle as soon as possible. It is therefore likely that ease of construction would have been the main priority involved in the selection of microstructure. Modern mollusc shells are stronger than crustacean cuticles, but these shells are gradually secreted throughout life (Wainwright et al. 1976).

When trilobite cuticle was secreted, the prismatic layer formed first, with only a very thin principal layer present; as secretion continued, cuticle thickness increased by growth of the principal layer only (Miller and Clarkson 1980). This would suggest that the prismatic layer was relatively easy to make, and so deposited rapidly after ecdysis to give some degree of hardening to the cuticle. Bulk was added later to the exoskeleton to give greater strength. Trilobite prismatic layer with its regular crystal arrangement was probably quite strong under compressive forces acting normal to the cuticle surface, but would have had poor crack-stopping capabilities. A crack would have been able to travel unimpeded between crystals, and would only have been deflected on reaching the principal layer. Hence the need for a thin principal layer even in newly secreted cuticle.

Unlike molluscs, trilobites only ever developed two kinds of exoskeletal microstructure. However, the overall thickness of the cuticles and the relative proportions of the different layers do vary considerably, which would have been of mechanical significance. Different types of cuticular ultrastructure may have been related to mode of life, or may just have been a phylogenetic trait e.g. proetides have relatively thin prismatic layers.

7.7. EFFECTS OF TRILOBITE ARCHITECTURAL DESIGN ON MECHANICAL STRENGTH

Like most ostracode carapaces, the trilobite exoskeleton structurally most resembles a series of modified domes based on catenary arches (Fig. 7.4). The cephalon and pygidium can be regarded simply as half-domes. The horizontal thrusts at the margins of the

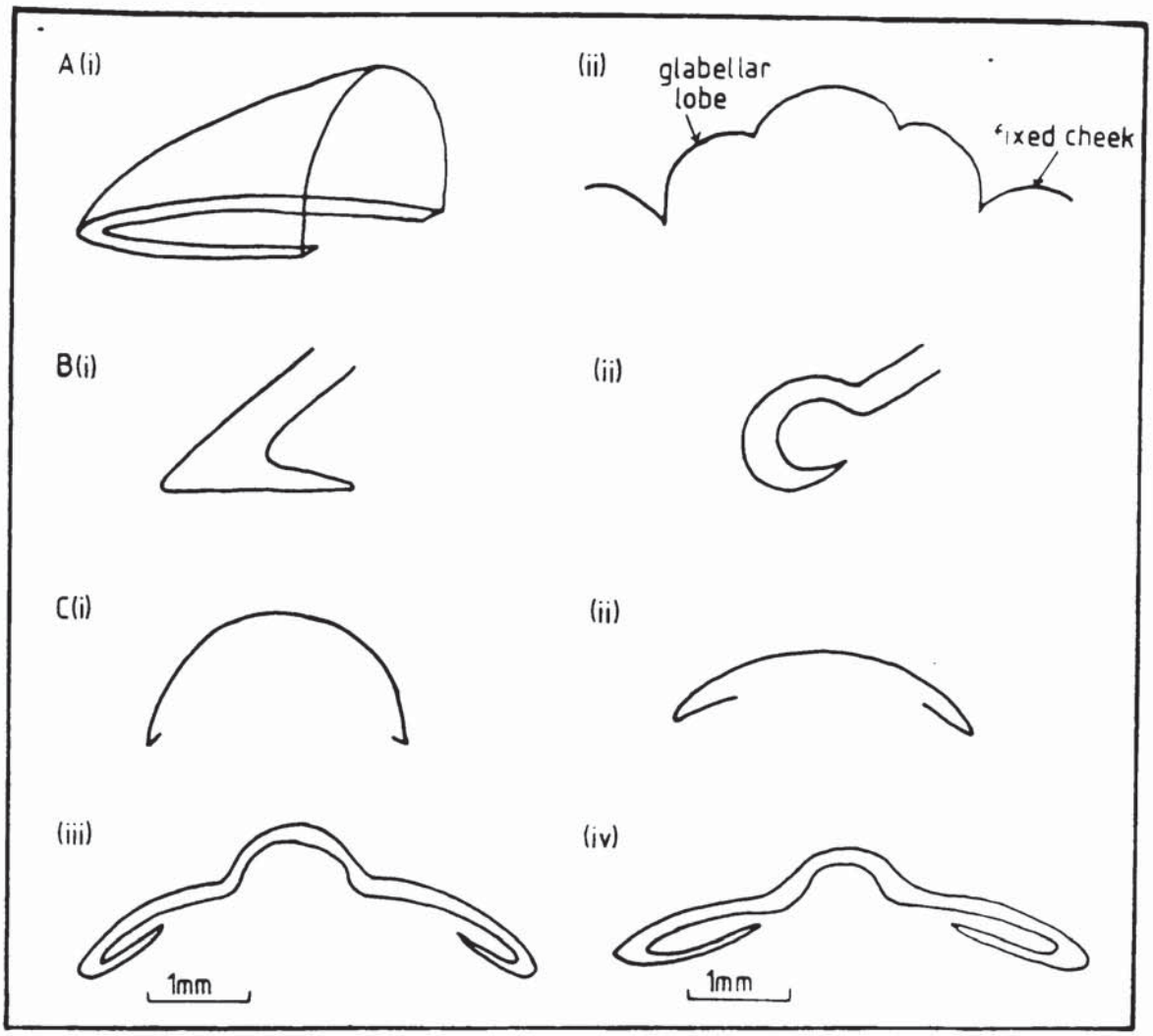

Figure 7.4. General form of cephala and pygidia.
A[i]. Trilobite cephala and pygidia can be regarded simply as half-domes.
A[ii]. Generalised transverse section through a cranidium. The basic shape of a half-dome has been modified by addition of extra domes.
B[i]. The doublure gives strength to the domed structure by increasing thickness at the base, and a change of direction.
B[ii]. The shape of the doublure is also important; cylindrical doublures such as those of certain proetids are very strong.
C. Flatter domes exert greater thrusts at the margins and therefore need longer doublures.
[i], [ii]. Diagrammatic representation of the relationship between convexity and doublure length.
[iii]. Transverse section through the pygidium of Proetus (Proetus) concinnus (Dalman) (based on specimen PRO 12).
[iv]. Transverse section through the pygidium of Warburgella (Warburgella) stokesii (Murchison) (based on specimen WAR 13).

Both these trilobites belong to the Proetacea yet have slightly different convexities, and hence dissimilar doublure lengths.

domes are resisted by the doublure, which confers strength by increased thickness and a change of direction. The inner edge of the doublure marks the point of attachment of the ventral membrane, but although the latter this was probably tough, its flexibility (Müller and Walossek 1987) would have given it negligible structural strengthening properties. Its main function would have been to constrain the positions of the body organs. As with the knee of a portal frame constructed of the same material throughout, the exoskeleton also had to be thicker at the doublure to resist shear forces at the change of direction. On average, cuticle thickness at least doubles across the doublure (Fig. 7.5). As slightly oblique sections through the doublure would give the impression of increased cuticle thickness, the minimum values recorded are the most significant. The width of the doublure is proportional to its strength, hence flatter domes exerting greater horizontal thrusts have to have longer doublures (Fig. 7.4C). However this general relationship is not necessarily valid for all trilobites (Fig. 7.6), as factors such as doublure shape, ultrastructure and overall cuticle thickness also exert an effect. Different types of trilobite doublure are illustrated in Plate 7.1. The addition of extra domes to the exoskeleton such as the glabella (Fig. 7.4Aii), is also a recognised practice in architecture .

Although in sagittal section, a trilobite is much more elongated and therefore resembles a shallower dome than in transverse section, the thorax is well jointed, and so dorso-ventral forces could have been taken up by flexure (Fig. 7.7Aiv).

Trilobite thoracic segments are a compromise in structure between the necessary mechanical strength to protect and support the underlying

organs, and permitting articulation. Some trilobites, such as certain illaenimorphs and homalonotids are characterised by their high convexity and effacement. Their thoracic segments resemble single arches (Fig. 7.7B) and are therefore structurally strong, and articulate only at the two fulcra (Lane and Thomas in Thomas 1978; Thomas and Lane 1984). The segments are arranged in an imbricate manner, and articulation is achieved by them sliding underneath one another (Thomas and Lane 1984, Text-fig. 2d). However this is not common for trilobites as a whole.

Most trilobites have various structures on the anterior and posterior margins of the thoracic segments which enable them to articulate. These may include an articulating half-ring anterior to the axial ring, flanges from the proximal parts of the pleurae to the fulcra, fulcral processes with corresponding sockets, and articulating facets on the distal parts of the pleurae. See Harrington (1959, p. 070-073, Figs.49-51), Bergström (1973), and Fortey and Owens (1979) for more detail about articulation and enrolment. Additionally, coaptative structures may exist on the cephalon and pygidium (Clarkson and Henry 1973; Henry and Clarkson 1975).

Many thoracic segments have the proximal parts of the pleurae extending horizontally from the axial furrows (Fig. 7.8). Although this is not very strong structurally, it is of great importance in articulation as the pleurae form a hinge plane. Strengthening of these thoracic segments is generated by the axial and pleural furrows (Bergström 1973; Müller and Walossek 1987) which are expressed ventrally as ridges (Fig. 7.8G), thus turning the cuticle into a folded sheet. Additional thickening of the exoskeleton in these areas also

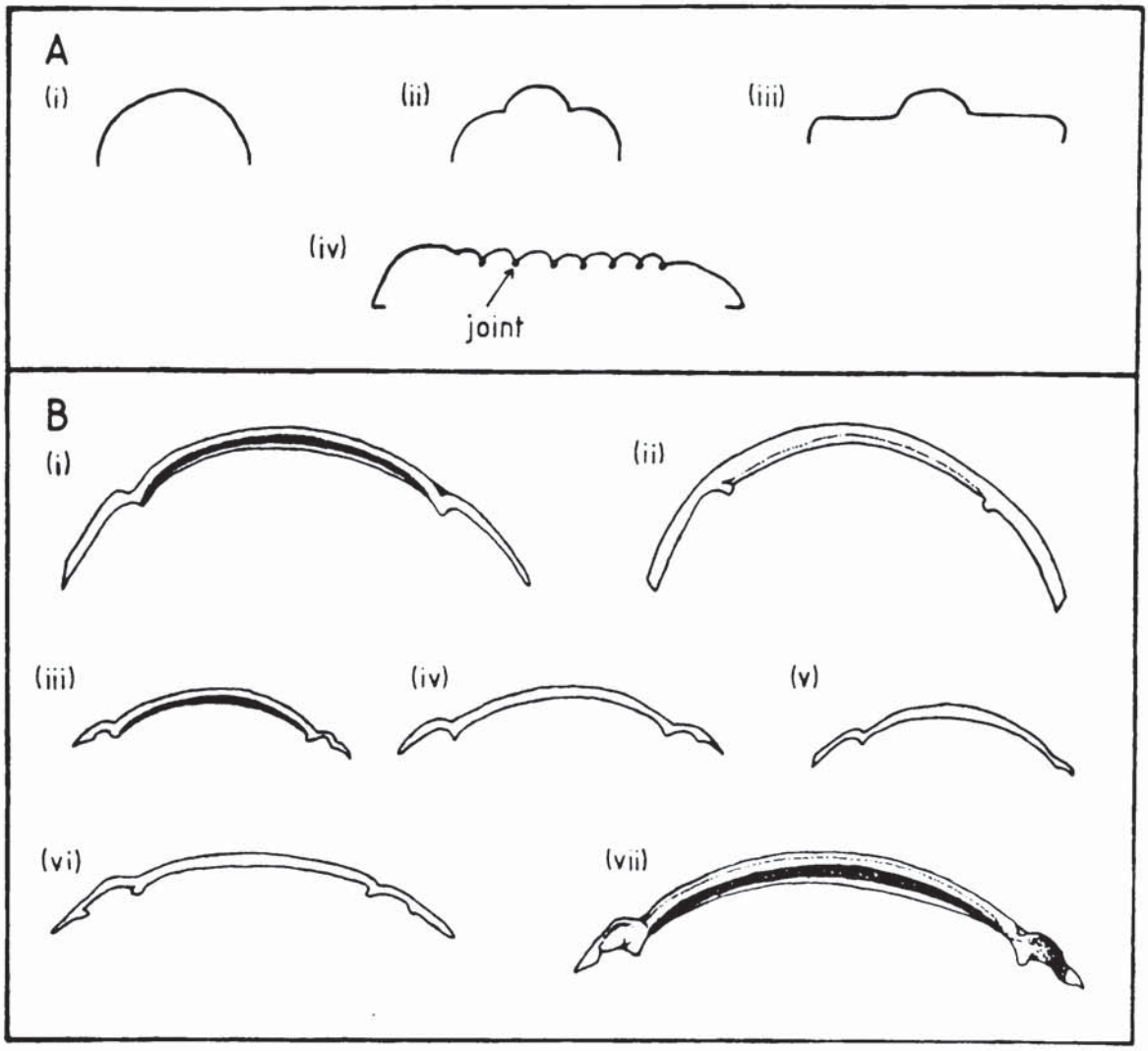

Figure 7.7. Trilobite thoracic segments.
A. Generalised forms of trilobite thoracic segments.
[i]. Single arch.
[ii]. Arch on arches.
[iii]. Horizontal pleurae.
[iv]. Simplified sagittal section through a trilobite, emphasizing the relatively low convexity compared with transverse sections, and the jointed nature of the thorax.
B. Single arch thoracic segments.
[i], [ii]. Bumastus (Bumastoides) lenzi Chatterton and Ludvigsen, (Illaenidae) anterior and posterior views of thoracic segments x3.8. Based on Chatterton and Ludvigsen (1976), pl. 5, figs. 27, 31.
[iii]-[vii]. Failleana calva Chatterton and Ludvigsen, (Styginidae) thoracic segments based on Chatterton and Ludvigsen (1976), pl. 6.
[iii]. Anterior view x3 (Fig. 18).
[iv]. Posterior view x4.3 (Fig. 21).
[v]. Posterior view x2.9 (Fig. 24).
[vi]. Posterior view x4.3 (Fig. 22).
[vii]. Anterior view x3.5 (Fig. 27).

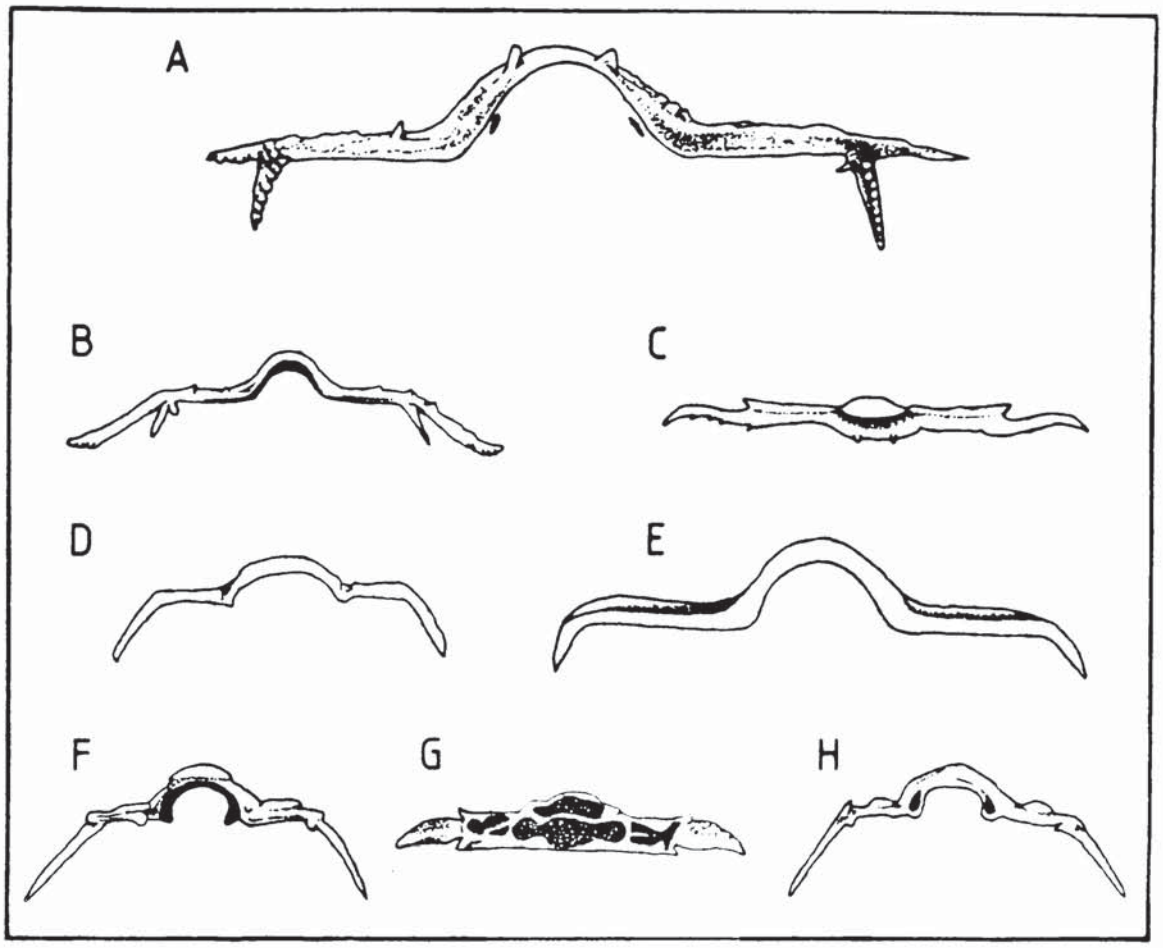

Figure 7.8. Thoracic segments with horizontal pleurae.
A. Ceratocephala lacinata Whittington and Evitt, (Odontopleuridae) posterior view of thoracic segment x10. Based on Whittington and Evitt (1954), pl. 8, fig.8.
B, C. Acidaspis (Asidaspis) lesperancei Chatterton and Perry, (Odontopleuridae) posterior and anterior views of thoracic segment x10. Based on Chatterton and Perry (1983), pl.21, figs. 15, 16.
D. Nanillaenus mackenziensis Chatterton and Ludvigsen, (Illaenidae) anterior view of thoracic segment x2.9. Based on Chatterton and Ludvigsen (1976), pl. 4, fig. 15.
E. Dolichoharpes. aff. D. reticulata Whittington. (Harpedidae) posterior view of thoracic segment x7. Based on Chatterton and Ludvigsen (1976), pl.7, fig. 24.
F-H. Ceraurinella typa Cooper, (Cheiruridae) anterior, ventral and posterior views of thoracic segment x2. Based on Whittington and Evitt (1954), pl. 11, figs. 1, 4, 5.

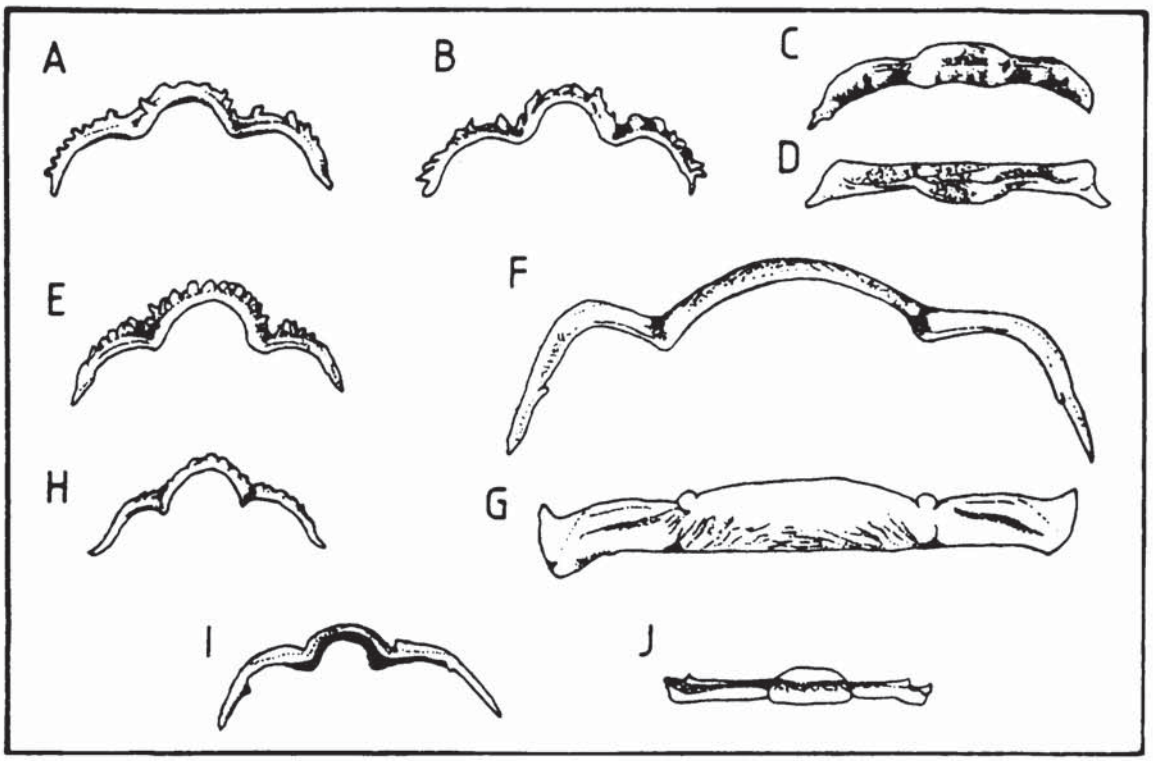

Figure 7.9. Arch on arch thoracic segments.
A-D. Dimeropyge virginensis Whittington and Evitt, (Dimeropygidae) thoracic segments x15. Based on Whittington and Evitt (1954), pl. 3, figs. 8, 11, 1, 5.
E. Dimeropyge clintonensis Shaw, (Dimeropygidae) posterior view of thoracic segment x15. Based on Chatterton and Ludvigsen (1976), pl. 18, fig. 11.
F, G. Isotelus parvirugosus Chatterton and Ludvigsen, (Asaphidae) posterior and dorsal views of thoracic segment x2.9. Based on Chatterton and Ludvigsen (1976), pl. 2, figs. 19, 20.
H. Acanthoparypha chiropyga Whittington and Evitt, (Cheiruridae) posterior view of thoracic segment x3.2. Based on Whittington and Evitt (1954), pl. 29, fig. 25.
I, J. Encrinuroides rarus (Walcott), (Encrinuridae) posterior and dorsal views of thoracic segments x5.5. Based on Chatterton and Ludvigsen (1976), pl. 15, figs. 39, 40.

increases the strength of the structure, especially in areas of muscle attachment such as the axial furrows.

Other thoracic segments are intermediate in form between these two end members and resemble arches on arches, but with several articulating processes (Fig. 7.9). Therefore, although the cephalon and pygidium of a trilobite are well designed for mechanical strength, the shape of thoracic segments are also a function of their role in articulation.

Occasionally a network of polygonal structures can be seen on the surface of trilobite cuticles, for example Homagnostus obesus (Chapter 6) which gives the appearance of space frames, such as geodesic domes. However, as trilobite exoskeletons were constructed predominantly from low-magnesian calcite that resisted compressive forces, presumably with tensile chitin fibrils parallel to the surface; their space-enclosing structure is more analogous to the monocoque shell, which resists forces throughout its skin, not just in members of a grid system.

The polygonal structures are simply the external expression of epidermal cells which generated the cuticle, but the network of ridges they create can give the 'thin shell' some additional strength. When examined in detail, the cell polygons are essentially curved plates with reinforced ridges on their edges (Fig. 7.10A,B). In section, the ridges are acting as T-beams (Fig. 7.10C), which are much stronger than ordinary beams since there are no joints. Although in architecture these are normally inverted, the principles involved remain valid for trilobites. Altogether, a strengthening meshwork has been produced over the external surface, the structural significance of which is most marked in thin cuticles such as those of agnostid trilobites, where the

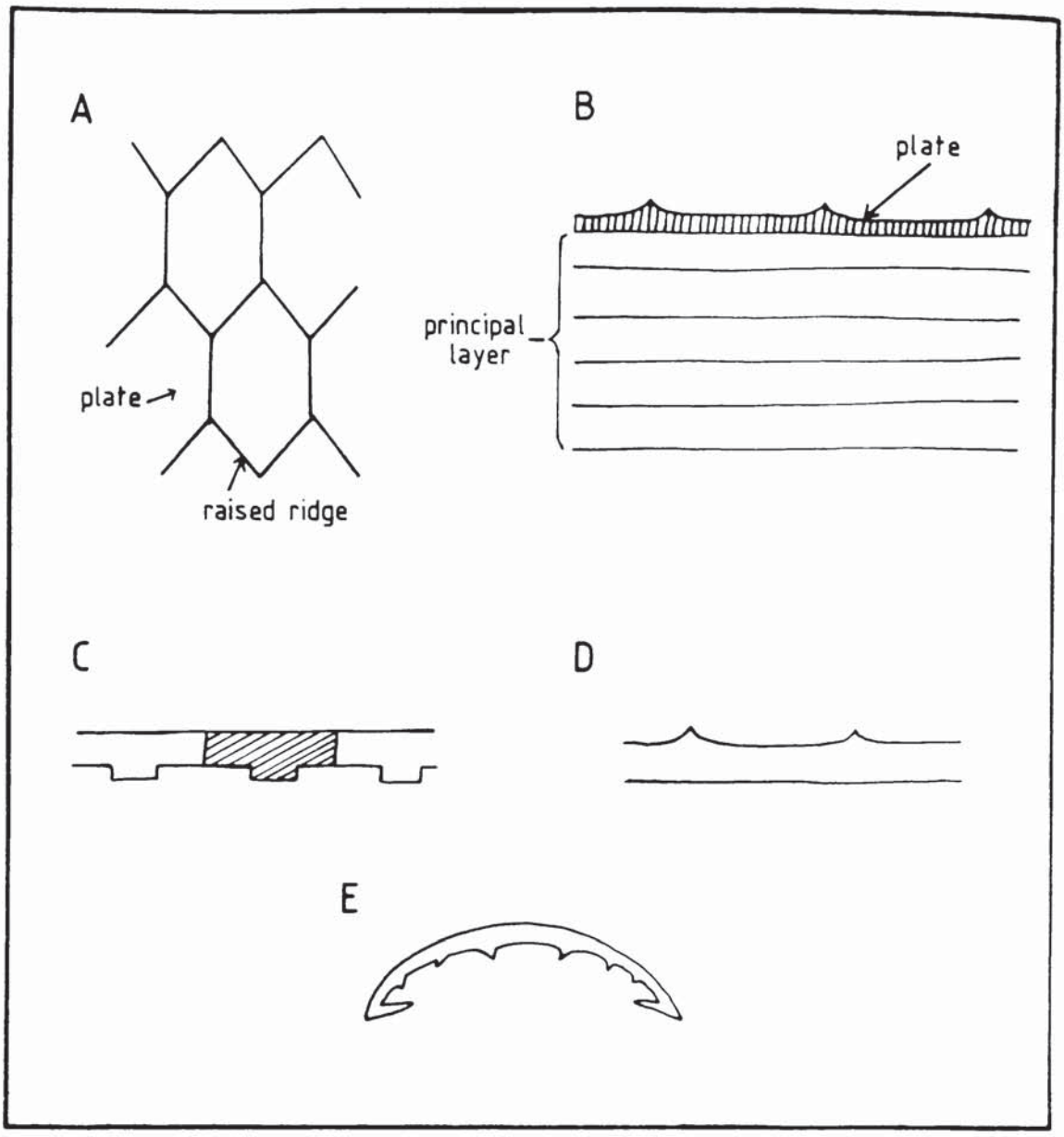

Figure 7.10. T-beams.

A. Plan view of cell polygons on trilobite cuticle.

B. Schematic transverse section through trilobite cuticle, not to scale.

C. A T-beam, as used in architecture.

D. Transverse section through an agnostid cuticle.

E. Schematic transverse section through an effaced pygidium showing ribs on ventral surface.

ridges can form as much as 15% of the total cuticle thickness. The presence of an external strengthening mesh is very useful in curved structures as it helps to transmit forces, applied on the structural shell. However they are rarely used in man-made structures as external meshes are subject to corrosion; as a compromise, they have to be placed within the structure. In this respect therefore, trilobite exoskeletons are better designed than most buildings, although an external mesh was applied to the Philips Pavilion, designed by Le Corbusier at the Brussels Exhibition in 1958. As the building was just a temporary exhibit, corrosional effects were unimportant.

Additional structures on trilobite exoskeletons acting as T-beams occur on the ventral surfaces of some effaced cuticles (Fig. 7.10E). For example, the pygidium of Leiolichas is strengthened by a series of radiating ribs (Thomas and Holloway 1988, pl. 9, fig. 208). As mentioned previously, ridges on the ventral surface are generally more prominent than the corresponding dorsal furrows, although this is probably primarily for muscle attachment rather than for strengthening purposes. Other larger-scale features such as terrace ridges and tubercles will have strengthened the exoskeleton by increasing the thickness of the cuticle. As most terrace ridges only have relief on the external surface of the exoskeleton, they too acted as reinforcing ridges to the 'sheet', and often occur on the margins or doublure where strains were greatest. Those that have relief on both dorsal and ventral surfaces of the cuticle (Chapter 4) will have acted as folded plates.

7.8. CONCLUSIONS

1. For the first time, the mechanical characteristics of a fossil exoskeleton have been related to its composition, microstructure, and architecture.

2. Trilobite cuticles are best regarded as ceramics which are linearly elastic, as they were predominantly composed of low-magnesian calcite with only a small proportion of organic matter.

3. Calcification was probably the most economical method of strengthening the cuticle in the marine environment, due to the abundance of the relevant ions.

4. Trilobite exoskeletons were composites that could resist both tensile and compressive forces. Calcite is strong under compression, whereas probable chitin fibrils orientated parallel to the cuticle surface resisted tensile forces.

5. The small size of the calcite crystals reduced the risk of crack formation, and the progression of fractures was slowed by the changes of direction at each crystal boundary.

6. Prismatic layer was probably the easiest microstructure to construct rapidly after ecdysis, and would have been strong under compressive forces acting normal to the cuticle surface. The underlying principal layer functioned as a crack-stopper and added bulk to the exoskeleton.

7. The relative proportions of prismatic layer to principal layer would have been of mechanical significance.

8. Structurally, the trilobite exoskeleton is a monocoque shell in the form of a series of modified domes. The doublure, cell polygons, and terrace ridges all strengthened the cuticle. Strongly convex trilobites had shorter doublures than shallower forms.

9. The shape of thoracic segments is a compromise between mechanical strength and their function as articulating structures.

7.9. REFERENCES

ABBY-KALIO, N,J. 1982. Aspects of feeding in Carcinus maenus (Linnaeus): functional anatomy and food-harvesting strategies. Ph.D. thesis (unpubl.), Reading University.

BARTH, F. G. 1973. Microfibre reinforcement of an arthropod cuticle. Z. Zellforsch. mikrosk. Anat. 144, 409-433.

BENSON, R. H. 1974. The role of ornamentation in the design and function of the ostracode carapace. Geoscience and Man, 6, 47-57.

BENSON, R. H. 1975. Morphologic stability in Ostracoda. Bull. Am. Paleont. 65 (282), 13-46.

BENSON, R. H. 1981. Form, function and architecture of ostracode shells. Ann. Rev. Earth Planet. Sci. 9, 59-80.

BENSON, R. H. 1982. Comparative transformation of shape in a rapidly evolving series of structural morphotypes of the ostracod Bradleya. In BATE, R. H., ROBINSON, E. and SHEPPARD, L.M. (eds.). Fossil and Recent Ostracods. 147-164, British Micropalaeont. Soc. Series, Ellis Horwood Ltd., Chichester.

BERGSTRÖM, J. 1973. Organisation, life and systematics of trilobites. Fossils Strata, 2, 1-69, pls.1-5.

BERMAN, A., ADDADI, L. and WEINER, S. 1988. Interactions of sea-urchin skeleton macromolecules with growing calcite crystals - a study of intracrystalline proteins. Nature, 331, 546-548.

BOULIGAND, Y. 1965. Sur une architecture torsadée répandue dans de nombreuses cuticules d'arthropodes. C. r. hebd. Séanc. Acad. Sci. Paris, 261, 3665-3668.

BUCKLE, I. G. (ed.). 1977. W. Morgan's "The elements of structure". (Second edition) xi + 252 pp. Pitman Publishing Ltd., London.

CHATTERTON, B. D. E. and LUDVIGSEN, R. 1976. Silicified Middle Ordovician trilobites from the South Nahanni River area, District of Mackenzie, Canada. Palaeontographica, Abt. A, 154, Lfg.1-3, 1-109, pl. 1-22.

CHATTERTON, B. D. E. and PERRY, D. G. 1983. Silicified Silurian odontopleurid trilobites from the Mackenzie Mountains. Palaeontographica Canadiana, 1, 1-127, pls.1-36.

CLARKSON, E. N. K. and HENRY, J-L. 1973. Structures coaptatives et enroulement chez quelques Trilobites ordoviciens et siluriens. Lethaia, 6, 105-132.

COOK, J. and GORDON, J. E. 1964. A mechanism for the control of crack propagation in all-brittle systems. Proc. R. Soc. A282, 508-520.

COWAN, H. J. 1980. Architectural structures: an introduction to structural mechanics (Metric edition). xvi + 320 pp. Pitman Publishing Ltd., London.

CRAIG, J. R. and VAUGHAN, D. J. 1981. Ore microscopy and ore petrography. xii + 406 pp. John Wiley and Sons, Inc., New York.

CURREY, J. D. 1969. The mechanical consequences of variation in the mineral content of bone. J. Biomechanics, 2, 1-11.

CURREY, J. D. 1975. The effects of strain rate, reconstruction and mineral content on some mechanical properties of bovine bone. J. Biomechanics, 8, 81-86.

CURREY, J. D. 1976. Further studies on the mechanical properties of mollusc shell material. J. Zool., Lond. 180, 445-453.

CURREY, J. D. 1979. Mechanical properties of bone tissues with greatly differing functions. J. Biomechanics 12, 313-319.

CURREY, J. D. 1980. Mechanical properties of mollusc shell. Symp. Soc. exp. Biol. 34, 75-97.

CURREY, J. D., NASH, A. and BONFIELD, W. 1982. Calcified cuticle in the stomatopod smashing limb. J.Mats. Sci. 17, 1939-1944.

CURREY, J. D. and TAYLOR, J. D. 1974. The mechanical behaviour of some mollusc hard tissues. J. Zool., Lond. 173, 395-406.

DALINGWATER, J. E. 1969. Some aspects of the chemistry and fine structure of the trilobite cuticle. Ph.D. thesis (unpubl.), University of Manchester.

DALINGWATER, J. E. 1973. Trilobite cuticle microstructure and composition. Palaeontology. 16, 827-839, pls.107-109.

DALINGWATER, J. E. 1985. Biomechanical approaches to eurypterid cuticles and chelicerate exoskeletons. Trans. R. Soc. Edinb. 76, 359-364.

DALINGWATER, J. E. and MILLER, J. 1977. The laminae and cuticular organisation of the trilobite Asaphus raniceps. Palaeontology. 20, 21-32, pls.9-10.

DENNELL, R. 1978. Balken orientation in three coleopteran cuticles. Zool. J. Linn. Soc. 64, 15-26.

DORRINGTON, K. L. 1980. The theory of viscoelasticity in biomaterials. Symp. Soc. exp. Biol. 34, 289-314.

FORTEY, R. A. and OWENS, R. M. 1979. Enrolment in the classification of trilobites. Lethaia. 12, 219-226.

GORDON, J. E. 1980. Biomechanics: the last stronghold of vitalism. Symp. Soc. exp. Biol. 34, 1-11.

HACKMAN, R. H. 1974. The soluble cuticular proteins from three arthropod species: Scylla serrata (Decapoda: Portunidae), Boophilus microplus (Acarina: Ixodidae), and Agrianome spinicollis (Coleoptera: Cerambycidae). Comp. Biochem. Physiol. 49B, 457-464.

HARRINGTON, H. J. 1959. General description of Trilobita. In MOORE, R. C. (ed.). Treatise on invertebrate paleontology. Part O. Arthropoda 1. O38-O117. Geological Society of America and University of Kansas Press, New York and Lawrence, Kansas.

HENRY, J-L. and CLARKSON, E. N. K. 1975. Enrolment and coaptations in some species of the Ordovician trilobite genus Placoparia. Fossils Strata. 4, 87-95, pls.1-3.

HEPBURN, H. R., JOFFE, I., GREEN, N. and NELSON, K. J. 1975. Mechanical properties of a crab shell. Comp. Biochem. Physiol. 50A, 551-554.

HILLERTON, J. E. 1980. The hardness of locust incisors. Symp. Soc. exp. Biol. 34, 483-484.

HILLERTON, J. E. 1984. Cuticle: mechanical properties. In BEREITER-HAHN, J., MATOLTSY, A. G. and SYLVIA RICHARDS, K. (eds.). Biology of the integument. Volume 1. 626-637. Springer-Verlag, Berlin, Heidelberg, New York.

HILLERTON, J. E., REYNOLDS, S. E. and VINCENT, J. F. V. 1982. On the indentation hardness of insect cuticle. J. exp. Biol. 96, 45-52.

JOFFE, I., HEPBURN, H. R. and ANDERSON, S. O. 1975. On the mechanical properties of Limulus solid cuticle. J. comp. Physiol. 101, 147-160.

KER, R. F. 1980. Small-scale tensile tests. Symp. Soc. exp. Biol. 34, 487-489.

KRAMPITZ, G., DROLSHAGEN, H., HAUSLE, J. and HOF-IRMSCHER, K. 1983. Organic matrices of mollusc shells. In WESTBROEK, P. and DE JONG, E. W. (eds.). Biomineralisation and biological metal accumulation. 231-247. D. Reidel Publ. Co., Dordrecht, Holland.

LANE, P. D. and THOMAS, A. T. 1978. Family Scutelluidae. In THOMAS, A. T. British Wenlock Trilobites (Part 1). Palaeontogr. Soc. [Monogr.], 1, 8-25.

LIVOLANT, F., GIRAUD, M-M. and BOULIGAND, Y. 1978. A goniometric effect observed in sections of twisted fibrous materials. Biol. Cellulaire, 31, 159-168.

LOWENSTAM, H. A. 1981. Minerals formed by organisms. Science, N. Y. 211, 1126-1131.

MANN, S. 1988. Molecular recognition in biomineralisation. Nature, 332, 119-124.

MILLER, J. 1976. The sensory fields and mode of life of Phacops rana (Green 1832) (Trilobita). Trans. R. Soc. Edinb. 69, 337-367, pls.1-4.

MILLER, J. and CLARKSON, E. N. K. 1980. The post-ecdysial development of the cuticle and the eye of the Devonian trilobite Phacops rana milleri Stewart 1927. Phil. Trans. R. Soc. Ser. B. 288, 461-480, pls.1-7.

MÜLLER, K. J. and WALOSSEK, D. 1987. Morphology, ontogeny, and life habit of Agnostus pisiformis from the Upper Cambrian of Sweden. Fossils Strata, 19, 1-124, pls.1-33.

MURDOCK, G. R. and CURREY, J. D. 1978. Strength and design of shells of the two ecologically distinct barnacles Balanus balanus, Semibalanus (Balanus) balanoides (Cirripedia). Biol. Bull. mar. biol. Lab., Woods Hole. 155, 169-192.

NERVI, L. 1951. Il ferro-cemento: sue carattieriche e possibilita. L' Ingegnere, 1.

NEVILLE, A. C. 1970. Cuticle ultrastructure in relation to the whole insect. Symp. R. ent. Soc. Lond. 5, 17-39.

NEVILLE, A. C. and LUKE, B. M. 1969. A two-system model for chitin-protein complexes in insect cuticles. Tissue and Cell. 1, 689-707.

RICHARDS, A. G. 1951. The integument of arthropods. xvi + 411 pp. University of Minnesota Press, Minneapolis.

TAYLOR, J. D. and LAYMAN, M. 1972. The mechanical properties of bivalve (mollusca) shell structures. Palaeontology, 15, 73-87.

TEIGLER, D. J. and TOWE, K. M. 1975. Microstructure and composition of the trilobite exoskeleton. Fossils Strata, 4, 137-149, pls.1-9.

THOMAS, A. T. 1978. British Wenlock Trilobites (Part 1) Palaeontogr. Soc. [Monogr.], 1, 1-56, pls 1-14.

THOMAS, A. T. and HOLLOWAY, D. J. 1988. Classification and phylogeny of the trilobite Order Lichida. Phil. Trans. R. Soc. Lond. Ser. B 321, 179-262, 16 pls.

THOMAS, A. T. and LANE, P. D. 1984. Autecology of Silurian trilobites. Sp. Pap. Palaeontology, 32, 55-69.

VINCENT, J. F. V. 1980. Insect cuticle: a paradigm for natural composites. Symp. Soc. exp. Biol. 34, 183-210.

VINCENT, J. F. V. 1982. Structural biomaterials. xi + 206 pp. The Macmillan Press Ltd., London.

VINCENT, J. F. V. and HILLERTON, J. E. 1979. The tanning of insect cuticle - a critical review and revised mechanism. J. Insect. Physiol. 25, 653-658.

VAINWRIGHT, S. A., BIGGS, W. D., CURREY, J. D. and GOSLINE, J. M. 1976. Mechanical design in organisms. xii + 423 pp. Edward Arnold, London.

VATABE, N. 1984. Shell (Mollusca). In BEREITER-HAHN, J., MATOLTSY, K. and SYLVIA RICHARDS, K. (eds.). Biology of the integument. 448-485. Springer-Verlag, Berlin, Heidelberg, New York.

WEINER, S., TRAUB, W. and LOWENSTAM, H. A. 1983. Organic matrix in calcified exoskeletons. In WESTBROEK, P. and DE JONG, E. W. (eds.). Biomineralization and biological metal accumulation. 205-224. D. Reidel Publ. Co., Dordrecht, Holland.

WELINDER, B. S. 1974. The crustacean cuticle 1. Studies on the composition of the cuticle. Comp. Biochem. Physiol. 47A, 779-787.

WHATLEY, R. C., TRIER, K. and DINGWALL, P. M. 1982. Some preliminary observations on certain mechanical and biophysical properties of the ostracod carapace. In BATE, R. H., ROBINSON, E. and SHEPPARD, L. M. (eds.). Fossil and Recent ostracods. 76-104. The British Micropalaeont. Soc., Ellis Horwood Ltd.

WHITTINGTON, H. B. and EVITT. W. R. 1954. Silicified Middle Ordovician trilobites. Mem. geol. Soc. Am. 59, 1-135, pls.1-33.

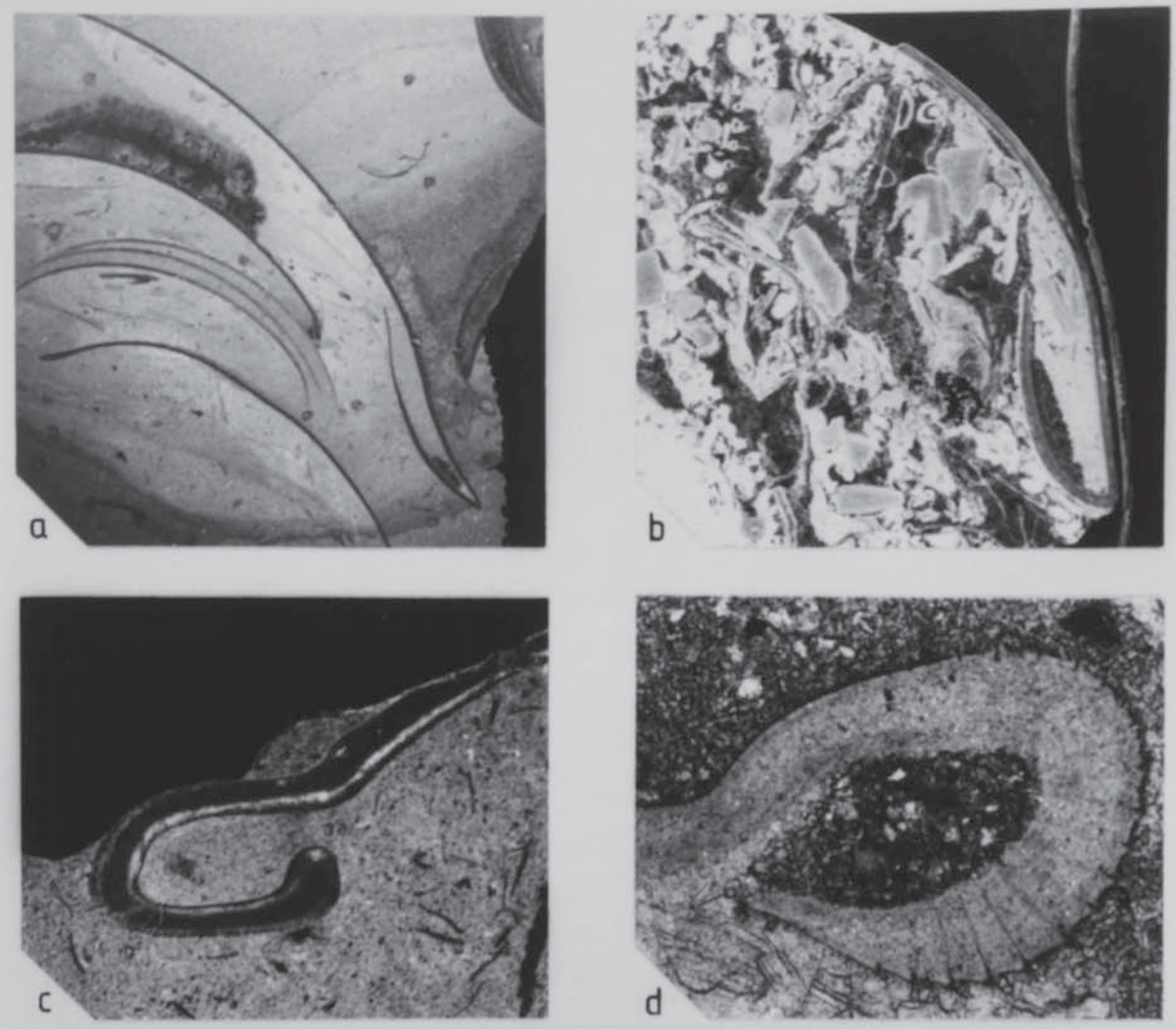

Plate 7.1. Different types of doublure.

a, Illaenus sp. Boda Limestone, Dalarna, Öland (Ordovician). (JED)2.II.66. Pygidial doublure. x15.

b, Cybantyx anaglyptos Lane and Thomas. Much Wenlock Limestone Formation, Wren's Nest, Dudley (Wenlock). NW43.1. Longitudinal section through pygidium. x7.

c, Dalmanites myops (König). Hill End Farm Borehole, Walsall (Wenlock). NW34.1. Longitudinal section through pygidium. x10.

d, Warburgella (Warburgella) stokesii (Murchison). Locality 28 of Thomas (1978) (Wenlock). 14.10. Transverse section through the lateral border of a free cheek. Note the canals opening out at the crests of the terrace ridges. x70.

APPENDIX 1

A. A. analyses

Specimen	%Ca^{2+}	%$CaCO_3$	%Mg^{2+}	%$MgCO_3$	Total $CaMgCO_3$	%Fe^{2+}	Sr^{2+}
1	33.65	84.13	0.55	1.93	86.06	0.63	0.29
2	32.45	81.13	0.55	1.93	83.06	0.52	0.28
3	35.79	89.48	0.63	2.21	91.69	0.37	0.33
4	37.86	94.65	0.50	1.75	96.40	0.43	0.31
5	36.77	91.93	0.24	0.84	92.77	0.67	0.16
6	35.63	89.08	1.01	3.54	92.62	0.28	0.17
7	33.91	84.78	1.01	3.54	88.32	0.47	0.27
8	36.08	90.20	1.37	4.80	95.00	0.56	0.09
9	37.50	93.75	0.35	1.23	94.98	0.60	0.36
10	37.90	94.75	0.56	1.96	96.71	0.48	0.15
11	32.66	81.65	1.58	5.53	87.18	0.30	0.35
12	36.07	90.18	1.37	4.80	94.98	0.72	0.13
13	34.08	85.13	3.18	11.13	96.26	0.29	0.07
14	28.27	70.68	0.41	1.44	72.12	0.56	0.27
15	8.16	20.40	0.31	1.09	21.49	0.91	0.06
16	32.72	81.80	0.41	1.44	83.24	0.56	0.27
Average (1-10)	35.75	89.36	0.68	2.37	91.76	0.50	0.24

Specimens 11 and 13 were not used for averages as the %$MgCO_3$ values were unrealistic. All samples were collected from the Much Wenlock Limestone Formation. Locality numbers refer to those of Thomas (1978).

1. Warburgella pygidium, Loc. 43.
2. Proetus pygidium, Loc. 43.
3. Dalmanites pygidium, Loc.43.
4. Calymene cephalon, Loc. 43.
5. Dalmanites pygidium, Loc. 64.
6. Dalmanites free cheek, Loc. 64.
7. Dalmanites pygidium, Loc. 43.
8. Cybantyx cephalon, Loc. 64.
9. Dalmanites genal spine, Loc.64.
10. Dalmanites genal spine, Loc.43.
11. Dalmanites pygidium, Loc. 43.
12. Dalmanites free cheek, Loc. 64.
13. Dalmanites free cheek, Loc.64.
14. Matrix, Loc. 43.
15. Matrix, Loc. 43.
16. Matrix, Loc, 43.

APPENDIX 2

Carbon and oxygen stable isotope values

K. T. RATCLIFFE DATA.

Specimen	$\delta^{13}C_{PDB}$	$\delta^{18}O_{PDB}$	$\delta^{18}O_{SMOW}$
DEB1 Cr	4.38	-4.47	25.95
DEB2 Cr	4.30	-5.62	25.07
DEB3 Cr	4.12	-5.74	24.94
DEB1 Br	-3.42	-5.68	25.01
DEB2 Br	0.46	-5.79	24.90
DEB3 Br	0.22	-5.35	25.35
DEB4 Br	0.16	-5.12	25.58
DEB5 Br	-1.68	-5.46	25.23
WN1 Tril	3.09	-5.83	24.85
WN3 Tril	-0.65	-5.56	25.12

N. V. WILMOT DATA.

B1	1.16	-5.36	25.33
B2	1.21	-5.75	24.93
B3	1.05	-5.70	24.98
B4	1.24	-5.82	24.86
C3	2.47	-6.20	24.47
NW C4	5.05	-6.85	23.80
NW C5	5.19	-7.04	23.60
NW C6	3.16	-7.19	23.45
NW C7	2.98	-6.17	24.49
NW C8	2.52	-6.62	24.04
NW C9	2.61	-6.75	23.91
NW C10	2.95	-6.29	24.38
NW1	1.27	-7.44	23.19
NW2	0.89	-6.67	23.98
NW3	0.99	-6.71	23.94
NW4	-0.01	-7.87	22.75
NW5	1.08	-6.87	23.78
NW7	1.68	-6.27	24.39
NW8	1.05	-7.61	23.02

NW9	-0.46	-5.35	25.34
NW10	-0.05	-5.27	25.43
NW11	0.98	-5.83	24.85
NW13	0.72	-6.54	24.12
NW14	0.40	-4.80	25.91
NW15	0.60	-6.67	23.99
NW16	1.09	-6.61	24.05
NW17	0.39	-8.09	22.52
NW19	0.19	-10.65	19.88
NW20	0.88	-6.83	23.82

APPENDIX 3

Trilobite cuticle thicknesses

AGNOSTIDA	Thickness (μm)
Agnostus pisiformis	8-15
Homagnostus obesus	5-10
Ptychagnostus gibbus	10-12
Peronopsis interstrictus	5-15
Leiopyge laevigata	10
REDLICHIIDA	
Paradoxides	340-400
Ellipsocephalus polytunus	115-350
CORYNEXOCHIDA	
Corynexochus (Bonnia) fieldensis	130
Bonnia	35-70
PTYCHOPARIIDA	
Komaspidacea	
Carolinites	45
Elrathia	110
Olenidae	
Olenus	5-50
Parabolina	15
Balnibarbi	20
Hypermecaspis	20
Svalbardites	8
Peltura	15-50
Asaphidae	
Gog	35-45
Asaphus	250
Nileidae	
Poronileus	160
Peraspis	140
Nileus	140

Ceratopygidae	
Ceratopyge	70
Trinucleidae	
Cryptolithus	100
Onnia	180
Tretaspis	130
Raphiophoridae	
Ampyx	20-150
Illaenidae	
Illaenus	130
Stenopareia	125-300
Styginidae	
Turgicephalus	70
Bumastus	145-350
Cybantyx	325
Opsypharus	270
PROETIDA	
Proetus (Proetus) concinnus	65-160
Warburgella (Warburgella) stokesii	40-160
W. (W.) scutterdinensis	80
Cyphoproetus depressus	95
Archegonus (Cyrtoproetus) cracoensis	70-130
Aulacopleura socialis	130
Harpidella (Harpidella) maura	25-75
Cummingella	90-160
PHACOPIDA	
Phacopina	
Phacops granulatus	470
Phacops rana crassituberculata	485-520
Phacops rana milleri	390-560
Toxochasmops extensus extensus	160-250
Dalmanites myops	300-370
Acaste dowingae	150

Cheirurina	
Ceraurus	120-180
Encrinurus tuberculatus	180
Encrinurus punctatus	250-310
Calymenina	
Calymene puellaris	230
Calymene blumenbachi	350-420
LICHIDA	
Hemiarges bucklandii	150-230
Dicranopeltis woodwardi	150

APPENDIX 4

Trilobite doublure thicknesses

Genus	Cuticle thickness (μm)	Thickness at doublure (μm)	% increase
Carolinites	45	90	200
Nileus	140	500	357
Illaenus	130	280	215
Bumastus	145	335	231
	350	590	168
Cyphoproetus	95	195	205
Archegonus	110	230	209
	70	200	286
Aulacopleura	130	270	208
Cummingella	160	340	213
	90	320	355
Proetus	120	240	200
Warburgella	115	300	260
Phacops	470	940	200
Toxochasmops	160	340	213
Dalmanites	300	590	197
	360	900	250
	370	1060	286
Ceraurus	180	410	228
Encrinurus	180	330	183

APPENDIX 5

Doublure length relative to convexity

All specimens are from the British Museum (Natural History), London.

Species	Specimen no.	Convexity (w:h)	Relative doublure length (w:dl)
PHACOPIDA			
Flexicalymene meeki	In58237	1:2.68	1:10.2
	In31803	1:3.02	1:9.2
	In31802	1:2.34	1:13.75
Flexicalymene senaria	In19844	1:2.51	1:7.75
	38414	1:3.8	1:10.1
Calymene blumenbachi	58793	1:2.8	1:8.58
	44212	1:3.55	1:9.23
	I316	1:2.55	1:14.9
	I1473	1:2.33	1:10.07
	44213	1:2.74	1:8.66
	I1473	1:3.25	1:9.32
	112	1:2.69	1:12.43
	58984	1:2.34	1:10.06
Calymene senaria	38414	1:3.23	1:9.83
	59735a	1:2.63	1:8.64
	59735b	1:2.76	1:15.8
	59735c	1:2.11	1:9.9
	59735d	1:2.6	1:15.4
	59735e	1:2.78	1:16.3
	42053	1:2.22	1:10.75
	42052a	1:3.08	1:11.93
	42052b	1:3.06	1:16.33
Calymene meeki	In31803	1:2.86	1:16.6
Encrinurus punctatus	59028	1:2.36	1:15.07
Dalmanites socialis	I5446	1:6.24	1:7.14
	42339	1:2.9	1:6.45
	59826	1:3.48	1:6.19
Deiphon forbesi	In28843	1:1.43	1:19.2

Calliops loxorhachis	In12460	1:2.09	1:9.57
	In12461	1:2.22	1:11.3
	In12462	1:2.59	1:7.38
Acastocepha dudleyensis	In36153	1:2.65	1:5.22
Phacops milleri	In36136	1:3.16	1:21.3
Phacops socialis	In28512	1:2.86	1:6.72
Phacops turio	It14185	1:2.6	1:8
	It14184	1:2.55	1:10.89
PROETIDA			
Proetus latifrons	58967	1:3.85	1:22.5
	46425	1:5.55	1:22.2
Dechenella rowi	It14275	1:3.6	1:13.3
Cummingella jonesi jonesi	59839	1:2.6	1:18.5
PTYCHOPARIIDA			
Ogygia desiduata	I3748	1:5.27	1:9.9
Asaphus raniceps	I5746	1:3.23	1:7.6
Asaphus expansus	In28407	1:3.76	1:10
Isotelus gigas	59485	1:2.58	1:7.4
Symphysurus dorsatus	It20532a	1:1.66	1:4.26
Symphysurus palpebrosus	It20923a	1:2.52	1:4.97
Ptychoparia striata	42371	1:4.44	1:12.6
	42374	1:7.72	1:16.3
Broeggeralithus broeggeri	In50879	1:4	1:9.14
	In50907	1:3.8	1:9.25
Harpes venulosus	It1611	1:3.18	1:4.95
Illaenus murchisoni	I1272	1:1.82	1:9.96
	I641	1:2.05	1:17.2
Bumastus barriensis	I1029	1:1.54	1:10.36

APPENDIX 6

List of specimens

NMW 88.22G.1 Crinoid ossicles (Wenlock), Much Wenlock Limestone Formation, Daw End, West Midlands.

NMW 88.22G.2 Gastropod, brachiopod and trilobite fragments (Wenlock) Much Wenlock Limestone Formation, Daw End, West Midlands.

NMW 88.22G.3 Ferroan brachiopod fragments (Wenlock) Much Wenlock Limestone Formation.

NMW 88.22G.4 Ferroan brachiopod fragments (Wenlock) Much Wenlock Limestone Formation.

NMW 88.22G.5 Warburgella (Warburgella) stokesii (Wenlock) Much Wenlock Limestone Formation. Large 14.10

NW1 Asaphus sp. (Ordovician) Asaphus Limestone, Muggerudkleiva, Norway.

NW2a Ptychagnostus sp. (M. Camb.) Slemmestad, Norway.

NW3 Peltura scarabaeoides (U. Camb.) Slemmestad, Norway.

NW4 Paradoxides sp. (M. Camb.) Slemmestad, Norway.

NW5 Elrathia sp. (M. Camb.) Peary Land, Greenland.

NW6 Bonnia sp. (L-M. Camb.) Peary Land, Greenland.

NW7 Bumastus nudus (Ordovician) Kullsberg Limestone, Osmundbjergte, Dalarne, Sweden.

NW8 Aulacopleura socialis (Llandovery) Washington Land, Greenland.

NW9 Ceraurus sp. and Cryptolithus sp. (Ordovician) Trenton Limestone, Quebec.

NW10 Cyphoproetus depressus and Bumastus? phrix (Wenlock) Limestone nodule in a shale band, Dolyhir and Nash Scar Limestone Formation. Exposure in old railway track 550m WNW of Dolyhir Brigde (SO 2403 5825).

NW11 Ellipsocephalus polytunus (Cambrian) Bornholm, Öland.

NW12 Agnostus pisiformis (U. Camb.) Hornes Udde, Öland.

NW13 Stenopareia glaber (Ordovician) Norway.

NW14 Stenopareia glaber (Ordovician) Norway

a, pygidium (internal mould)

b, pygidial doublure

c, pygidial doublure

d, cephalon

e, cephalon

NW15 Silicified trilobites. Lower part of the Edinburg Limestone, Hupp Hill, at entrance to Battlefield Crystal Caverns, and in field oppsite (east) side of U.S. Highway 11, approx. 1½ miles north of Strasburg, Shenandoah County, Virginia.

NW17 Dalmanites myops (Wenlock) Much Wenlock Limestone Formation, Eastnor Castle quarry (SO 7322 3629).

NW18 Dalmanites myops (Wenlock) Much Wenlock Limestone Formation, Eastnor Castle quarry (SO 7322 3629). Pygidium.

NW19 Dalmanites myops (Wenlock) Much Wenlock Limestone Formation, Eastnor Castle quarry (SO 7322 3629). Pygidium

NW20 Dalmanites myops (Wenlock) Much Wenlock Limestone Formation, old quarry 800m N. of Eastnor Castle (SO 7354 3774). Pygidium.

NW21 Nileus sp. (Ordovician) Lower 'raniceps' Limestone, Haget, Öland. Cephalon.

NW22-25 Ampyx sp. (Ordovician) Lower 'raniceps' Limestone, Haget, Öland. Cephala.

NW26 Ceratopyge sp. (Tremadoc) 'Ceratopyge' Limestone, Oslo Fjord, Norway.

NW27 Cryptolithus sp. (Ordovician) Eden Formation, central south Ohio.

NW28 Isotelus sp. (Ordovician) Drakes Formation, west side of Cowans Lake Spillway, Clinton County, Ohio.

NW30 Opsypharus convexus (Wenlock) Oslo Fjord, Norway. Pygidium.

NW31 Peronopsis interstricta (M. Camb.) Utah.

NW32 Leiopyge laevigata (M. Camb.) Asker Naöke, Sweden.

NW33 Ogygiocaris sp. (M. Ord.) Ogygiocaris shale, Huk Peninsula, Oslo, Norway.

NW34 Dalmanites myops (Wenlock) Hill End Farm borehole, Walsall. Pygidium.

NW39 Peltura sp. (U. Camb.) Slemmestad, Oslo Fjord, Norway.

NW40 Onnia sp. (Caradoc).

NW41 Tretaspis anderssoni (Ashgill) Frognøyn Shale Member, Venstop Formation, near Fjellstad, Ringerike, Norway.

NW42 Tretaspis anderssoni (Ashgill) Sørbakken Formation, Frognøya, Ringerike, Norway.

NW43 Cybantyx anaglyptos (Wenlock) Much Wenlock Limestone Formation. Pygidium.

NW44 Cybantyx anaglyptos (Wenlock) Much Wenlock Limestone Formation. Free cheek.

O.w. Olenus wahlenbergi and Homagnostus obesus (U. Camb.) Andrarum, Skåne, Sweden.

P.s. Parabolina spinulosa (U. Camb.) Andrarum, Skåne, Sweden.

KC1 Dalmanites myops (Wenlock) Cinder Hill cemetry borehole, Sedgely. Pygidium.

KC2 Warburgella (Warburgella) stokesii (Wenlock) Cinder Hill cemetry borehole, Sedgely. Pygidium.

DALM 1 Dalmanites myops free cheek, Locality 14 of Thomas (1978).

DALM 2 Dalmanites myops thoracic segment, Locality 14 of Thomas (1978).

DALM 3 Dalmanites myops thoracic segment, Locality 14 of Thomas (1978).

CALY 1 Calymene blumenbachi thoracic segment, Locality 14 of Thomas (1978).

AA 4-6 Specimens used for atomic absorption analyses.

INW 11-20 Specimens used for carbon and oxygen stable isotope analyses.

CAI 1-5 Specimens used for colour alteration experiments.

Silicified material.

E4Bb Edinburg Limestone (M. Ord) Virginia. Locality 4 of Whittington (1959).

AV4 126T Delorme Formation (Wenlock) Mackenzie Mountains, approximately 10km east of Avalanche Lake (see Chatterton and Perry 1983).

Recap Top of the Recaptaculites Limestone, New South Wales. Locality A of Chatterton (1971).

BH1 540 Cape Philips Formation (Wenlock), Baillie-Hamilton Island.

Specimens from Much Wenlock Limestone Formation (Wenlock), Wren's Nest, Dudley.

D1-3 Dalmanites myops cephala.

D4, D7, D9-11, D14, D16, D20 Calymene blumenbachi cephala.

D6 Encrinurus punctatus.

D24 Dalmanites myops pygidium.

D32 Hemiarges bucklandii pygidium.

D33 Hemiarges bucklandii cranidium.

D37 Cybantyx anaglyptos free cheek.

D38 Calymene? sp. Enrolled specimen.

RCC Calymene sp. cephala (Wenlock) Mulde Beds, Goll, Eksta parish, Blåhäll, Gotland.

RCP Calymene sp. pygidia (Wenlock) Mulde Beds, Goll, Eksta parish, Blåhäll, Gotland.

REP Encrinurus (Encrinurus) punctatus pygidia (Wenlock) Slite Marl, Sanda parish, Valbgtte, Gotland.

Specimens from Silica Shale (Middle Devonian), Silica, Ohio.

NE1-4, NE6 Phacops rana crassituberculata.

NE5, NE7 Phacops rana milleri.

Thin-sections of *Warburgella (Warburgella) stokesii*.

All locality numbers refer to those of Thomas (1978).

WAR.1 Pygidium, locality 75.

WAR.2-3 Free cheeks, locality 75.

WAR.4 Free cheek, locality 49.

WAR.5 Free cheek, locality 75.

WAR.6 Cranidium, locality 49.

WAR.7-9 Cranidia, locality 75.

WAR.10-20 Pygidia, locality 64.

WAR.21 Cranidium, locality 64.

WAR.22 Pygidium, locality 64.

WAR.23-26 Pygidia, locality 43.

WAR.27-28 Pygidia, locality 64.

WAR.29-31 Free cheeks, locality 43.

VAR.32-33 Free cheeks, locality 64.

VAR.34-40 Cranidia, locality 43.

VAR.41-42 Cranidia, locality 64.

Thin-sections of *Proetus (Proetus) concinnus.*

All locality numbers refer to those of Thomas (1978).

PRO.1 Pygidium, locality 49.

PRO.2-3 Pygidia, locality 75.

PRO.4 Free cheek, locality 75.

PRO.5-6 Free cheeks, locality 49.

PRO.7-9 Pygidia, locality 43.

PRO.10-14 Pygidia, locality 64.

PRO.15 Pygidium, locality 43.

PRO.16-21 Free cheeks, locality 64.

PRO.22-24 Cranidia, locality 64.

PRO.25 Cranidium, locality 43.

PRO.26-29 Pygidia, locality 43.

PRO.30-31 Enrolled specimens, locality 64.

PRO.32-33 Cranidia, locality 43.

PRO.34-35 Free cheeks, locality 43.

PRO.36 Pygidium, locality 43.

PRO.37-40 Pygidia, locality 64.

PRO.41 Pygidium, locality 43.

PRO.42 Cranidium, locality 64.

PRO.43 Free cheek, locality 64.

PRO.44-46 Free cheeks, locality 43.

PRO.47 Cranidium, locality 64.

Thin-sections of *Harpidella (Harpidella) maura.*

All specimens are from locality 14 of Thomas (1978).

HAR.1-12 Cranidia.

HAR.13-16 Free cheeks.

HAR.17-26 Cranidia.

HAR.27-28 Thoracic segments.

HAR.29-32 Free cheeks.

SEM stubs of *Warburgella (Warburgella) scutterdinensis.*

All specimens are from locality 38 of Thomas (1978).

War.scutt.1 Pygidium.

War.scutt.2 Free cheek.

War.scutt.3 Cranidium and free cheek.

War.scutt.4 Hypostome (counterpart to War.scutt.3).

SEM stubs of *Warburgella (Warburgella) stokesii.*

Locality numbers refer to those of Thomas (1978).

WAR.1 Pygidium, locality 43.

WAR.2 Free cheek, locality 43.

WAR.3-5 Cranidia, locality 43.

WAR.6-9 Free cheeks, locality 43.

WAR.10-11 Free cheeks, locality 64.

WAR.12 Cranidium, locality 64.

WAR.13-17 Pygidia, locality 64.

WAR.18 Cranidium, locality 64.

WAR.19 Free cheek, locality 64.

WAR.20 Pygidium, locality 64.

WAR.21 Free cheek, locality 64.

WAR.22-23 Cranidia, locality 64.

WAR.24 Pygidium, locality 43.

WAR.25 Pygidium, locality 64.

WAR.26 Free cheek, locality 64.

SEM stubs of *Proetus (Lacunoporaspis) oppidanus.*

All specimens are from locality 26 of Thomas (1978).

Pro.opp.1-3 Pygidia.

Pro.opp.4 Thoracic segment.

Pro.opp.5-6 Cranidia.

Pro.opp.7-8 Free cheeks.

SEM stubs of *Proetus (Proetus) concinnus.*

All locality numbers refer to those of Thomas (1978).

PRO.1-6 Cranidia, locality 43.

PRO.7-13 Free cheeks, locality 43.

PRO.14-16 Pygidia, locality 43.

PRO.17 Hypostome, locality 64.

PRO.18-19 Cranidia, locality 64.

PRO.20 Thoracic segment, locality 43.

PRO.21 Hypostome, locality 43.

PRO.22 Hypostome, locality 64.

PRO.23-24 Pygidia, locality 43.

PRO.25-28 Pygidia, locality 64.

PRO.29-31 Cranidia, locality 64.

PRO.32 Free cheek, locality 43.

PRO.34-37 Free cheeks, locality 64.

PRO.38 Cranidium, locality 64.

PRO.39-42 Pygidia, locality 64.

PRO.43-44 Pygidia, locality 43.

PRO.45 Hypostome, locality 43.

PRO.46 Cranidium, locality 43.

PRO.47-48 Free cheeks, locality 43.

SEM stubs of *Harpidella (Harpidella) maura.*

All specimens are from locality 14 of Thomas (1978).

HAR.1-12 Cranidia.

HAR.13-14 Free cheeks.

HAR.15 Pygidium.

HAR.16 Cranidium.

HAR.17 Pygidium.

HAR.18-19 Thoracic segments.

HAR.20-22 Free cheeks.

HAR.23-34 Cranidia.

SEM stubs of *Cyphoproetus depressus.*

All specimens are from a limestone nodule in a shale band, Dolyhir and Nash Scar Limestone Formation (Wenlock). Exposure in old railway track 550m WNW of Dolyhir Bridge (SO 2403 5825).

CYP.1-6 Free cheeks.

CYP.7-8 Pygidia.

SEM stubs of *Bumastus? phrix.*

All specimens are from a limestone nodule in a shale band, Dolyhir and Nash Scar Limestone Formation (Wenlock). Exposure in old railway track 550m WNW of Dolyhir Bridge (SO 2403 5825).

BUM.1-3 Free cheeks.

BUM.4-6 Cranidia.

BUM.7 Free cheek.

BUM.8-10 Cranidia.

Sedgwick Museum specimens of *Warburgella (Warburgella) stokesii.*

Thin-sections.

A95352a

A95353a

A95358a

SEM stubs.

A95208

A95217a

A95322a

A95332a

A95335

A95397a

A95401a

A95403

A95341a

A95348a

A95382a

A95396

A95399a

A95400a

A95409

A95424

A95433

A95439a

A95450

Sedgwick Museum specimens of *Proetus (Proetus) concinnus.*

Thin-sections.

A95471a

A95512

A95524

A95649a

SEM stubs.

A95612a

A95631

A95657

A95681a

A95845a

Specimens from the Naturhistoriska Riksmuseet, Stockholm; figured by Lindström (1901).

Hand specimens.

Ar.27029 Bumastus sp.

Mo.2274c,b Bumastus barriensis

Ar.30223 Encrinurus punctatus

Ar.32860 Homalonotus knighti

Ar.2282 Bumastus sulcatus

Ar.46992a,b. Bronteus sp. indet

Ar.10916 Bronteus laticauda

Ar.10917 Bronteus laticauda

Ar.26570 Bumastus

Ar.10919 Bronteus laticauda

Ar.46993 Bronteus irradians

Ar.26973 Bumastus sp.

Ar.29497 Bronteus polyactin

Ar.10920 Bronteus laticauda

Ar.26505 Bumastus

Thin-sections.

Ar.2024b

Ar.48936

Ar.48939

Ar.29538b

Ar.29494b

Ar.48940

Ar.48938

Ar.48937

Ar.29498b

Ar.29499b

Ar.26506

Ar.30586c

Ar.30586b

Ar.48942

Ar.48941

Specimens from the Paleontologisk Museum, Oslo.

SEM stubs of Toxochasmops extensus extensus.

PMO-un1

PMO-un2

PMO6476

PMO69390

PMO81010

PMO81011

PMO69511

Thin-sections of Toxochasmops extensus extensus.

PMO 6476

PMO 69517

PMO 80990

Thin-sections from Størmer (1980).

PMO94398a,b

PMO94416a,b

PMO69349

PMO21999a,b

PMOA38817a-e

Specimen from British Geological Survey, Keyworth.

FOR.2393 Ptychagnostus gibbus (M. Camb.)

Specimens from the Geology Museum Louisiana State University, Baton Rouge.

8270 Greenops boothi (Middle Devonian)

8269.3 Phacops rana (Middle Devonian)

8271 Phacops rana (Middle Devonian)

Specimens from National Museum of Wales, Cardiff.

NMW.71.8G.3 Paradoxides pinus (Camb.)

NMW.71.8G.13 Ellipsocephalus polytnus (Camb.)

NMW.71.8G.26 Agnostus pisiformis (Camb.)

NMW.80.34G.362A Eodiscus punctatus punctatus (Camb.)

NMW.82.15G.55 Hedstroemia delicata (Wenlock)

NMW.76.6G.297 Proetus (Proetus) concinnus (Wenlock)

NMW.G.449 Dalmanites (Phacops) caudatus (Wenlock)

NMW.20.341.G9 Acaste dowingiae (Wenlock)

NMW.83.2G.2 Warburgella (Warburgella) stokesii (Wenlock)

NMW.71.6G.230 Acaste dowingiae (Wenlock)

NMW.71.6G.228 Acaste dowingiae (Wenlock)

NMW.6G.199 Encrinurus tuberculatus (Wenlock)

NMW.78.1G.344 Eocyphinium sp. (Dinantian)

NMW.71.7G.42 Archegonus (Cyrtoproetus) cracoensis (Dinantian)

NMW.71.7G.36 Archegonus (Cyrtoproetus) cracoensis (Dinantian)

NMW.78.1G.244a Griffithides sp. (Dinantian)

NMW.78.1G.147 Cummingella carringtonesis (Dinantian)

NMW.78.1G.143 Cummingella carringtonesis (Dinantian)

NMW.78.1G.181 Cummingella sp. (Dinantian)

NMW.74.29G.336 Cummingella sp. (Dinantian)

NMW.83.31G.879 Brachymetopus ornatus (Dinantian)

NMW.83.31G.889a Brachymetopus ornatus (Dinantian)

NMW.29G.196 Archegonus (Cyrtoproetus) cracoensis (Dinantian)

NMW.74.27G.16 Cummingella sp. (Dinantian)

NMW.22.11.G23 Corynexochus (Bonnia) fieldensis

NMW.82.15G.57 Hedstroemia delicata

NMW.75.45G.144a Porterfieldia punctata

NMW.71.8G.44 Ceratopyge forticula

NMW.82.15G.126 Calymene puellaris

NMW.82.15G.127 Calymene puellaris